Quantum Effects in the Search for New Physics

Dissertation submitted for the award of the title
"Doctor of Natural Sciences"
to the Faculty of Physics, Mathematics and Computer Science of
Johannes Gutenberg University Mainz

Prisco Lo Chiatto
born in Modena, Italy

Mainz, 30 September 2024

JOHANNES GUTENBERG
UNIVERSITÄT MAINZ

JG|U

Date of submission: 30/09/2024
Date of defence: 18/03/2025

Abstract

Quantum field theory is the backbone of modern particle physics. As the name implies, it is based on quantum mechanics, of which it is the consistent expansion to include special relativity. However, its quantum nature is not as evident when performing calculations for observables at collider experiments. Indeed, by construction, perturbation theory at leading order coincides with a classical theory, and quantum effect act as a parametrically small correction. Trying to bridge this gap, this thesis explores purely quantum phenomena as a discovery tool for new physics.

We start with an account of entanglement at colliders, focusing on the concrete example of 4-fermion scattering in the electroweak theory and including new physics dipole moments. We show that angular correlations of the fermions' decay products can restore ("resurrect") interference contributions that are otherwise suppressed by small masses in cross sections, thus unlocking a quantum phenomenon. We also critically evaluate the new physics sensitivity of entanglement markers, by interpreting the angular correlations as spin correlation of the parent fermions; we show that there is no advantage in using entanglement markers, and the angular correlations perform equally or better.

We then move to a scenario where quantum interference plays an even more dramatic role. We study a new gauge boson that is nearly degenerate with the Standard Model Z boson and show how interference between the two fundamentally alters predictions. We correct inconsistent treatments in older works, which worked in an uncontrolled approximation that suppressed interference. Surprisingly, we find that the quantum Zeno effect is critical to understanding the phenomenology of this system. This effect, which is not widely known in the particle physics community, is due to the mismatch of unitary evolution and the non-unitary nature of particle decay.

Finally, we shift our attention to nonrelativistic quantum mechanics, specifically exploring the connection between the quantum vacuum and the classical limit. Here, we uncover a surprising relationship between large-multiplicity scattering amplitudes and tunneling, offering new insights into how quantum effects persist even as systems approach classical behavior. This finding provides a fresh perspective on the interaction between quantum and classical mechanics in high-energy physics.

Throughout this thesis, we emphasize the importance of quantum effects that go beyond minor corrections to classical predictions. These effects represent fundamental shifts in behavior that must be accounted for when searching for new physics. In doing so, we highlight areas where quantum interference and related phenomena offer unique insights into physics beyond the Standard Model.

List of Publications

This thesis is based on the following works, that have already appeared on the arXiv repository, and are awaiting referral for publication. Each work forms the majority of one main part of this thesis. We highlight the contributions of the author to each work.

- P. Lo Chiatto *Interference Resurrection of the τ Dipole through Quantum Tomography* [1]: Single-authored paper.

- P. Lo Chiatto, F. Yu *Consistent Electroweak Phenomenology of a Nearly Degenerate Z' Boson* [2]: All figures were generated by the author, and all analytical and numerical calculations were first performed by the author. Both authors contributed to the text of the manuscript, as well to the generation of the *Feynarts* file that was necessary for the numerical calculations. The analytical arguments are also due to both authors.

- P. Lo Chiatto, S. Schenk, F. Yu *Quantum Imprint of the Anharmonic Oscillator* [3]: All authors contributed to the text of the manuscript. The author and S. Schenk created the Mathematica notebook that was used to derive the coefficient of the $\hbar$ expansion of the quantum volumes. This notebook was in turn based on code by S.Schenk that computes the necessary Picard-Fuchs operators. All authors contributed to the interpretation of the "quantum imprint rule", the main result of the paper.

Contents

Introduction

CHAPTER I

Introduction

We live in a quantum world. This statement is nowadays completely uncontroversial among anyone with even so much as a passing interest in physics. It might be then easy to forget the paradigm shift that had to take place for us to accept that the triumph of physics of the 18th and 19th century, Newtonian mechanics, cannot be a theory of everything, and that the world of the exceedingly small does not follow the laws of Lagrange and Hamilton. QM (quantum mechanics) not only describes with incredible precision the physics of atoms and subatomic particles, but it is also required to explain certain everyday phenomena, for instance the stability of matter [4–6]. This unparalleled explanation power came at an epistemological cost: it takes a large degree of abstraction to accept the quantum description of the world, as anybody sitting in (or teaching) a quantum mechanics class for the first time can confirm. Even sidestepping the question of how to interpret QM, certain phenomena are so in contrast with our everyday experience that, if both the theory and experimental data did not force them on us, we would regard them as downright absurd.

One of the most bewildering concept is entanglement, experimentally confirmed by the observation of Bell inequality violation [7–9]. The fact that two causally disconnected systems cannot be described separately, if they interacted in the past and left unperturbed, implies that only two of three previously held as sacred principles can be satisfied at once. Namely, the quantum mechanical world cannot be local (only the near-vicinity of an object influences it), realist (there are underlying properties of the world that exist independently of observers and their definitions) and causal (there exists a cause-effect link between phenomena). Another important conceptual leap in the early days of QM was the discovery of quantum tunnelling: mass can be transported around an energy barrier in finite time, even if the total energy of the system is less than the height of the barrier. Indeed, failure to account for tunnelling resulted in a wrong prediction for the stability of the Hydrogen ion molecule by Pauli in his PhD thesis, which in turn was one of the driving factor to move away from the old conception of QM (see *e.g.* ref. [10] for an account of this interesting story).

The success of QM notwithstanding, Newtonian mechanics works well, and indeed in its regime of validity it does not have rivals in terms of both ease of calculation and explanatory power. In a reductionist manner, we would like to be able to reduce classical mechanics to some limit of QM. For instance, the other great revolution in fundamental physics that happened in the early 1900s, special relativity, can easily be shown to smoothly approach Galilean relativity in the formal limit $c \to \infty$, or more properly in the $v/c \to 0$ limit, with c the speed of light and v the highest velocity involved in the process. A similar procedure should, we feel, be able to be performed in QM. This is the so-called correspondence limit, that we recall in Section I.1.3. Formally, this is attained in

the $\hbar \to 0$ limit, the Planck constant being the measure of all things quantum. However, a quantum mechanical system has a countably infinite amount of states, which somehow need to correspond to an uncountably infinite number of trajectories in the classical case, signalling that the situation may not be as clear-cut as special relativity, where no discontinuity of this kind is found during the limiting procedure [11]. This underlines that the statement in the opening of this thesis, while ingrained into any practising physicist in the 21st century, is not a clear *prediction* of the theory: to the best of the author's knowledge, there is no physical system for which we can reliably calculate using both quantum and classical mechanics, without having to resort to hand-waving. This means that deciding whether macroscopic objects could in principle display quantum coherence, or whether it even makes sense to talk about the wavefunction of macroscopic objects, is strictly speaking still an open question. We elaborate on this point in Section I.1.7.

The two phenomena of tunnelling and entanglement, as different as they appear, are both consequences of the principle of superposition. The superposition principle is also responsible for interference between different states. In this thesis, we will be broadly speaking concerned with consequences of the superposition principle. In particular, this thesis will be concerned with leveraging quantum effects for the search of NP (new physics)– *i.e.* physics not included in the Standard Model of particle physics – which we will also refer to as beyond the Standard Model. The focus will be on effects, familiar to the QM practitioner but often forgotten by the high-energy phenomenologist, that are not just a correction to classical behaviour but a qualitative shift from the classical mechanics prediction.

The structure of this thesis is as follows. In Part I of this thesis, we will study entanglement at collider experiments, and analyse how they can restore quantum effects, namely interference between different processes, that a simple cross-section study would be completely blind to. We also study whether the additional sensitivity afforded by this restoration is a consequence of probing the quantum nature of the model at hand, that is, if probing the quantum nature of correlations directly is necessary for improved NP sensitivity.

The answer to this question will unfortunately be negative, so we will move in Part II to a situation where interference between processes qualitatively changes the expectations with respect to the incoherent sum. Namely, we will study the collider phenomenology of a new gauge boson that is nearly degenerate with a known particle, and emphasise the need to correctly take into account the interference between the two particles. Surprisingly, we will find that considering the quantum Zeno effect, which we review in Section I.1.2, is necessary to understand the resulting phenomenology.

In Part III, we will return to nonrelativistic QM and study the relation between the classical limit and the quantum vacuum, by uncovering an unexpected link between large-multiplicity amplitudes and tunnelling amplitudes. We conclude in Chapter V by summarising the work, as well as interesting lines of inquiry for the future.

In the rest of this prologue we collect the necessary background for this thesis, emphasising where the standard material serves as inspiration for the original material presented in this thesis, and paying attention to currently unresolved questions. We have split the introduction in two sections: in Section I.1 we will focus on single-particle nonrelativistic QM, while Section I.2 is dedicated to QFT (quantum field theory).

I.1 Quantum Mechanics

I.1.1 Bell Inequalities and Coherence

Quantum correlations are one of the most spectacular deviations from classical expectations. In the 1960s, John Bell proposed a test to experimentally discriminate between the type of probabilistic interpretation we ascribe to QM and that of a hidden variable model, where only stochasticity is present [7]. The simplest possible scenario that showcases the essence of this test is the two-party Bell test, involving a bipartite two-qubit state [8]. That is, take two parties, Alice and Bob, each measuring two observables, say the x and z component of the spin of two spin 1/2 fermions, S_x, S_z, where we take $S_z \left|\downarrow\right\rangle = -\left|\downarrow\right\rangle, S_z \left|\uparrow\right\rangle = \left|\uparrow\right\rangle$. If we assing to positive spin a value of 1 and to negative spin 0, the following combination of expectation values

$$\mathcal{I}_2 = \left\langle S_x^1 S_x^2 \right\rangle + \left\langle S_x^1 S_z^2 \right\rangle + \left\langle S_z^1 S_x^2 \right\rangle - \left\langle S_z^1 S_z^2 \right\rangle , \tag{I.1}$$

cannot be higher than 2 in classical mechanics, *viz.* if we assume that the outcomes come from a pre-determined set of possible answers. This would be the case for a hidden-variable theory, where the apparent probabilistic nature of QM is actually a stochastic phenomenon due to yet-undiscovered high-frequency degrees of freedom that act classically [7]. However, QM predicts a maximum value of $2\sqrt{2}$ for this quantity [7]. A quick calculation shows that the maximum value can be attained *e.g.* by the state

$$\left|\psi_B\right\rangle = \frac{1}{\sqrt{2}} \left(\left|\uparrow\downarrow\right\rangle + \left|\downarrow\uparrow\right\rangle\right) . \tag{I.2}$$

It is important to note that the only reason why a higher value than 2 can be attained in QM is due to interference, which is absent in classical mechanics. Indeed, if one does not take coherence into account,

$$\mathcal{I}_2(\left|\psi_B\right\rangle)^{\text{Incoherent}} \equiv \frac{1}{2} \left(I_2(\left|\uparrow\downarrow\right\rangle) + I_2(\left|\uparrow\downarrow\right\rangle)\right) = 2 , \tag{I.3}$$

which is, indeed, the classical maximum. Thus, coherence plays a crucial role in distinguishing quantum and classical behaviour, a common theme in this thesis. We will come back to this point in Part I, where it will play an important role in establishing the sensitivity a Bell test performed at collider experiments can have to NP. We now discuss a phenomenon that, by disrupting coherence, freezes the time evolution of a system, the so-called Zeno effect.

I.1.2 Quantum Zeno

The basis of the quantum Zeno effect is the mismatch between unitary evolution and non-unitary measurement. To illustrate it, we follow the pedagogical treatment of ref. [12]. Consider the survival probability $p(t)$ of a system prepared in the state $\left|\psi\right\rangle$ at time $t = 0$, under the evolution of a Hamiltonian H

$$p(t) = \left|\langle\psi(0), \psi(t)\rangle\right|^2 = \left|\langle\psi(0)\right| \mathrm{e}^{-iHt} \left|\psi(0)\right\rangle\Big|^2 . \tag{I.4}$$

Expanding the exponential for small times t, one obtains

$$p(t) = 1 - \left(\frac{t}{\tau_Z}\right)^2 + \mathcal{O}\left(\left(\frac{t}{\tau_Z}\right)^4\right) , \tag{I.5}$$

where we defined the Zeno time τ_Z by the relation

$$\frac{1}{\tau_Z^2} = \langle\psi(0)|\, H^2\, |\psi(0)\rangle - \langle\psi(0)|\, H\, |\psi(0)\rangle^2 \,. \tag{I.6}$$

Importantly, even though the wave function evolves linearly away from the initial state, the probability function evolves quadratically with respect to time away from unity. Consider now performing N equally spaced projective measurements, *i.e.* check N times, at intervals of $t_M = t/N$, whether the system is still in the state $|\psi(0)\rangle$. Now consider what happens if the answer is affirmative: the system is projected onto its initial state, and the evolution starts over. Then, the next measurement will still have the same probability $p(t)$. If $t_M \ll \tau_Z$, one obtains

$$p(t;N) = p(t_M)^N \approx \left(1 - (\frac{t_M}{\tau_Z})^2\right)^N \,. \tag{I.7}$$

In the limit of large N this can be resummed into an exponential law with effective lifetime

$$\tau_{\text{eff}} = \frac{\tau_Z^2}{t_M} \,, \tag{I.8}$$

which is large with respect to τ_Z, by assumption. That is, frequent measurements have effectively frozen the evolution of the state. The quantum Zeno effect is so called because of similarity with the paradoxes of motion formulated by an Eleatic philosopher from the 5th century BCE of the same name.

Consider now a two-level system with a non-hermitian absorption term:

$$H = \begin{pmatrix} 0 & \Omega \\ \Omega & -i2V \end{pmatrix} \,; \tag{I.9}$$

we set $|\psi(0)\rangle = (1,0)^T \equiv |+\rangle$. For $V = 0$, the system would simply oscillate back and forth from $|-\rangle \equiv (0,1)^T$ (Rabi oscillations [13]), but nonzero V adds a decay term for $|-\rangle$. The survival amplitude can be easily derived [12]:

$$p(t) = \left(\frac{1}{2}(1 + \frac{V}{h})\mathrm{e}^{-t(V-h)} + \frac{1}{2}(1 - \frac{V}{h})\mathrm{e}^{-t(V+h)}\right)^2 \,, \tag{I.10}$$

where we defined $h = \sqrt{V^2 + \Omega^2}$. It can then be observed that, for large V, the coefficient $V - h$ of the first exponential is much smaller than $V + h$ in the second, which means the system has one fast and one slow decay mode. By expanding around $\Omega/V = 0$, one obtains

$$p(t) \approx \mathrm{e}^{-\frac{\Omega^2}{V}t} \,. \tag{I.11}$$

This result is somewhat counter-intuitive: by enlarging the decay probability of $|-\rangle$, we also boost the probability of the system to remain in the state $|+\rangle$, almost as if it knew its inevitable fate if it were to oscillate into $|-\rangle$. By comparing the effective lifetime in this example and the previous example of N projective measurements, one finds the curious correspondence [14]

$$V \leftrightarrow \frac{1}{t_M} \,. \tag{I.12}$$

This lends to the following interpretation: the fast decay channel of $|-\rangle$ effectively prevents $|+\rangle$ from oscillating by acting as a continuous measurement: if V is large, as soon as $|-\rangle$

is populated it decays within a time $\sim 1/V$, that is the transition from $|+\rangle$ to $|-\rangle$ is immediately measured by the decay process of $|-\rangle$. By the Zeno effect, this prevents evolution from taking place. We will use this interpretation in Part II.

We now go back to the old days of QM, to set the stage for our discussion of tunnelling, the divergence of perturbation theory, and their connection in the realm of high-multiplicity amplitudes.

I.1.3 The Correspondence Principle

Quantum mechanics, as it was conceptualised in the first decades of the 1900s, had a strict relationship with classical mechanics. The "correspondence principle" was the driving conceptual force behind the relation, which in turn relied on the success of classical mechanics to explain physics at length scales much bigger than the atomic ones. Then, if one imagines an atomic level with a macroscopically big Bohr radius, classical mechanics should be able to describe it well. Indeed, in this limit its angular momentum is very large in comparison to $\hbar$. Bohr arrived at what is now called the quantisation condition of the "old quantum theory" by pondering on this exact principle, which he considered a basic law of Nature [15]. By quantising the phase-space of the hydrogen atom in units of $\hbar$, he arrived at the condition

$$\oint_{H(p,q)=E} p\,\mathrm{d}q = n\hbar \tag{I.13}$$

where $H(p,q)$ is the Hamiltonian functional, depending on action-angle variables q and p, as well implicitly on the energy E and the quantum number $n \in \mathbb{N}$. Dirac later formulated the correspondence principle through what is now called canonical quantisation [16]:

$$\{A, B\} \to \frac{1}{i\hbar}[\hat{A}, \hat{B}]\,. \tag{I.14}$$

Poisson brackets in classical Hamiltonian formalism are replaced by commutators, with the Planck constant again making its appearance. The mathematical justification for this intuition, which at the same time justified the correspondence principle, is found in Ehrenfest's theorem [17]:

$$\frac{\mathrm{d}}{\mathrm{d}t}\langle A\rangle = \frac{1}{i\hbar}\langle[A, H]\rangle + \left\langle\frac{\partial A}{\partial t}\right\rangle\,, \tag{I.15}$$

that is, the expectation values follow a law that is structurally equivalent to Liouville's theorem in classical mechanics.

Therefore, we are presented with two possible avatars of the correspondence principle: either we consider larger and larger quantum numbers, or we consider the formal limit $\hbar \to 0$. In both cases, we should recover a theory that is semi-classical, *i.e.* which retains features of the quantum theory but is approximated better and better by classical physics.

Deviations from classical trajectories come then from the mismatch between the expectation value of the potential at a given point and the potential evaluated on the expectation value of $\hat{x}$, which only agree for quadratic potentials, which correspond to a theory free of interactions:

$$\langle V(x)\rangle^2 = \langle V(x)^2\rangle \Leftrightarrow V(x) \propto x^2\,. \tag{I.16}$$

Conversely, for a highly localised wavefunction, these two are approximately the same, a fact that will come in handy when considering semi-classical approximations. By pondering on this fact, we will also draw connections to some interesting phenomena that become easily calculable in the correspondence limit.

I.1.4 WKB, Instantons and Tunnelling

A particle rolling back and forth in a conservative potential $V(x)$, classically, can be found at position x with a probability $P(x)$ that is inversely proportional to its velocity $\dot{x}$ and its period T:

$$P(x) = \frac{2}{T\dot{x}} = \frac{1}{T}\frac{2m}{E - V(x)}\,, \tag{I.17}$$

which is then maximal (and indeed diverging) at points where the velocity of the particle vanishes. These points are called *turning points* and are equivalently characterised as those where the energy is purely potential and the kinetic energy is thus zero. This simple observation is the basis of the WKB (Wentzel-Kramers-Brillouin) method [18–20]: in the correspondence limit, this fact needs to be recovered, which forces the wavefunction to be highly peaked in the vicinity of the classical turning points. Beyond the turning points, there is no classical motion, but the wavefunction is defined all over the classical axis, for finite barriers. By analogy with the Beer-Lambert extinction law for classical waves, we can postulate that in the classically forbidden region the probability decays exponentially, with a parametric dependence such that in the $\hbar \to 0$ limit the classical result of zero probability is recovered

$$P_{\text{forbidden}}(x) \sim \mathrm{e}^{-S(x)/\hbar}\,, \tag{I.18}$$

where $S(x)$ has the dimensions of an action by dimensional analysis. On the other hand, the wavefunction on the allowed region is expected to be an oscillatory function, again by analogy with classical waves. We can then substitute the ansatz $\psi(x) = \exp(iS(x)/\hbar)$ into the Schrödinger equation, expand $S(x)$ in a power series around $\hbar = 0$ and retain only the lowest order, which gives us [21]

$$S(x) = \pm \int \mathrm{d}x\, \sqrt{2m(E - V(x))} + \mathcal{O}(\hbar)\,. \tag{I.19}$$

In the classically allowed region, the exponent is then imaginary, hence the wavefunction oscillates in space, as expected. In the classically forbidden region, both an exponentially growing and exponentially decaying solution are present, because the exponent is real, and we will have to discard the latter solution. It is also clear that the normalisation of ψ will be proportional to $1/\sqrt{E - V}$, so that at the turning points the wavefunction is ill-defined. We will see in Part III that this is only an artifact of the uncontrolled approximation we used. Nonetheless, for our current purposes, we only need the wavefunction away from the turning point, so we will not introduce additional complication.

The WKB wavefunction is particularly useful to grasp basic features of tunnelling. We will, for the remainder of this section, be concerned with the potential

$$V(x) = -x^2 + gx^4\,, \tag{I.20}$$

with g a positive constant, assumed to be small, $g \ll 1$. Classically, this potential has two minima, symmetric around $x = 0$. A naive perturbative approach would then conclude that there must be two energy levels with degenerate energy, but this would violate a basic theorem of ODE (ordinary differential equations) theory, that states that no such degeneracy can arise for smooth 1-dimensional potentials defined over the whole real axis [22]. We now follow Rubakov's book [23] to resolve this conundrum, in the process examining a deep connection between WKB and nontrivial classical trajectories.

Perturbation theory has to be performed around a nearly harmonic point, so we expand around one of the two degenerate minima $v_\pm$. The choice is at this point completely

arbitrary, except for the localisation of the wavefunction around either v_+ or v_-. These two states have the same energy to all orders in perturbation theory, because any energy difference can perturbatively be expressed in terms of the expectation of the potential $V(x)$ and powers of it, which all respect parity. However, one can build symmetric and antisymmetric wavefunctions by either summing or subtracting the wavefunction centered around the two minima. These linear combinations are, by linearity, also eigenfunctions of the Hamiltonian, and they are perturbatively degenerate because they are a linear combination of degenerate eigenfunctions.

Another clue to the solution of the puzzle comes from the fact that the symmetric wavefunction has no nodes, while the antisymmetric features one node, so they should be the ground state and the first excited state, respectively.

Indeed, we will now show that the perturbative wavefunctions, constructed around the two minima, are not eigenfunctions of the hamiltonian, and that the two functions we built out of them are not actually degenerate. To see this, consider the effect of tunnelling. The perturbative wavefunctions must be smooth deformations of the ground state of the harmonic oscillator, which is simply a Gaussian function. To zeroth order in perturbation theory the overlap between the perturbative ground states is then

$$\langle \psi_+ \,|\, \psi_- \rangle \approx \frac{1}{\sqrt{\pi}} \int_{-\infty}^{\infty} \mathrm{d}x \, \mathrm{e}^{-(x-v_-)^2/2} \mathrm{e}^{-(x-v_+)^2/2} = \mathrm{e}^{-1/(4g^2)} \,, \tag{I.21}$$

with $\psi_+ \, (\psi_-)$ the wavefunction defined around $v_+ (v_-)$. While exponentially small for small g, this is nonzero. This means that the wavefunctions defined around the harmonic vacuum do not form an orthonormal basis for the double well hamiltonian, with the overlap due to tunnelling. We can instead construct eigenstates of the Hamiltonian that are also eigenstates of the spatial parity operator P, since it commutes with the Hamiltonian. The wavefunctions confined around either of the two minima are not eigenstates of P, but they get transformed into one another by the action of P:

$$P\psi_\pm = \psi_\mp \,. \tag{I.22}$$

We can then define the symmetric and antisymmetric wavefunctions, as advertised before:

$$\psi_{S/A} = \frac{1}{\sqrt{2}} (\psi_+ \pm \psi_-) \,, \tag{I.23}$$

that are eigenstates of P and are actually orthogonal to one another. The normalisation we chose is actually nonperturbatively different from unity, due to the original wavefunctions being not orthogonal, but this will be no problem for us. We now estimate the energy splitting, following the so-called surface integral method developed independently by Holstein, Herring, and Smirnov [23–26]. The two wavefunctions in Eq. (I.23), should satisfy the stationary Schrödinger equation:[1]

$$\psi_S = 2(E_S - V)\psi_S \,, \tag{I.24}$$

$$\psi_A = 2(E_A - V)\psi_A \,. \tag{I.25}$$

By multiplying the first (second) equation by $\psi_A (\psi_S)$ and integrating over $\mathrm{d}x$ from 0 to ∞, the difference of the two equations gives us the energy splitting [23]:

$$E_A - E_S = \frac{1}{2\int_0^\infty \psi_A \psi_S \mathrm{d}x} \left(\psi_A' \psi_S - \psi_S' \psi_A \right)\big|_{x=0} \,. \tag{I.26}$$

[1] Of course, the symmetric and antisymmetric wavefunctions are no more eigenfunctions than the original harmonic eigenfunctions, but they at least explicitly respect parity and can be used to learn about the true ground state of the system.

The second term between parenthesis vanishes because the antisymmetric wavefunction has a node at zero, and the integral evaluates to 1/2 since $\psi_A(x) = \psi_S(-x)$ by definition. Then, one obtains

$$E_A - E_S = 2\psi_+(0)\frac{\mathrm{d}\psi_+(x)}{\mathrm{d}x}\bigg|_{x=0} . \tag{I.27}$$

The energy splitting is proportional to the wavefunction, as well as its derivative, evaluated at zero, that is deep inside the barrier. They can be evaluated using the WKB wavefunction we sketched before:

$$\psi_+(0) \sim \frac{\mathrm{d}\psi_+(x)}{\mathrm{d}x}\bigg|_{x=0} \sim \exp\left(-\int_0^{v_+}\sqrt{2V(x)}\mathrm{d}x\right) . \tag{I.28}$$

Finally, for the double well potential Eq. (I.20), one obtains

$$E_A - E_S \sim \mathrm{e}^{-1/(6g^2)} \equiv \mathrm{e}^{-S_I} , \tag{I.29}$$

where we defined the instanton action S_I. To recap, the energy splitting is determined, in the leading semiclassical approximation, by the instanton action. We now proceed to give another picture of tunnelling, which will explain the name "instanton action".

We are interested in finding a solution of the stationary Schrödinger equation with zero energy, given that we are interested in the ground state. As argued before, in the classically forbidden region, the wavefunction should be exponentially decreasing as a function of the distance from the classical minimum of the potential, v_+. If we input the ansatz

$$\psi(x) = A(x)\mathrm{e}^{-S(x)} , \tag{I.30}$$

the exponent has to satisfy

$$\frac{\mathrm{d}S}{\mathrm{d}x} = \sqrt{2V(x)} \tag{I.31}$$

with boundary condition $S(v_+) = 0$, which guarantees that the wavefunction is not exponentially small at the classical minimum. Equation (I.31) is exactly the Hamilton-Jacobi equation, with vanishing energy, for a system whose trajectory $x(\tau)$ starts at $x = v_+$ at time $\tau = -\infty$ and passes by x at a time τ. Assuming, as we need to do for perturbation theory, that the potential is quadratic near the minimum, the solutions to the Hamilton-Jacobi equation take the form [23]

$$S(\tau) = \int_{-\infty}^{\tau(x)} \frac{1}{2}\left(\frac{\mathrm{d}x}{\mathrm{d}\tau}\right)^2 + V(x)\,\mathrm{d}\tau . \tag{I.32}$$

The trajectories $x(\tau)$ that minimise this quantity are then classical solutions of the system. It should be noted, at this point, that the potential appearing in this and the preceding equation has *the wrong sign*, meaning we are studying trajectories in the flipped potential $-V(x)$. In particle physics language, we performed a Wick rotation, by sending $\tau \to i\tau$ in the path integral, and are thus studying the theory in Euclidean signature instead of Lorentzian signature. The splitting in Eq. (I.29) can easily be seen to refer then to a path that arrives at the second minimum v_- of the Lorentzian potential, which is a maximum of the Euclidean potential, at time $\tau = \infty$. For the double well, the trajectory can be calculated by straightforward application of the Euler-Lagrange equations:

$$x_I(\tau) = \frac{1}{2g}\tanh\left(-\frac{\sqrt{2}\tau + \tau_0}{4}\right) , \tag{I.33}$$

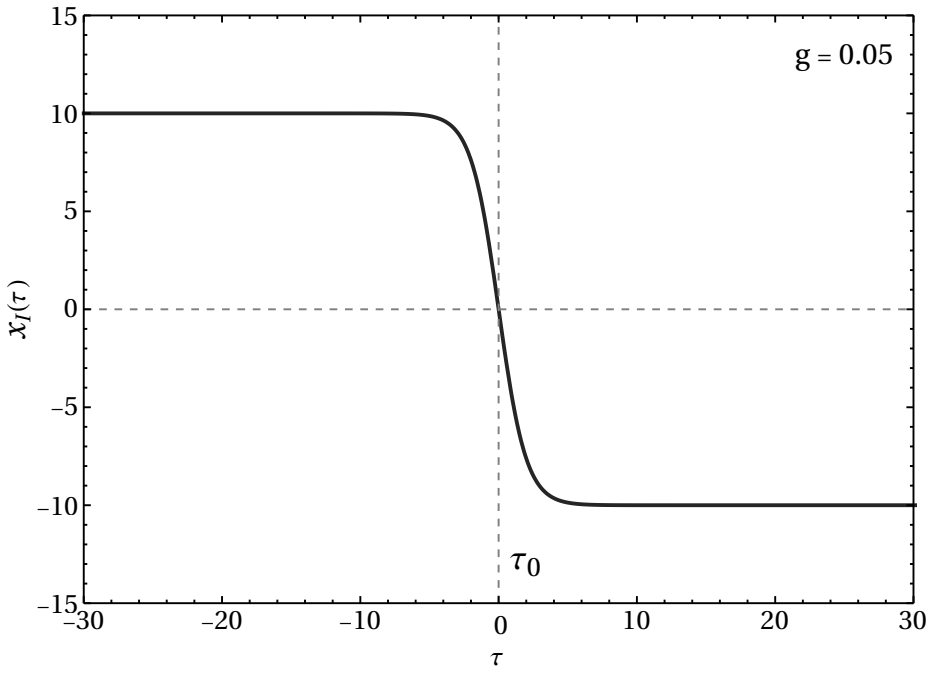

Figure I.1: Plot of the instanton trajectory in Eq. (I.33), for $g = 0.05$, $\tau_0 = 0$, interpolating from $x = v_+$ to $x = v_-$.

where the free parameter τ_0 cannot be fixed by imposing boundary conditions (that indeed have already been imposed). By looking at the graph of this function in Fig. I.1, we can explain the name "instanton": The trajectory is almost flat at all times except for the vicinity of the integration constant τ_0, so this configuration is non-trivial only for an *instant* in Euclidean time. To summarise, in this section we elucidated the connection between exponentially small energy splittings, tunnelling, and instantons, which are classical solutions of the Euclidean (*i.e.* flipped-sign) potential with minimal action. We should add, at this point, that this identification is well-established only at zero energy, that is in tunnelling out of the lowest level of the local minimum, but for excited states there are still big conceptual and technical issues, although promising steps forward have been made in the past few years, see *e.g.* [27–30] and references therein.

Something else has been left unanswered: why was perturbation theory unable to see the energy splitting? To answer this, we will have a detour in the theory on asymptotic series.

I.1.5 Asymptotic Series and Borel-Laplace Summation

We review Borel-Laplace summation with an explicit example, closely following the presentation in Ref. [31]. This will set the stage for our discussion of the shortcoming of perturbation theory and how to go past them to uncover quantum behaviour.

A partial series $\phi = \sum_{i=0}^{N} a_i x^i$ is said to be asymptotic to a function $f(x)$ if, for fixed

N and $x \ll 1$, its partial sum approximates f to polynomial accuracy,

$$|f(x) - \phi(x; N)| \sim \mathcal{O}\left(x^{N+1}\right) . \tag{I.34}$$

The first thing to note is that "being asymptotic to" is not a one-to-one relation, but one-to-many. Indeed, consider the function $\exp(-1/x)$, whose Taylor expansion at zero is trivial, given that for all terms, at each order n,

$$\frac{\mathrm{d}^n}{\mathrm{d}x^n} \mathrm{e}^{-1/x}\bigg|_{x=0} = 0 . \tag{I.35}$$

Hence, if ϕ is asymptotic to $f(x)$ around $x = 0$, then it is also asymptotic to $f(x) + \exp(-1/x)$, and indeed to an infinity of functions. This explains why the perturbation series of the energy levels in the anharmonic oscillator in the previous section was insensitive to the tunnelling contribution. The second thing to note is that the definition of an asymptotic series tells us nothing about the limit for fixed x, $N \to \infty$ which is used to assess convergence of ϕ to $f(x)$ along the whole range of x. Asymptotic series indeed can be divergent, and even display zero radius of convergence.[2] Nonetheless, an asymptotic divergent series is not devoid of information and together with a resummation procedure it can be used – in favourable cases – to reproduce the exact answer to the problem at hand.

Borel-Laplace summation is perhaps the simplest and best known resummation method. Given a formal series ϕ, we define its Borel-Laplace summation as the function $\hat{\phi} = \mathcal{L}\mathcal{B}\phi$. Here, we have defined the Borel transform $\mathcal{B}$,

$$\phi = \sum_{n=0}^{\infty} a_n z^n \to \mathcal{B}(\phi) = \sum_{n=0}^{\infty} \frac{a_n}{t^{n+1} n!} , \tag{I.36}$$

defining a map between series defined around zero ($z \ll 1$) and series defined around infinity ($t \gg 1$), or vice versa, and the Laplace transform $\mathcal{L}$,

$$\mathcal{L}\phi(z) = \int_0^{\infty} \mathrm{d}t\, \mathrm{e}^{-zt} \phi(t) . \tag{I.37}$$

As an example of this resummation procedure, consider the equation

$$\frac{\mathrm{d}\Phi}{\mathrm{d}z} = \Phi + \frac{1}{z} , \tag{I.38}$$

and plug a series ansatz $\Phi = \sum_{n=0}^{\infty} c_n z^{-1-n}$, $z \gg 1$, which easily leads to

$$c_n = -n c_{n-1} \Rightarrow c_n = (-1)^n n! . \tag{I.39}$$

The coefficients of the series Φ clearly exhibit factorial growth and hence the power series has zero radius of convergence, *i.e.* it only formally converges in the limit $z \to \infty$. The Borel transform of Φ is

$$\mathcal{B}\Phi = \sum_{n=0}^{\infty} (-1)^n t^n , \tag{I.40}$$

[2] In the remainder of this thesis, we will follow common usage and say, with a slight abuse of language, that a series is "asymptotic", without specifying what function it is asymptotic to, when we simply want to say that it does not converge while retaining apparent convergence for a possibly large number of terms.

which should be a convergent series for $t \ll 1$. Indeed, it is nothing other than the geometric series

$$\mathcal{B}(\Phi) = \frac{1}{1+t}\,, \tag{I.41}$$

and the pole at $t = -1$ is a consequence of the divergence of the original Euler series. The Laplace transform of the geometric series gives a particular solution of Eq. (I.38) with finite behavior at infinity,

$$\mathcal{L}(1+t)^{-1} = -\mathrm{e}^{z}\,\mathrm{Ei}(-z)\,, \tag{I.42}$$

where

$$\mathrm{Ei}(-z) = -\int_{z}^{\infty} \mathrm{d}t\,\frac{\mathrm{e}^{-t}}{t} \tag{I.43}$$

is the exponential integral function, defined for all positive z. We have thus turned a divergent power series into a function.

In this simple example, the basic motivation behind why Borel-Laplace resummation works is evident: namely, it relies on the interchange between summation and integration using the integral representation of the Gamma function:

$$\sum_{n=0}^{\infty} (-1)^n\, n!\, z^{-n-1} = \sum_{n}^{\infty} (-1)^n \left(\int_0^{\infty} \mathrm{d}t\, \mathrm{e}^{-t}\, t^n\right) z^{-n-1} \tag{I.44}$$

$$= \int_0^{\infty} \mathrm{d}t\, \mathrm{e}^{-t} \frac{1}{z(1+t/z)} = \int_0^{\infty} \mathrm{d}z\, \mathrm{e}^{-zt} \frac{1}{1+t}\,. \tag{I.45}$$

It is also easy to see when this procedure fails: If $\mathcal{B}(\phi)$ has poles along the real axis, the Laplace transform cannot be performed. For instance, consider taking the absolute value of each summand of the Euler series, $\tilde{\Phi} = \sum_n n!\, z^{-(n+1)}$. This formally solves the equation

$$\frac{\mathrm{d}\tilde{\Phi}}{\mathrm{d}z} = \tilde{\Phi} - \frac{1}{z}\,. \tag{I.46}$$

Its Borel-Laplace transformation is

$$\mathcal{L}\mathcal{B}\,\tilde{\Phi} = \int_0^{\infty} \mathrm{d}t\, \frac{\mathrm{e}^{-zt}}{1-t}\,, \tag{I.47}$$

which is not well-defined because the integrand has a pole at $t = 1$. However, we can consider slight deformations by ϵ on the positive or negative imaginary axis, defining

$$\mathcal{L}^{\pm\epsilon}\mathcal{B}\tilde{\Phi} \equiv \int_0^{\infty} \mathrm{d}t\, \frac{\mathrm{e}^{-zt}}{1-t\pm i\epsilon}\,. \tag{I.48}$$

Both of these integrals converge but not to the same value,

$$\mathcal{L}^{+\epsilon}\mathcal{B}\tilde{\Phi} - \mathcal{L}^{-\epsilon}\mathcal{B}\tilde{\Phi} = 2\pi i \mathrm{e}^{-z}\,. \tag{I.49}$$

Series that display such behavior are said to be non Borel-Laplace summable. It should be noted that the same difficulty would be reached while trying to analytically continue Eq. (I.42) to negative values of z: to reach $Re(z) < 0$, the singular ray on the negative imaginary axis needs to be crossed, leading to an ambiguity on how to reach negative real parts of z. This ambiguity, however, is present in the original problem: we have not fixed the boundary conditions, and as such the solution to Eq. (I.38) is a one-parameter family

$$\Phi = -\mathrm{e}^{z} Ei(-z) + C\,\mathrm{e}^{z}\,,\ C \in \mathbb{C}\,. \tag{I.50}$$

The difference between any two solutions, as it should, is simply a solution of the corresponding homogeneous differential equation. This is, in essence, one of the main observations of the theory of "resurgence" [32–34]: analytical continuation of the resummed perturbation series is capable of uncovering exponentially small contributions that are invisible to perturbation theory. In the case of the absolute value Euler series, ignorance of non-perturbative (*viz.* invisible to perturbation theory) contributions cause an ambiguity in the resummation procedure. For the original Euler series, on the other hand, we could have completely missed the non-perturbative contributions. Nonetheless, the two situations are two sides of the same coin.

Resurgence can do even more: the knowledge of large orders of perturbation theory informs us directly about the singularity in the Borel plane, and vice-versa. We can heuristically understand this phenomenon with simple complex analysis considerations [35]: Cauchy's coefficient formula lets us write the n-th coefficient of the power series of a function $f(z)$ as

$$a_n = \frac{1}{2i\pi}\int_\gamma f(z)\frac{\mathrm{d}z}{z^{n+1}}\,. \tag{I.51}$$

Consider then the case $f(z) = (1-z)^{-\alpha}$, $\alpha > 0$: this function has a power-law singularity at $z = 1$. We can then deform the integration contour γ to come within a distance $1/n$ of the singularity, and perform the change of variable $z \to 1 + t/n$:

$$a_n = \frac{n^{\alpha-1}}{2i\pi}\int_\gamma (-t)^\alpha (1+\frac{t}{n})^{-n-1}\mathrm{d}t\,. \tag{I.52}$$

As we are interested in large orders of perturbation theory, we can formally send $n \to \infty$ inside the integral and use the asymptotic form of the exponential to obtain

$$a_n = \frac{n^{\alpha-1}}{2i\pi}\int_\gamma \mathrm{d}t\,(-t)^\alpha e^{-t}\left(1+\mathcal{O}(\frac{1}{n})\right) = \frac{n^{\alpha-1}}{\Gamma(\alpha)}\left(1+\mathcal{O}(\frac{1}{n})\right)\,. \tag{I.53}$$

Thus, knowing the large order of perturbation theory gives us precise information about α, the degree of divergence of $f(z)$ around $z = 1$. Similar arguments can be used for other singularities such as square root, logarithm and so on, which would give different asymptotic forms for a_n, allowing to diagnose the type of singularity from perturbation theory only [21]. This type of argument is sometimes said to follow from the "Darboux principle" [21], although Darboux's method is strictly speaking a different way to extract the growth of coefficients from singularity analysis [35].

We can now study the connection between singularities and large orders in the context of Borel-Laplace resummation: the singularities of the Borel transform of a series determine its large-order terms, which in turn are related to the original power series by the definition of Borel transform itself. Since, as we have seen in the previous example, the singularities of the Borel transform encode non-perturbative information, this information was present, all along, in the large-order terms of perturbation theory. This clarifies our statement at the beginning of this section that a divergent power series is not devoid of information: indeed, its early terms are a good approximation of the perturbative sector of the theory, while the late terms decode the non-perturbative sector.

In the path integrals formulations of QM, we need to calculate integrals of the form

$$\int e^{f(t)/\alpha}\,\mathrm{d}t \tag{I.54}$$

with $|\alpha| \ll 1$. These integrals are usually approximated by the method of steepest descent: an expansion around the stationary points of $f(t)$, called saddle points f_s, is employed

to turn this integral into a Gaussian-times-power-series type, that is then solved order by order in α. In particular, in most cases only the dominant saddle point, *i.e.* that for which $\mathrm{Re}(f_s)$ is largest, is considered, and the change of variable $w = \sqrt{f_s - f}$ is performed to obtain

$$\int e^{-w^2/\alpha} \frac{\mathrm{d}t}{\mathrm{d}w} \, \mathrm{d}w \,, \tag{I.55}$$

and finally the Jacobian factor is expanded in powers of α. The exchange of integration and summation in this procedure makes the resulting power series an asymptotic function, as argued in the early days of QED (quantum electrodynamics) by Dyson [36] on the basis of analiticity, in an argument we reproduce in Section I.1.6. We can then hope to extract, from the expansion around one given saddle point, the effects of other saddle points, in particular those whose singularities are closest to the origin in the Borel plane. Given that a saddle point is a stationary point of $f(t)$, if the quantity of interest is a path integral the saddle points are actually classical solutions of the classical EOM (equations of motion), *i.e.* a solution of the Euler-Lagrange equation. These solutions can usually be understood in QFT as extended field configurations in time-space: one important class of solutions are instantons, that we already encountered in the last section. Indeed, tunnelling is a prime example of a non-analytical, exponentially small quantity in QM that qualitatively changes the behaviour of a system.

I.1.6 Divergence of Perturbation Theory and High Multiplicity

Let us review Dyson's argument [36]. Perturbation theory stipulates that observables can be calculated as power series in the coupling α, that is the power series

$$\mathcal{O} \equiv \sum_{k}^{\infty} c_n \alpha^k \tag{I.56}$$

converges to the exact value for $\alpha \ll 1$. But this means that $\mathcal{O}$ is an analytic function of α: from complex analysis we know this means that if we complexify α, the RHS (right-hand side) of Eq. (I.56) converges in a disk around $\alpha = 0$. Dyson considered the situation $\alpha < 0$, and constructed a physical argument against $\mathcal{O}$ being analytical for negative coupling. This, in turn, means that $\mathcal{O}$ cannot be analytical for positive coupling, either, and thus the power series cannot converge (to the right answer). The argument for the non-analyticity of the negative-coupling theory goes as follows: Like charges attract in the negative-coupling theory, hence we can imagine creating two large bodies made up of negative and positive charges only, respectively, by pair production from the vacuum. Pair production from the vacuum has an energy cost associated to it, but there is no cost associated to separating the e^+e^- pair an asymptotically infinite distance, as unlike charges repel in this theory. Now, any charge feels a large potential energy at asymptotic infinity because it is attracted by the body with large charge at infinity, and thus the energy cost in creating a pair out of the vacuum is overcome by the energy gain in bringing the charge from the origin to spatial infinity. This means that the perturbative "vacuum", *i.e.* the state with no particles, is energetically disfavoured with respect to the state with a huge number of particles organised like above. This is a runaway process, since pair production is now a favoured process. Note here that, at this point, we do not necessarily need to conclude that the theory with negative coupling is ill-defined; it suffices to conclude that the negative-coupling theory must at least have complicated, non-analytical dependence on α in its equation of motion to somehow make sense of the classical runaway vacuum. This completes the argument and suggests that the perturbation theory for QED can be at best asymptotic to the true answer.

We can also advance another argument for the lack of convergence of the perturbative series, which is less physically motivated but sets the stage for later considerations. Using again the double well potential, in the unbroken case $V(x) = x^2 + gx^4$, one can easily recognise that the deformation gx^4 can be larger than the harmonic contribution x^2 for $x > g^{-1/2}$. Given that the wavefunctions, and hence the energy levels, probe the whole real axis, perturbation theory should not converge exactly to the right answer, because there exists a regime where the assumption of perturbativity breaks down. In the book by Boyd on asymptotics [21], this example is used to advance the "principle of non-uniform smallness" for diagnosing asymptotic behaviour. This could also be put into contact with a perhaps more familiar heuristic for the breakdown of perturbative methods: the presence of many scales. Indeed, non-uniform smallness implies that there is an extra scale in the problem (in our example $g^{-1/2}$) that we did not explicitly take into account when formulating the perturbative series. Beyond $x = g^{-1/2}$, a better approximation would be to consider the harmonic contribution to be a deformation of $V(x) = gx^4$, and derive the wavefunction in that region following this approximation. By how much can we expect the answer to be changed by following such a procedure? The large x region is in the classically forbidden region, while the quasi-harmonic region coincides with the allowed region. Thus:

$$\frac{\psi_0(x \gg g^{-1/2})}{\psi_0(x=0)} \lesssim \frac{\mathrm{e}^{-x^2}}{x^2}\,, \tag{I.57}$$

So we can conclude that by approximating the wavefunction in this region by a deformed Gaussian, instead of the eigenfunctions of $V(x) = x^4$, we make at worst an exponentially small error. What about excited states? For the low-lying ones, the same story goes: so long as the turning points are before the large x region, we are fine. For multiply excited states, however, the large x region is partly in the allowed region, hence the modifications to the wavefunction can be large. In this case, the effect of perturbation theory being only asymptotic are expected to be relevant not only at asymptotically large orders in the perturbative series, but starting from the first few terms already. This is intuitive: as we raise the energy, the harmonic part of the potential is not what is relevant any more, because the particle is mostly localised around the turning points, where the largest effect comes from the deformation. By comparison of the turning point and the energy, one can estimate that for $n \gtrsim 1/g$, n being the label of the energy eigenstate, the perturbative series will stop being a good approximation for the wavefunction. We will now make this statement more precise, while introducing one of the puzzles that prompted the work in Part III.

Consider the transition amplitude from the n-th energy level to the ground state, induced by the position operator, $\langle n|\, x\, |0\rangle$. For large n, WKB can be used to argue for an exponential form of this transition amplitude (see *e.g.* [37]):

$$\langle n|\, x\, |0\rangle = \exp\left(\frac{F(n)}{g} + F_1(n) + \dots\right) \tag{I.58}$$

thus the process is exponential suppressed for $F(n) < 0$. In a Feynman diagram picture[3], we can split the contribution arising from tree-level diagrams from the rest. Given the usual expectation, from the correspondence principle that highly excited states are increasingly classical, the tree level answer is naively what contributes most in this scenario. The

[3]While obviously associated with the calculation of matrix elements in QFT, the Feynman diagram technique is nothing else than a useful pictorial representation of the perturbative expansion of path integrals near a critical point.

properly normalised tree-level amplitude has been calculated [38–40] to be

$$\langle n \,|\, x \,|\, 0 \rangle = \sqrt{\frac{n!}{2}} \left(\frac{g}{8}\right)^{\frac{n-1}{2}} (1 + \mathcal{O}(g)) \,. \tag{I.59}$$

It is easy to see that the power suppression gets overtaken at large n by the factorial growth due to combinatorics. This implies a loss of unitarity: by insertion of a partition of unity we can easily see that

$$\langle 0 | \, x^2 \, | 0 \rangle = \sum_{n=0}^{\infty} |\langle 0 | \, x \, | n \rangle|^2 \,; \tag{I.60}$$

if we now insert Eq. (I.59) the sum on the RHS diverges by the ratio test, while the LHS (left-hand side) clearly has to be finite. The only possibility is that the tree-level computation is not, in fact, dominant in the large n regime. This is surprising, because it means that quantum effects take over in a semiclassical regime. However, we recognise this as a fault of perturbation theory, and it is in fact related to the large-order divergence of perturbation theory. Indeed, Eq. (I.60) can be thought of as a perturbative expansion of the LHS, which we have already argued must be divergent in perturbation theory. From a Feynman diagram point of view, if the large-order (*i.e.* many loops) diagrams diverge factorially, then by the optical theorem so does the diagram where we cut through all the loops and set the legs on-shell. Thus, the two divergences are strictly related.

The resummation of all orders in g has been performed in [40], where a remarkable exponentiation was shown to take place, confirming semiclassical intuition. In the limit $n \to \infty$, $g \to 0$, with the 't Hooft-like [41] parameter $\lambda = ng$ kept constant, Ref. [40] finds:

$$F(\lambda) < 0 \; \forall \; \lambda \,. \tag{I.61}$$

The resummation thus prevented unitarity from being violated in the limit, or even saturated, because the process is suppressed for all values of λ. In contrast, for the tree-level result there is a critical value λ_c past which the exponential suppression is replaced by an enhancement.

That is, even for arbitrarily small coupling g, there is always an n where tree-level perturbation theory breaks down. To have any chance of recovering a sensible result, one then needs to consider and resum loop effects. As we will see in Part III, this hints to a curious correspondence between large-multiplicity amplitude and tunnelling effects in the double well.

We now conclude the QM section with a discussion of the importance of tunnelling in the macroscopic limit.

I.1.7 Macroscopic Quantum Mechanics

Anthony Leggett asked: "What experimental evidence do we have that quantum mechanics is valid at the macroscopic level?" in a seminal paper in 1980 [42]. He excluded often-cited examples of macroscopic quantum behaviour such as Debye's prediction of the specific heat of a solid [43], superfluidity (see [44] for a historical account) and superconductivity [45,46], and even the Aharonov-Bohm effect [47], on the basis that they "only" show that the dynamics of microscopic objects can sometimes conspire to give macroscopic effect by behaving roughly the same way as they would in isolation. The kind of question that Leggett was interested in answering, instead, is related to the reason why Schrödinger's

cat thought-experiments seems to us to be so paradoxical: How confidently can we say that a macroscopic object's state can be described by the linear superposition of two other macroscopic objects'? Without assuming (or, indeed, experimentally proving) that this should be the case, Schrödinger's thought experiment is void, because then the cat would not need to be in a linear superposition after all.

Towards the end of the paper, Leggett makes the proposal to test this assumption by the observation of quantum tunnelling of macroscopic objects. This choice is motivated by the following argument. The crucial QM feature that we would like to detect is coherence, *i.e.* the measurement of the relative phase of the wavefunction of the two macroscopic systems; but in a realistic experimental setup this requires that the two objects are not disturbed by the environment for a long time. In contrast, tunnelling has much less stringent requirements to be observed, while stemming from the same quantum mechanism. To illustrate this, consider a double well, that is a 1-dimensional potential $V(x)$ with two minima. First, we can consider the case where the minima are not degenerate. If one prepares the system in the higher of the two minima (the "false vacuum"), the system will eventually evolve towards the lower minimum (the "true vacuum") by tunnelling. WKB lets us express the tunnelling frequency Γ as

$$\Gamma \propto \exp\left(-\int \sqrt{2mV(x)}\,\mathrm{d}x\right), \tag{I.62}$$

which implies that we can describe the time evolution of the system by the linear superposition of the states localised in the two minima:

$$|\psi(t)\rangle = \exp\left(-\Gamma t\right)|\psi_{\text{false}}\rangle + \left(1-\exp(-\Gamma t)\right)|\psi_{\text{true}}\rangle\ . \tag{I.63}$$

However, for all practical purposes, the interference between the two states can be neglected, and the system treated as a classical superposition [48]. In contrast, as we reviewed in Section I.1.4, if the two minima are classically degenerate, to get the energy splitting due to tunnelling it is crucial to represent the state as a superposition and not just a classical admixture. This is then a coherent effect, of the kind Leggett wanted to test. Importantly, while coherence is needed to correctly describe the tunnelling between degenerate minima, the timescales involved for the two phenomena are widely separated. The quantum Zeno effect (see Section I.1.2) may be invoked to destroy coherence if the interaction with the environment is strong with respect to Γ. On the other hand, tunnelling semiclassically occurs on a timescale of the bounce time

$$\tau_B \equiv \int \frac{\mathrm{d}x}{\sqrt{2V(x)}}\,, \tag{I.64}$$

which is much smaller than $1/\Gamma$. Pictorially, Leggett explains this as the particle trying a large number of times to take the instanton trajectory to go to the other minimum, but only succeeding after a time $1/\Gamma$ [42]. However, a single try only takes a time τ_B, such that the quantum Zeno effect is only effective if the interaction with the environment is strong with respect to $1/\tau_B \gg \Gamma$. That is, tunnelling is a relatively stable quantum effect, that survives also in a properly defined macroscopic limit.

In the third part of this thesis, we will explore tunnelling in the anharmonic oscillator using the resurgent tools of exact WKB, and uncover an interesting link between large-multiplicity amplitudes and tunnelling in the correspondence limit. In this sense, we will explore similar questions to those raised by Leggett in 1980, by showing the importance of tunnelling in the classical limit.

We now proceed by introducing concepts from QFT that will be important for the main parts of this thesis.

I.2 Quantum Field Theory

Quantum field theory is nothing else than the consistent extension of QM to relativistic velocities. As such, it respects all the tenets of QM, and has all the quantum "weirdness" as well. Nonetheless, the interest in scattering experiments has brought particle theory to be, if not conceptually, at least in practice quite far from QM.[4] In the process, many defining features of QM took a back seat. Indeed, we rarely need to discuss tunnelling, with virtually the sole exceptions being the theta vacuum of QCD (quantum chromodynamics) [50,51] and the study of phase transitions [52–54], both of which influence collider physics only tangentially. Similarly, entanglement is not discussed at all in an introductory course on QFT. More generally, it is not often that we speak of quantum phenomena that are *qualitatively* different from their classical field theory analogue: of course, any loop calculation is the calculation of a quantum effect, but the result is just a quantitative shift from the classical result, which by definition of perturbation theory needs to be small. In this thesis we would like to consider a different kind of quantum effect, namely those that have a large, and possibly qualitative, effect on the end results. Having framed the question like this, it is quite obvious that answering it will not only bring us advancements in the theoretical side of particle physics, but also on its phenomenology.

I.2.1 The Standard Model

The SM (Standard Model) of particle physics is a gauge theory with underlying Lie algebra $\mathfrak{su}(3)_C \otimes \mathfrak{su}(2)_L \otimes \mathfrak{u}(1)_Y$, whose adjoint representations furnish the 8 gluons $g_a\,,\ a = 1 \dots 8$, and 4 electroweak bosons $W^{\pm}, Z, \gamma$, the spin 1 bosons that are the force carriers for all known forces except gravity. In addition to the force carriers, the SM also contains three generations of quarks, spin 1/2 fermions charged under all of the gauge groups, and three generations of leptons, which are doublet of $SU(L)$ and uncharged under the colour group $SU(3)_C$. A generation is only differentiated from another because of the mass of its components, with all other quantum numbers remaining the same between generations. With the addition of the higgs boson, that unitarises the theory [55] and was historically theorised to explain the masses of the electroweak bosons [56, 57], the SM comprises all the known elementary particles known so far, and it is arguably one of the best-tested theories in all of science, along with general relativity.

However, the SM is not without shortcomings. For starters, as implied before, the framework of quantum field theory has not to date been convincingly demonstrated to be compatible with the description of general relativity. A naive power counting suggest that the theory should break down at around $M_{Pl} \approx 10^{19}$ GeV, which is the mass of a particle whose Compton wavelength and Schwarzschild radius are of the same order of magnitude, begging for a unified description of gravity and quantum forces. If one does not see the need of unification, at even higher energies the apparent triviality of both $U(1)$ and ϕ^4 theory [58], describing the hypercharge and higgs sector of the SM respectively, also call out for an explanation and preclude us from thinking the SM can be a valid theory up to arbitrarily high energy. This is actually a good thing because, while an extremely successful description of particle physics, the SM is arguably an "ugly" – meaning *ad hoc* – theory, with many adjustable parameters (around 25, depending on the definition of what is the precise particle and global symmetry content of the SM [59]) that are organised in a hierarchical way. On a less aesthetic note, there are also experimental concerns: particle

[4] The interested reader can find in ref. [49] a historical account of how the shift from the calculation of spectral properties to that of scattering morphed from the quantum theory of Schrödinger and Heisenberg to what is now familiar to the practicing particle physicist.

physics is able to describe the physics of the extremely large, *i.e.* cosmology, in the form of the ΛCDM model, only if a cosmological constant Λ and cold DM (dark matter) are postulated to exist [60]. Neither of these can be found in the particle content of the SM. If QFT is to describe Nature as a whole, then a particle nature for these two entities is highly desirable, and indeed it is currently the hypothesis under which most searches for DM operate. There is, finally, the questions of experimental anomalies, that is experimental results that are, at face value, in disagreement with the theoretical predictions of the SM. Suffice to say that, so far, none of them have passed the extremely stringent requirements that particle physicists impose to claim a discovery, but as the recent review paper [61] stresses, they span many orders of magnitude in energy and a plethora of experimental techniques. If a coherent picture of these anomalies were to be accepted in the future, particle physics would enter a new era.

All in all, for a host of different reasons, a large portion of particle physicists today is actively thinking about ways to extend the SM, trying to fix one or another problem that afflicts it. The mathematical structure of QFT permits an uncountably infinite number of possible models (consider *e.g.* adding one $U(1)$ for each possible real value of the unit charge e), and at present there is no way to forbid any of them on purely theoretical grounds, so a survey of all possible models is obviously impossible. A survey of the finite set of popular models, while in principle possible, is beyond the scope of this thesis.

While studying a specific model has its merits, in many cases much can be done without referring to specific models, with the benefit of being able to make sweeping assessments on entire classes of models in one go. This will, of course, come at the price of introducing a modicum of theoretical bias. In the next subsection, then, we will deal with effective field theories.

I.2.2 The Standard Model as an Effective Field Theory

A key feature of QFT is the ability to make precise a basic idea of Science: that one can perform useful calculations and measurements without needing to know the theory of everything, so long as one is okay with measuring "fundamental" constants of the system at hand. An often-repeated analogy involves civil engineering [62]: one does not need to know QM to build a bridge, as long as the (macroscopic) properties of steel, for instance, can be measured prior to drawing the blueprint for the bridge, and a theory of macroscopic elasticity has been formulated. Indeed, let alone QM, one does not even need to know anything about what steel is made from in the first place. This almost self-evident statement belies a deep truth: one can make progress in physics without needing to formulate a fundamental theory. Two assumptions are however needed for this reasoning to make sense: the underlying fundamental theory needs to be local, such that its macroscopic description can be thought of as being factorised into a microscopic unknown part, and a macroscopic part. Ignorance of the microscopic part can then be hidden in the macroscopic part, which can be directly measured. Just like measuring the properties of steel allows one to design a bridge, a finite number of measurements should then suffice to fix ignorance of the microscopic theory, and then allow useful predictions about phenomena different from those used to fix the parameters of the macroscopic theory. The other assumption is that the microscopic dynamics is happening at a scale too small to resolve, *i.e.* that a separation of scales exists; Coming back to the bridge example, if we want to know how the bridge reacts to being bombarded by α particles, a macroscopic theory of elasticity will not do us any good.

In QFT, the intuitions outlined in the previous paragraph are formalised thanks to

two ideas: the Wilsonian idea of renormalisation as coarse-graining, and the Appelquist-Carrazzone decoupling theorem. The first can be understood as follows: one starts from a microscopical theory, valid at a high scale Λ, which we will say is "in the UV (ultraviolet)", and applies a coarse-graining operation, meaning one takes the average in a momentum shell going from Λ to $\Lambda - dk$. By repeatedly applying this operation one can reach the low scale μ where one wishes to perform experiments: the averaged theory now has information about the full theory, but encoded differently [63]. This coarse-graining process is exactly what one does when describing steel, which we know is made up of individual particles and, from a classical perspective, mostly of empty space, as a continuous material. At the low scale, only some of the degrees of freedom of the high-scale theory re-organise in a way that is more suitable for a low-scale description. It should be noted that the view we just outlined of how an EFT (effective field theory) arises from a fundamental theory is considered by some EFT practitioners to be "old-fashioned" [62], since many currently used EFTs do not arise from a coarse-graining process. This includes, for instance, the theory to treat soft and collinear radiation (SCET) [64–66], and other theories whose main aim is to re-sum large logarithms in the renormalisation group evolution. Nonetheless, many EFTs can still be thought to arise from a purely Wilsonian process, and the Wilsonian framework is a useful tool to understand how low-energy physics "forgets" the detail of the high-energy theory. The EFT we will use in this thesis is one that is purely Wilsonian in nature, just as Fermi theory for beta decay [67], and heavy-quark effective theory [68], for instance.

Having understood the mechanism that allows one to deal with the appropriate degrees of freedom at a given energy, we now introduce another key piece in the conceptualisation of an EFT. The Appelquist-Carrazzone theorem [69] deals with a field theory of massless gauge fields A_μ coupled to massive fermions Ψ of mass m, and it is a statement about 1PI Feynman graphs. Generalisations to other theories are relatively straightforward, even though counter-examples can arise if the generalisation is not carefully constructed [62]. The statement of the Appelquist-Carrazzone theorem is that any 1PI Feynman graph with external gauge bosons, but with only fermions in the internal lines, is suppressed by powers of m with respects to graphs that do not feature internal fermions, so long as the external momenta squared are small relative to m^2. The last requirement is needed because if the fermions are allowed to go on shell, they would considerably modify the structure of the amplitude. Instead, the restriction to low momenta allows us to state the second part of the theorem: the only other possibility other than the $1/m$ suppressed interactions is coupling constant and field strength renormalisation. Given that we work at low momenta, the fermions with large mass m cannot be excited, so the low-energy experiments are blind to them. We can then express, at lower momenta, the theory just in terms of the degrees of freedom with low mass, and then parametrise the effect of higher-mass particles by considering the coupling constants of the low-energy fields to be free parameter, as well as introducing operators that are suppressed by powers of $1/m$. Building an EFT, then, is reduced to the task of choosing the relevant fields and symmetries, then building all the operators consistent with said symmetries out of those fields. The operators in the EFT Lagrangian are constructed as polynomials in the fields, as well as their covariant derivatives that are invariants under the desired gauge and global symmetries, as well as space-time symmetries.

The problem of constructing the EFT Lagrangian at a given order seems then to be a simple combinatorics problem, but there are two complications: integration by part and field redefinitions. Indeed, we know that total derivatives do not contribute to S-matrix elements in perturbation theory, so two operators that differ only by a total derivative

give the same contribution to the S-matrix, and in that sense adding them both to the Lagrangian is redundant. Then, to construct a non-redundant basis at a given order one needs to make sure that no operators in the basis can be related to one another by integration by parts. Moreover, field redefinitions also do not alter the S-matrix, as a consequence of the reparametrisation invariance of the path integral, while they can obviously alter the form of the Lagrangian, so they need to be accounted for in the same way as total derivatives.[5] The lack of clear signals of physics beyond the SM prompted the construction of an EFT using SM fields only, the idea being that the lack of discoveries is a consequence of the new states living at a scale much higher than the higgs vev (vacuum expectation value) $\Lambda \gg v \approx 250$ GeV. Moreover, the experimental discovery of a scalar particle compatible with the higgs boson of the SM is taken up to mean that the mass generation mechanism is indeed the Brout-Englert-Higgs mechanism for $SU(2) \times U(1) \to U(1)$. This EFT is the so-called SMEFT (Standard Model EFT) We point out that this is not the only assumption consistent with current data, and indeed a low-energy EFT that does not assume the SM symmetry breaking has been constructed, the so-called HEFT (higgs EFT). The difference in assumptions that go in the HEFT and SMEFT provide different outcomes that are experimentally testable [71–73], due to the different realisation of the electroweak vacuum. In any case, we will proceed talking about the SMEFT only.

The Appelquist-Carrazzone theorem guarantees that at low energy we can parametrise NP effects with a tower of higher-dimensional operators, suppressed by powers of $1/\Lambda$. Explicitly:

$$\mathcal{L}_{\text{SMEFT}} = \mathcal{L}_{\text{SM}} + \sum_{i=5}^{\infty} \frac{1}{\Lambda^{i-4}} \mathcal{L}^{(i)} \,, \tag{I.65}$$

$$\mathcal{L}^{(i)} = \sum_{k=1}^{N_i} c_k \mathcal{O}_k^{(i)} \,, \tag{I.66}$$

where $\mathcal{L}_{SM}$ is the SM Lagrangian, containing all operators of dimension 4 or lower consistent with the SM gauge symmetries as well as Lorentz symmetry, and $\mathcal{L}^{(i)}$ is a sum of the N_i non-redundant dimension i operators made up of SM fields and their derivatives. At each order in mass dimension, the SMEFT Lagrangian respects the SM gauge symmetries and Lorentz invariance. Since $\mathcal{L}^{(i)}$ has mass dimension i, we extracted a dimensionful parameter Λ^{4-i} in front of it, consistently with the Appelquist-Carrazzone theorem. The dimensionless parameters c_k that appear in front of the operators are called "Wilson coefficients". They are in principle calculable in a given UV model, but from the EFT perspective they are simply free parameters to be measured (or constrained). Of course, only the ratio between the Wilson coefficient and the cutoff scale Λ to the appropriate power affects the S-matrix, and such an ambiguity can only be resolved by committing to a given UV theory.

At dimension 5, exactly two operators consistent with the SM gauge symmetries exist, and they generate Majorana masses for left-handed neutrinos. As such, they violate an accidental symmetry of the SM, namely lepton number L, and it is consistent with naturalness that they are suppressed by a scale $\Lambda_{\not L}$ that is much higher than the scale Λ at which new operators consistent with the global symmetries of the SM arise. Increasing the dimensionality, the number of operators in $\mathcal{L}^{(i)}$ grows quickly, even after imposing baryon

[5] It is sometimes stated that the relevant field transformations are the classical EOM (equations of motion), but this statement is misleading and coincides only in special cases with the more general statement that we formulate above [70].

and lepton number conservation, as can be proven using Hilbert series techniques [74]. The basis of non-redundant operators at dimension 6, first derived in [75] is commonly known as the "Warsaw basis".

In Part I, we will employ the SMEFT to study the sensitivity of measures of quantum correlation to NP. We now describe a usual approximation for unstable states, and its possible shortcoming.

I.2.3 The Narrow Width Approximation

An easily forgotten fact of QFT is that only stable particles can be incoming or outgoing states of a scattering process, because the LSZ (Lehmann-Symanzik-Zimmermann) [76] formalism that is at the basis of S-matrix calculations requires the limit of infinite separation between the states, and an unstable particle has, by definition, to decay at some point. Even more neglected is the fact, derived by Veltman [77], that cutting rules can only be consistently formulated if the lines of unstable particles are never cut through, essentially because of the same reason: The cutting rules involve setting the cut propagator on shell, and then applying the LSZ rules. Instead, unstable particles are only to be treated as internal lines. Nonetheless, for long lifetime, an unstable particle should be amenable to being treated as quasi-stable. This intuition is behind the NWA (narrow-width approximation) [78], which deals with the factorisation of a process $AB \to V \to CD$, with V an unstable resonance exchanged in the s-channel, into production and decay. The matrix element of this process can be written by resummation of the so-called Dyson series (see *e.g.* [79] for a recent account), where the tree-level propagator of V is modified by adding insertions of the renormalised, all-order, 1PI (1-particle irreducible) self energy $\Sigma(s)$:

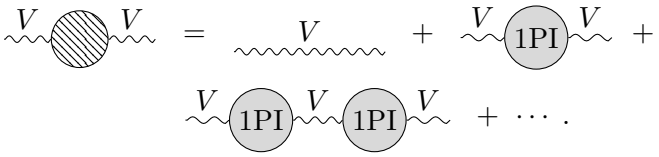

(I.67)

The resulting propagator, resummed with the help of the geometric series, is then used to write the matrix element as:

$$\mathcal{M}_{AB\to CD} = \frac{f(s)}{p^2 - m^2_{V,\,\text{tree}} + \Sigma(s)} = \frac{f(s)}{p^2 - m_V^2 + i\Gamma_V m_V}\,, \tag{I.68}$$

where we split the renormalised self-energy into its real part $m_V^2 - m^2_{V,\,\text{tree}}$ and its imaginary part $\Gamma_V m_V$, and defined the width as usual making use of the optical theorem in the one-loop approximation [79],

$$\Gamma_V = \frac{\text{Im}(\Sigma(m_V^2))}{m_V}\,. \tag{I.69}$$

The instability of the particle, which necessarily induces a width, also prevents the of tree-level s-channel scattering from being divergent at $s = m^2_{V,\,\text{tree}}$: the pole of the S-matrix element is now shifted into the complex plane, and by working with real squared momenta only the singularity is never encountered. If we also assume that $f(s)$ is only significantly different from zero in the region $s \in [(m_V - \Gamma_V)^2, (m_V + \Gamma_V)^2]$, as well as slowly varying in this region, we encounter a tremendous simplification when calculating the total cross-section:

$$\sigma_{AB\to CD} \approx \sigma_{AB\to V}\Gamma_{V\to CD} \int_{(m_V-\Gamma_V)^2}^{(m_V+\Gamma_V)^2} \frac{\mathrm{d}s}{2\pi} \frac{2m_V}{|s - m_V + im_V\Gamma_V|}\,, \tag{I.70}$$

where the assumptions on $f(s)$ let us separate the production process, encoded in the cross-section $AB \to V$, from the decay, encoded in the partial width $\Gamma_{V\to CD}$ which is calculated from the imaginary part of the contribution from the final state CD in the self-energy of V. The integral can then be further simplified by making use of the known limit, in the sense of distributions, of the Breit-Wigner function:

$$\frac{1}{\left|s - m_V^2 + i m_V \Gamma_V\right|^2} \overset{\Gamma_V \to 0}{\to} \frac{\pi}{m_V \Gamma_V} \delta(s - m_V^2)\,, \tag{I.71}$$

which implies

$$\sigma_{AB\to CD} = \sigma_{AB\to V} \frac{\Gamma_{V\to CD}}{\Gamma_V} + \mathcal{O}(\frac{\Gamma_V}{m_V})\,, \tag{I.72}$$

the ratio on the RHS being the definition of the branching ratio of V into CD. Thus, the assumption of narrow width, together with the additional assumptions on $f(s)$, have allowed to completely factorise the production of the unstable particle from its decay. Failure to comply with the aforementioned assumptions can cause the Γ_V/m_V estimate of the corrections to fail, see for instance [80–82] and references therein. Physically, the assumption on $f(s)$ can be interpreted as the absence of thresholds or other resonances in the region of interest $[(m_V - \Gamma_V)^2, (m_V + \Gamma_V)^2]$, which would cause $f(s)$ to vary abruptly, as well as neglecting the interference with nonresonant contributions, which can make $f(s)$ differ significantly from zero outside the region of integration considered in the NWA. We will consider a failure of the former assumption in Part II of this thesis.

I.2.4 High Multiplicity and the Electroweak Vacuum

As reviewed in Section I.1.6, high multiplicity amplitudes cause a breakdown of perturbation theory, since naive perturbation theory is not simply an expansion in small coupling but also simultaneously in small wave amplitude. This concept carries over to QFT; unlike in QM, explicit analytical control is much harder to attain, which made the issue controversial. In this subsection, we review the parts relevant to this thesis. We do not plan to be exhaustive, but we want to underline the areas of current research that prompted the work reported in Part III. The existence of an Adler-Bell-Jackiw anomaly [83, 84] in the electroweak sector prevents the quantum number $B + L$ to be conserved at the quantum level, even though both baryon number B and lepton number L are good global symmetries in the SM [85, 86]. As such, different vacua arise, labeled by the value of $B + L$. Manton and Taubes showed in the 1980s [86, 87] that there exists a barrier between the vacua, and a semiclassical field configuration can be responsible for the interpolation between different vacua. These field configurations are named sphalerons, and they have an associated mass equal to the height of the barrier that divides the vacua, which has been calculated to be around 9 TeV in the SM [88]. For energies much lower than the barrier height, a suppression due to tunnelling of the order $\exp\left(-(4\pi/g_W)^2\right) \approx 10^{-163}$, with $g_W \approx 0.65$ the weak coupling constant, is expected [88], rendering the process unobservable. If the energy of a process is high enough to excite the sphaleron, then the transition rate is unsuppressed, in analogy with above-the-barrier transmittance in QM. But to be able to excite a macroscopic field excitation, one needs to first excite a number $\sim 1/\alpha_W$ of electroweak bosons [37], a process which requires to go to such a high order in perturbation theory to reintroduce an effectively exponential loop suppression. However, this lore was questioned in 1990 by various authors [89–92], on the basis of the arguments we put forward in Section I.1.5: at high orders in perturbation theory a factorial growth in the number of diagrams allows one to overcome any suppression factor, and thus in the

multi-TeV regime unsuppressed $B + L$ violation can occur. More recently, unsuppressed sphaleron production at colliders has been argued in ref. [93–95] by analogy with Bloch waves in crystals, starting another discussion [96]. It should be mentioned that sphalerons have a special role in cosmology, as the $B + L$ violation allows converting L violation into B violation [97], thus satisfying one of Sakharov conditions for baryogenesis [98], that is the generation of a baryon-antibaryon asymmetry from a symmetric starting condition. The situation in cosmology is however different because the thermal plasma can supply the required energy to jump over the barrier and excite the sphaleron, and the multiplicity suppression is also taken care of by particles in the thermal bath [97].

More generally the possibility of enhanced amplitudes at high multiplicity is one that is of interest in and of itself, because it might signal the existence of new phenomena in one of the easiest QFTs, ϕ^4 theory [38, 39, 92, 99–108]. Large multiplicity is also of interest when performing large charge expansion in CFTs (conformal field theories) [109]. In a different context, large charge is important for so-called classicalisation of a QFT [110, 111], that allows for instance to make statements about black holes in the context of QFT, as well as a possible resolution to UV-complete nonrenormalisable theories [112].

In Part III of this thesis, we re-examine large-multiplicity amplitudes in QM, uncovering an unexpected link with the structure of the vacuum. We speculate on how this can bring advancements in the context of large multiplicity in QFT in Chapter V.

We will now move to the main parts of the thesis, starting with a study of the usefulness of Bell tests for uncovering NP at colliders.

Part I

Entanglement at Collider Experiments

CHAPTER II

Entanglement at Collider Experiments

II.1 Introduction

The search for deviations from the SM has entered an era of precision tests. NP whose characteristic scale Λ is well-separated from the EW (electroweak) scale v can be described with the tools of EFT to a largely model-independent extent. As we described in Section I.2.2, the SMEFT [113, 114] is one such EFT, which encodes the effect of heavy NP in a tower of operators, organised according to the number of derivatives and fields. In most cases, NDA (naive dimensional analysis) can be used to argue that the leading deviation from the SM prediction for a given observable is due to operators with canonical mass dimension 6. In particular, the leading deviation from the SM in observables is expected to arise at order $1/\Lambda^2$, corresponding to the interference between the SM matrix at dimension-6. However, (approximate) symmetries and selection rules can cause this expectation to fail [115–117]. In such cases, operators with higher mass dimension, loop corrections and multiple insertions of dimension 6 operators can have parametrically larger contributions than the interference. In Ref. [117], it was shown that a selection rule arises whenever the SM and SMEFT contribute to mutually exclusive helicity amplitudes; in the high-energy limit, the chiral nature of the SM forces certain helicity amplitudes to vanish, so selection rules that are only lifted by finite masses emerge.

In cases where noninterference happens, the sensitivity that a given observable has to NP effects is lowered by additional inverse powers of the large scale Λ. Noninterference can be circumvented by looking at different observables or different final states, in a process dubbed "interference resurrection". For instance, if the final states are allowed to decay, the full process does not need to respect the helicity selection rule, and the interference is resurrected. One phenomenologically relevant case that has received much attention is triple gauge coupling, both for triple-W [118–120] and triple-gluon [121] case.

In this section, we consider resurrection in 4-fermion scattering, which is relevant for searches at both lepton and hadron collider experiments.

We show, through a quantum mechanical example, that the measurement of the spin correlations of final-state leptons in the process $f\bar{f} \to \ell\bar{\ell}$ can resurrect the interference of operators that generate electric and magnetic dipole moments, elucidating at the same time why the same procedure fails with other noninterfering operators. We therefore focus on the anomalous dipole moment of the τ, $g_\tau - 2$. Unlike the anomalous dipole moment of the lighter leptons, the short lifetime of the τ prevents $g_\tau - 2$ from being measured at low energies. Viable probes are then forced to be at high energies, and as such they suffer

from noninterfence. Spin correlation then offer an interesting window on the anomalous dipole moments by resurrecting the interference.

Recently, the study of spin correlations at colliders has gained renewed interest, after the prediction [122] and successful measurement [123] of entanglement between the spins of a top quark pair at the LHC (Large Hadron Collider), as discussed in the review section Ref. [124]. Following the formalism of the celebrated Bell inequalities [7], and of the groundbreaking experimental and theoretical efforts of the 1960s [8, 9], so-called "Bell tests" were developed. They aim to exclude hidden variable theories by measuring correlations between spins that could not arise in theories based on local realism. At colliders, the correlation between the polarisation of the final states from hard scattering events are measured only indirectly. For unstable particles, the angular distribution decay product can be used instead, relying on angular momentum conservation.[1] This also explains, in part, why the measurement of spin correlations can resurrect the interference.

From a phenomenological and model building point of view, much of the recent effort on observables related to entanglement has been on establishing their sensitivity to physics BSM (beyond the Standard Model). For top quark pair production, it has been shown [127] that quantum information observables either surpass or complement the sensitivity of both the integrated cross-section and other angular observables. This seems to tie in perfectly with the fact that spin correlations can be used for interference resurrection, enhancing the sensitivity with respect to the cross-section. To test whether access to uniquely quantum phenomena is a necessary ingredient for increased sensitivity, we then evaluate the reach of different quantum information observables, and compare it to the spin correlation coefficients, which do not distinguish between classical and quantum correlations. We show that quantum information observables are suboptimal probes for 4-fermion operators, when compared with spin correlations, for instance because they partly erase the CP information. Indeed, we find that different choices for the phase of the Wilson coefficients lead to polarisation along different axes. Quantum information observables, combining all spin correlation in one measure, are unable to differentiate between different choices for the phase of the Wilson coefficients, causing the information about CP properties to be lost. We also evaluate the possible reach of present and future colliders to one class of noninterfering dimension-6 operators that display resurrection, the dipole operators of the τ.

The section is structured as follows: in Section II.2, we introduce noninterference and resurrection of interference, then use a simple quantum mechanical example to explain the features of the resurrection mechanism. In Section II.3 we introduce the formalism to describe spin correlations, as well as the quantum information observables. In Section II.4 we calculate the spin observables for both lepton and hadron colliders, and critically analyse their NP reach. We conclude in Section II.5.

II.2 Interference Suppression and Resurrection in 4-Fermion Scattering

Heavy BSM physics generically impacts low energy observables through virtual corrections, which in the infrared are indistinguishable from higher dimensional operators; this observation, coupled with the experimental fact that the symmetries of the SM seem to be a valid at low energy, lets us organise SM contributions in a largely model-independent

[1] This measurement strategy is known to generate a loophole in Bell tests, see Refs. [125, 126]. Since the focus of this section is not a test of quantum mechanics, this will not be an issue for us.

way by considering all operators in an EFT built up from the SM fields in increasing mass dimension [113, 114]. We will adopt the SMEFT in this section to discuss new physics effects, under the assumption that the underlying theory lives at a scale $\Lambda \gg v$.

In this section, we will be interested in $f\bar{f} \to \ell\bar{\ell}$, with f a charged SM fermion and ℓ a charged SM lepton. At dimension 6 — the lowest dimension higher than 4 to affect this process at LO (lowest order) — the full list of SMEFT operator is well-known [75, 113]. Truncating the operator basis at dimension 6, we can compute the squared matrix element. It contains both SM and SMEFT contributions:

$$\mathcal{M} = \mathcal{M}^{\mathrm{SM}} + \frac{1}{\Lambda^2}\mathcal{M}^{\mathrm{SMEFT}}\,, \tag{II.1}$$

$$|\mathcal{M}|^2 = |\mathcal{M}^{\mathrm{SM}}|^2 + 2\,\mathrm{Re}\left(\frac{1}{\Lambda^2}\mathcal{M}^{\mathrm{SM}}\mathcal{M}^{\mathrm{SMEFT}*}\right) + \frac{1}{\Lambda^4}|\mathcal{M}^{\mathrm{SMEFT}}|^2\,, \tag{II.2}$$

$$\equiv |\mathcal{M}|^{2(0)} + \frac{1}{\Lambda^2}|\mathcal{M}|^{2(2)} + \frac{1}{\Lambda^4}|\mathcal{M}|^{2(4)}\,. \tag{II.3}$$

Using NDA (naive dimensional analysis), one can estimate the energy scaling for $|\mathcal{M}|^{2(n)}$; the interference contribution gives in most cases the leading deviation from the SM, simply because it carries fewer powers of the small ratio (E/Λ) than the SMEFT squared piece, where E is the energy scale of the hard interaction. However, as will be discussed shortly, selection rules can make the interference contribution vanish, rendering the SMEFT squared piece the leading deviation from the SM. In this case, the experimental sensitivity to this operator is expected to be much weaker than if the selection rule were absent, due to the energy suppression.[2] Such a situation has been known since the 1990s to arise in the case of triple-gluon interaction [128, 129], and strategies to circumvent the suppression where quickly proposed [121]. Recently, this topic has attracted renewed interest [115, 117, 130, 131], mostly for the phenomenologically important case of pair production of electroweak bosons; in this context, strategies to circumvent the helicity suppression go under the name of "interference resurrection" [132], that we will use throughout this section.

Because the SM is a chiral theory, 4-fermion effective operators exhibit accidental selection rules in the limit of vanishing fermion masses, where helicity coincides with chirality. For instance, the three-point operators $f\bar{f}V$ $(V = \gamma, Z)$, only allow f and $\bar{f}$ to have opposite helicities, if the vector is transversely polarised. That is, the helicity matrix element $\mathcal{M}_{h_V h_f, h_{\bar{f}}}$, with h_X the helicity of particle X, satisfies

$$\mathcal{M}_{T--} = \mathcal{M}_{T++} = 0\,. \tag{II.4}$$

This implies specific helicity configurations for SM lepton pair production $f\bar{f} \to \ell\bar{\ell}$ mediated by electroweak gauge bosons at tree level. We will be interested in the cases $f = e, \mu, u, d, s$, all of which have small masses; since the coupling of fermions to longitudinally polarised gauge boson scales with the mass, we only need to consider transverse polarisation of the gauge boson. Then, the helicity matrix element $M_{h_f h_{\bar{f}} h_\ell h_{\bar{\ell}}}$ is nonvanishing only when $h_f(h_\ell)$ is opposite to $h_{\bar{f}}(h_{\bar{\ell}})$. In the following, we will denote this by saying that the SM imposes the helicity structure $(h_f, h_{\bar{f}}, h_\ell, h_{\bar{\ell}}) = (+-+-), (-++-), (+--+), (-+-+)$. For nonzero lepton masses, the other helicity structures are suppressed by powers of $m_\ell/m_{\ell\ell}$, where $m_{\ell\ell}$ is the invariant mass of the di-lepton pair, and the longitudinal polarisation of the gauge bosons are likewise suppressed. In conclusion, in the

[2] Note that, if the dimension-6 squared contributions are considered, then the contributions of dimension-8 and loop-induced contributions can be of the same order and should generally to be considered when evaluating the sensitivity. This is beyond the scope of this section.

Operator	Helicity Structure
$\bar{\ell}\gamma_\mu \ell A^\mu, \bar{\ell}\gamma_\mu \ell Z^\mu, \bar{\ell}\gamma_\mu\gamma^5 \ell A^\mu, \bar{\ell}\gamma_\mu\gamma^5 \ell Z^\mu$	$(+-T), (-+T)$
$\mathcal{O}_{\ell\ell}, \mathcal{O}_{\ell edq}, \mathcal{O}_{\ell u}, \mathcal{O}^1_{\ell q}, \mathcal{O}^3_{\ell q}$	$(+-+-), (-++-), (+--+), (-+-+)$
$\mathcal{O}^1_{\ell equ}, \mathcal{O}^3_{\ell equ}$	$(+++), (---)$
$\mathcal{O}_{W\ell}, \mathcal{O}_{B\ell}$	$(++T), (--T)$

Table II.1: Operators that enter $\bar{f}f \to \bar{\ell}\ell$ up to dimension 6 in the SMEFT, and their helicity structure in the chiral limit. For the SMEFT operators we follow the notation of [75].

SM:

$$\mathcal{M}^{\rm SM}_{h_f h_{\bar{f}} h_\ell h_{\bar{\ell}}} = 0 + \mathcal{O}(\frac{m_\ell}{m_{\ell\ell}}) \quad \text{if } h_\ell = h_{\bar{\ell}} \text{ or } h_f = h_{\bar{f}}\,. \tag{II.5}$$

Given that SM leptons are light, at energies $m_{\ell\ell} \gtrsim 40$ GeV helicity-violating contributions are heavily suppressed even for the heaviest lepton, the τ. We refer to this as helicity suppression, and we call helicity selection rule the emerging selection rule in the exact chiral limit.

We now add dimension-6 SMEFT operators, whose helicity structures are summarised in Table II.1. Most operators that enter lepton pair production at dimension 6 in the SMEFT are unconstrained by helicity selection rules, because they have the same helicity structure as the SM. Only two classes of operators suffer from helicity suppression in the interference: the left-right quark-lepton 4-fermion operators $\mathcal{O}^1_{\ell equ}, \mathcal{O}^3_{\ell equ}$, and the dipole operators $\mathcal{O}_{W\ell}, \mathcal{O}_{B\ell}$. In both cases, in the chiral limit it is impossible to construct a non-zero interference $\mathcal{M}^{(\rm SM)}_{s_\ell s_{\bar{\ell}}} \mathcal{M}^{(2)\,*}_{s_\ell s_{\bar{\ell}}}$, with $s_\ell(s_{\bar{\ell}}) = \pm 1$ the helicity of $\ell(\bar{\ell})$. We underline that in the calculation of the (differential) cross-section for on-shell particles, no product of matrix elements with different helicities can appear, but as we will see this is not true for a generic observable. Indeed, the only way to resurrect interference is to find an observable that is built out of different helicity structures. In the next subsection, using a simple quantum mechanical example, we argue that spin observables can indeed display resurrection of interference.

II.2.1 Resurrection in Spin Observables: a Quantum Mechanics Example

Since leptons are spin 1/2 particles, the spin state of a $\ell\bar{\ell}$ pair is represented by a bipartite two-qubit. That is, if we consider the initial state $\left|f\bar{f}\right\rangle$ to be a pure state, the final state can be expressed as:

$$|\psi\rangle = S\left|f\bar{f}\right\rangle = \sum_{s_\ell, s_{\bar{\ell}}} \mathcal{M}_{s_\ell s_{\bar{\ell}}} |s_\ell s_{\bar{\ell}}\rangle + \dots\,, \tag{II.6}$$

with S the scattering matrix, and the dots stand for all possible final states other than $\ell\bar{\ell}$. The spin state $|s_\ell s_{\bar{\ell}}\rangle$ is then, in general, not normalised, but it contributes to $|\psi\rangle$ weighted by the S matrix element $\mathcal{M}_{s_\ell s_{\bar{\ell}}}$. Consider the simple case where $|\psi\rangle$ is the following pure, unnormalised state:

$$|\psi\rangle = a\left(|{+}{+}\rangle + |{-}{-}\rangle\right) + b\left(|{+}{-}\rangle - |{-}{+}\rangle\right)\,, \tag{II.7}$$

where we have quantised the spins along the z-axis. We recognise this state to be a linear combination of a triplet and singlet state. Given that these two states are orthogonal,

they do not interfere in the modulus squared of the final state:

$$\langle\psi|\psi\rangle = \sum_{s_\ell s_{\bar{\ell}}} |\mathcal{M}_{s_\ell s_{\bar{\ell}}}|^2 = |a|^2 + |b|^2 \,. \tag{II.8}$$

We can consider also spin observables by insertion of the spin operators $S_i^\ell = \sigma_i \otimes \mathbb{1}_2$, $S_i^{\bar{\ell}} = \mathbb{1}_2 \otimes \sigma_i$, with σ the Pauli matrices. The correlation between the two spins, both measured along the z-axis, is given by

$$\left\langle \psi \middle| S_z^\ell S_z^{\bar{\ell}} \middle| \psi \right\rangle = |a|^2 - |b|^2 \,, \tag{II.9}$$

which, like the modulus squared, only depends on the two coefficients squared, so it receives no contributions from interference. It would be too hasty to conclude at this point that the orthogonality of the two states prevents them from interfering in all observables. Indeed, interference generates the polarisation of ℓ along the y-axis, because the S_y^ℓ operator causes a spin flip:

$$\begin{aligned} \left\langle \psi \middle| S_y^\ell \middle| \psi \right\rangle &= \langle\psi| \Big(a\left(|-+\rangle - |+-\rangle\right) + b\left(|--\rangle + |++\rangle\right) \Big) \\ &= 4\,\mathrm{Im}(ab^*) \,. \end{aligned} \tag{II.10}$$

And similarly we find a nonzero interference when considering the expectation value of $S_z^\ell S_x^{\bar{\ell}}$, which gives the correlation between the two spins when measured along the z- and x-axis, respectively:

$$\left\langle \psi \middle| S_z^\ell S_x^{\bar{\ell}} \middle| \psi \right\rangle = -2\,\mathrm{Re}(ab^*) \,. \tag{II.11}$$

Measuring the full set of spin observables, as well as the modulus square, can then be used to fully reconstruct $|\psi\rangle$. In contrast, a measurement of the modulus square alone cannot access the relative phase between a and b. This is the essence of a process called "quantum tomography" [133]; we discuss quantum tomography at colliders in Section II.3.2.

Let us now add the effect of classical uncertainty, to describe polarisation and other degrees of freedom. This is best done using a density matrix. We recall that for a given state $|\psi\rangle$, which is represented by a statistical ensemble of pure states $|\phi_i\rangle$, the density matrix ρ is the weighted sum of the projectors over $|\phi_i\rangle$:

$$\rho = |\psi\rangle\langle\psi| = \sum_i p_i \,|\phi_i\rangle\langle\phi_i| \,, \tag{II.12}$$

where $\{|\phi_i\rangle\}_i$ is a basis for the Hilbert space of the system, and the p_i sum to one. In the present case of a bipartite qubit, ρ will be a $2^2 = 4$-dimensional square matrix.

We will assume the initial state is an unpolarised beam, represented as an equiprobable ensemble ρ_i:

$$\rho_i = 1/4 \begin{pmatrix} 1 & 0 & 0 & 0 \\ 0 & 1 & 0 & 0 \\ 0 & 0 & 1 & 0 \\ 0 & 0 & 0 & 1 \end{pmatrix} \,. \tag{II.13}$$

We will have the scattering matrix S act on the pure states as:

$$\begin{cases} |++\rangle \to \sqrt{2}a|++\rangle \\ |--\rangle \to \sqrt{2}a|--\rangle \\ |+-\rangle \to b\left(|+-\rangle + |-+\rangle\right) + c\left(|++\rangle + |--\rangle\right) \\ |-+\rangle \to b\left(|+-\rangle + |-+\rangle\right) + c\left(|++\rangle + |--\rangle\right) \end{cases}, \tag{II.14}$$

that is, in matrix form

$$S = \begin{pmatrix} \sqrt{2}a & 0 & 0 & 0 \\ c & b & b & c \\ c & b & b & c \\ 0 & 0 & 0 & \sqrt{2}a \end{pmatrix}. \tag{II.15}$$

The action of S was chosen to mimic the 4-fermion interactions we study in this section. In particular, the action on the equal-sign states (a channel) mimics the $\mathcal{O}^1_{\ell equ}, \mathcal{O}^3_{\ell equ}$ operators, while the action on the mixed-sign states (b and c channels) mimics the SM and the dipole operators, respectively.

The trace of the final state, which computes the weighted average of all the pure states square modulus is

$$A = \mathrm{Tr}(S\rho_i S^\dagger) = |a|^2 + |b|^2 + |c|^2\,, \tag{II.16}$$

which does not receive contributions from interference. On the other hand, the correlation matrix of the two spins along the three axes is given by

$$\tilde{C} = \mathrm{Tr}(\mathbf{S}^\ell \otimes \mathbf{S}^{\bar{\ell}} S\rho_i S^\dagger) = \begin{pmatrix} |b|^2 + |c|^2 & 0 & 0 \\ 0 & |b|^2 - |c|^2 & 2\,\mathrm{Im}(bc^*) \\ 0 & 2\,\mathrm{Im}(bc^*) & |a|^2 - |b|^2 + |c|^2 \end{pmatrix}, \tag{II.17}$$

which shows interference between the b and c channels in the (yz) and (zy) components. The a channel, on the other hand, does not interfere with the other two channels because the initial states are in a classical admixture. If the a channel had a nonzero action on the mixed-sign spin configurations, it would interfere with the b channel, even though it induces an orthogonal spin configuration in the final state.

The simple examples in this subsection demonstrate how interference can be resurrected in spin correlations: The interference between orthogonal final states is generated by a spin-flip operator, but only if the states are in a quantum superposition.

We now introduce the necessary formalism for describing quantum tomography measurements at a collider experiment.

II.3 Spin Correlations and Quantum Tomography

We study spin correlations in 4-fermion scattering $f\bar{f} \to \ell\bar{\ell}$. As argued before, the final state $\left|\ell\bar{\ell}\right\rangle$ can be expressed in terms of a 4×4 density matrix, called the spin-density matrix, defined using the S-matrix elements as follows [134]:

$$R_{s_{\ell,1}s_{\ell,2},s_{\bar{\ell},1}s_{\bar{\ell},2}} \equiv \frac{1}{N^2} \sum_{f,\bar{f}\,\text{d.o.f.}} \mathcal{M}^*_{s_{\ell,2}s_{\bar{\ell},2}} \mathcal{M}_{s_{\ell,1}s_{\bar{\ell},1}}\,, \tag{II.18}$$

$$\mathcal{M}_{s_\ell s_{\bar{\ell}}} \equiv \left\langle \ell(k_1, s_\ell)\bar{\ell}(k_2, s_{\bar{\ell}})\right| S \left| f(p_1)\bar{f}(p_2)\right\rangle, \tag{II.19}$$

where $\mathcal{M}_{s_\ell s_{\bar{\ell}}}$ are the polarised scattering matrix elements with s_ℓ ($s_{\bar{\ell}}$) the ℓ (anti-ℓ) spin, taking values $+, -$.

We average over discrete degrees of freedom (d.o.f.), such as spin and color, by summing incoherently over them and dividing by an appropriate normalisation factor N for each initial state fermion. The sum is incoherent because we assume the initial state is a mixed state with uniform statistical distribution over the initial d.o.f. (i.e. we assume unpolarised beams). This results in the final state being mixed [134]. In contrast, the final state spin d.o.f. are in a quantum superposition. Note also that while we defined R to have four indices, the indices $(s_{\ell,1}s_{\bar{\ell},1})$ and $(s_{\ell,2}s_{\bar{\ell},2})$ can be combined to make R a 4×4 matrix.

Any 4×4 matrix can be decomposed in terms of products of Pauli matrices σ^i in terms of so-called Fano coefficients as follows [135]:

$$R = A\mathbb{1}_4 + \tilde{B}_i^+\sigma^i\otimes\mathbb{1}_2 + \tilde{B}_i^-\mathbb{1}_2\otimes\sigma^j + \tilde{C}_{ij}\sigma^i\otimes\sigma^j\,, \tag{II.20}$$

where we can recognise the spin operator acting on a single lepton, $S_i^+ = \sigma_i\otimes\mathbb{1}_2, S_i^- = \mathbb{1}_2\otimes\sigma_i$, as well as their product, $S_i^+S_j^- = \sigma_i\otimes\sigma_j$. The Fano coefficient can then be readily interpreted: A is the overall normalisation of R, the vector $\tilde{B}_i^-$ ($\tilde{B}_i^+$) quantifies the spin polarisation of the (anti-)lepton, while the matrix $\tilde{C}_{ij}$ contains the correlation between the spins of the two particles. The probability of a given spin configuration $(s_\ell, s_{\bar{\ell}})$ being measured is

$$P(s_\ell, s_{\bar{\ell}}) = \frac{1}{N^2}\sum_{\mathrm{f},\bar{\mathrm{f}}\,\mathrm{d.o.f.}} |\mathcal{M}_{s_\ell s_{\bar{\ell}}}|^2\,. \tag{II.21}$$

A is the trace of R, that is the sum of all the probabilities. This is, of course, proportional to the differential cross section:

$$\frac{d\sigma}{d\Omega} = \frac{\alpha^2\beta_\ell}{m_{\ell\ell}^2}A(m_{\ell\ell},\mathbf{k})\,, \tag{II.22}$$

where $m_{\ell\ell}^2 = (p_\ell + p_{\bar{\ell}})^2$ is the di-lepton invariant mass squared, α an appropriate coupling constant, $\beta_\ell = \sqrt{1-4m_\ell^2/(m_{\ell\bar{\ell}}^2)}$ is the ℓ velocity and Ω the solid angle defined by the direction $\mathbf{k}$.

On the other hand, the probability of the spin measurement on ℓ having the outcome (s_ℓ) can be obtained from the reduced density matrix, defined by tracing out the $\bar{\ell}$ spin d.o.f.:

$$\mathrm{Tr}_{\bar{\ell}}(R)_{s_\ell s'_\ell} = \sum_{s_{\bar{\ell}}}\mathcal{M}^*_{s'_\ell s_{\bar{\ell}}}\mathcal{M}_{s_\ell s_{\bar{\ell}}}\,, \tag{II.23}$$

$$P(s_\ell) = \frac{1}{N^2}\sum_{\mathrm{f},\bar{\mathrm{f}},\,\mathrm{d.o.f.}} |\sum_{s_{\bar{\ell}}}\mathcal{M}_{s_\ell s_{\bar{\ell}}}|^2 = \sum_{s_{\bar{\ell}}}P(s_\ell, s_{\bar{\ell}}) + 2(\mathcal{M}_{s_\ell,-}\mathcal{M}^*_{s_\ell,+}). \tag{II.24}$$

As we saw in the previous subsection, the probabilities of the spin measurements on a single particle, and thus also their correlations, depend not only on the matrix element squared, but also on the interference between matrix elements with different spin structures. Differently, the initial d.o.f. are in a classical admixture and do not interfere.

At this point, one can normalise the spin-density matrix as $\rho = R/\mathrm{Tr}[R]$ to obtain a proper density matrix. We can now expand ρ in the same form as the spin-production matrix (note the absence of tildes)

$$\rho = \frac{1}{4}(\mathbb{1}_4 + B_i^+\sigma^i\otimes\mathbb{1}_2 + B_i^-\mathbb{1}_2\otimes\sigma^i + C_{ij}\sigma^i\otimes\sigma^j)\,. \tag{II.25}$$

If the initial state is composite, like at a pp collider, the full density matrix can be factorised as a classical ensemble of the individual partonic contributions, weighted by the luminosity function I_q [122]:

$$\rho^{pp}_{ijkl} = \frac{\sum_q I_q R^{qq}_{ijkl}}{\sum_q I_q A^{qq}} \,. \tag{II.26}$$

The luminosity functions are defined as:

$$I_{qq}(\hat{m}) = \frac{2\hat{m}}{\sqrt{s}} \int_{\hat{m}}^{1/\hat{m}} \frac{dz}{z} q_q(\hat{m}z) q_{\bar{q}}\left(\frac{\hat{m}}{z}\right), \tag{II.27}$$

with $\hat{m} = m_{\ell\bar{\ell}}/\sqrt{s}$, and $q_q(x)$ is the PDF (parton distribution function) of the parton q. The numerical value of the PDFs are taken from the PDF4LHC collaboration [136] and evaluated with the help of the Mathematica interface ManeParse [137]. We will consider only $q = u, d, s$ because the luminosity functions of heavier quarks are negligibly small.

Finally, we will be interested in the density matrix integrated over the solid angle $d\Omega = \sin\theta d\theta d\phi \equiv dz d\phi$, with Ω the scattering angle of the hard scattering, so we define an integrated spin-production matrix and density matrix:

$$R^{\text{Integrated}} = \frac{1}{4\pi} \int dz d\phi R \,, \tag{II.28}$$
$$\rho^{\text{Integrated}} = \frac{R^{\text{Integrated}}}{A^{\text{Integrated}}} \,.$$

Having defined the necessary density matrix, we consider how to define the amount of entanglement it contains.

II.3.1 Entanglement Measures and Inequalities

A density matrix represents an entangled state if and only if its density matrix can be expressed as a convex combination of product states, i.e.

$$\rho = \sum_{ij} p_{ij} \rho_i^+ \otimes \rho_j^- \,, \tag{II.29}$$

where $\rho_i^\pm$ is a one-qubit state density matrix on the Hilbert space of the (anti-)particle and the real-valued p_{ij} are non-negative and sum to one. If such a decomposition does not exist, the state is said to be entangled [138], because knowledge about the Hilbert space of each subsystem does not translate to knowledge about the full Hilbert space, a purely quantum phenomenon. This formal definition does not provide however a quantitative handle on the entanglement; moreover explicitly checking whether a state is separable involves proving a negative, a generically hard task. For these reasons various quantities have been devised to measure entanglement (see e.g. [139] for a review). The specific case of two-qubit bipartite states is the best-understood one, and a plethora of so-called "entanglement witnesses" with explicit expressions are available. To be an entanglement witness, a measure of entanglement must attain its minimum value (usually zero) for pure states and its maximum value at maximally entangled states (such as Bell pairs).

Concurrence

One entanglement witness that is often used is the concurrence $\mathcal{C}[\rho]$ [140], defined in terms of the spin-flipped density matrix $\tilde{\rho} = (\sigma_2 \otimes \sigma_2)\rho^*(\sigma_2 \otimes \sigma_2)$. The decreasingly

ordered eigenvalues λ_i of the matrix $\omega = \sqrt{\sqrt{\tilde{\rho}}\rho\sqrt{\tilde{\rho}}}$ or, equivalently, the square root of the eigenvalues of the matrix $\Omega = \rho\tilde{\rho}$, are used to define [140]

$$\mathcal{C}[\rho] = \max(0, \lambda_1 - \lambda_2 - \lambda_3 - \lambda_4). \tag{II.30}$$

Null concurrence is attained for separable states, while the maximum value of 1 is attained for maximally entangled states.

CHSH Inequality

Arguably the most famous form of non-classical correlations is the violation of so-called Bell inequalities, which are always satisfied in local and realistic theories. A particularly useful form, the CHSH (Clauser-Horne-Shimony-Holt) inequality [8], allowed the first-ever experimental determination of Bell non-locality [9] and is still a cornerstone of quantum information studies.

For two-qubit systems, the so-called "Horodecki criterion" for violating the CHSH inequality can be calculated in terms of the spin correlation matrix C only [141]. One defines (m_1, m_2, m_3) as the eigenvalues of $M = C^T C$ in decreasing order. According to the Horodecki criterion, the CHSH inequality is violated if and only if [141]

$$\mathfrak{m}_{12} = m_1 + m_2 > 1\,. \tag{II.31}$$

Maximum violation is obtained at $\mathfrak{m}_{12} = 2$, and separable states have $\mathfrak{m}_{12} = 0$. It is worth noting that, in general, violation of Bell inequalities is a stronger condition than entanglement; the two notions coincide only for pure two-qubit bipartite states [142].

Simplified Criteria

It is clear that, if the polarisation vectors $B^{\pm}$ are vanishing, all the information about entanglement is contained in the correlation matrix C. This happens if the individual leptons are not produced in a polarised state by the interaction due to, for example, separate conservation of C and P parities [143]. In that case, the C matrix elements is also constrained to be block-diagonal [122]. Sufficient (but not necessary) conditions for Bell inequality violation and entanglement can be obtained from the Peres-Horodecki criterion [144] with reference only to the diagonal elements of the C matrix. We will not pursue this direction, because as we showed in Section II.2.1, resurrection of interference is active only in the off-diagonal elements of the C matrix. Moreover, EW interactions violate both P and C parities.

Quantum Discord

It has long been recognised [145] that there exist separable mixed states whose correlation cannot be described by a classical theory. This has prompted the search for finer discriminant between classical and quantum states, see Ref. [146] for a recent review. Various measures have been devised, focusing on different aspects of quantum mechanics, such as the fact that a local measurement on subsystems can induce disturbances in the overall system. Most of the measures of quantum correlations are called "discord", because they measure the difference between two generalisations of spin correlations that would coincide in the classical case. Many of the measures of discord involve complicated minimisation processes and are hence not easily amenable to calculations, without employing simplifying assumptions on the nature of the state, as for example can be done in top pair production [147].

In this chapter we will focus on one definition of quantum correlations that has a relatively simple expression, the LQU (local quantum uncertainty) [148]. It quantifies the irreducible quantum uncertainty in local measurements on a subsystem. The LQU is zero if and only if there exists at least one observable that can be measured on a subsystem that is not affected by quantum uncertainty. The LQU is defined as [148]

$$LQU(\rho) = 1 - \max(\mathrm{Eig}\,(W))\,, \tag{II.32}$$

$$W_{ij} = \mathrm{Tr}(\sqrt{\rho}(\sigma_i \otimes \mathbb{1}_2)\sqrt{\rho}(\sigma_j \otimes \mathbb{1}_2))\,. \tag{II.33}$$

We now consider how to experimentally measure spin polarisations and correlations.

II.3.2 Tomography

Collider experiments are generically not able to directly measure the spin of outgoing particles. Luckily, due to angular momentum conservation, the spin information of a decaying particle is imprinted in its decay products. By selecting one of the decay products $d^+(d^-)$ for the outgoing lepton (antilepton), we can relate the spin density matrix to the doubly-differential distribution in the decay product angles [149]. In particular, in the narrow-width approximation one obtains [134]

$$\frac{d\sigma}{d\cos\theta^i_\pm} \propto 1 \pm B^\pm_i \cos\theta^i_\pm\,, \tag{II.34}$$

$$\frac{d^2\sigma}{d\cos\theta^i_+ d\cos\theta^j_-} \propto 1 + C_{ij}\cos\theta^i_+\cos\theta^j_-\ln\cos\theta^i_+\cos\theta^j_-\,, \tag{II.35}$$

where we define the polar angle with respect to a given direction $\hat{u}_i$ through $\cos(\theta_\pm)^i \equiv \hat{d}^\pm \cdot \hat{u}_i$, with $\hat{d}^+(\hat{d}^-)$ the direction of flight of the decay product we picked for the lepton (antilepton). This is the basis of *quantum tomography*: from repeated measurement of angular correlations, one can reconstruct the density matrix, hence the state, of the outgoing $\ell\bar{\ell}$ pair. We note that many different ways have been devised to reconstruct the C matrix, by using different definitions of the notion of correlation, but they all perform similarly in terms of experimental uncertainties [150, 151].

We compute the density matrix in the helicity basis $\{\hat{r}, \hat{n}, \hat{k}\}$, where $\hat{k}$ points along the $\bar{\ell}$ 3-momentum and the other two unit vectors are defined with reference to a fourth unit vector $\hat{p}$:

$$\hat{p}\cdot\hat{k} = z\,, \tag{II.36}$$

$$\hat{r} = \frac{1}{\sqrt{1-z^2}}(\hat{p} - z\hat{k})\,, \tag{II.37}$$

$$\hat{n} = \frac{1}{\sqrt{1-z^2}}\hat{k}\times\hat{p}\,. \tag{II.38}$$

The helicity basis is event-dependent, thus the state that one reconstructs is in general not a proper quantum state but a so-called fictitious state [134]. Nonetheless, fictitious states retain the information of the single measurements that were used for its reconstruction, even though this information might get smeared [152].

We should note at this point that measuring the angular correlations of the decay products of ℓ requires a reconstruction of the momentum of ℓ, as well of the c.o.m. frame. At lepton colliders, the center of mass is known with precision, and possible invisible particles in the decay products can be reconstructed using impact parameters [153]. The

situation is more complicated at hadron colliders, where the composite nature of the hadron makes the c.o.m. frame of the hard scattering *a priori* unknown. We will revisit this issue later.

Based on the discussion in this section, we want to highlight a conceptual difference between the existing descriptions of interference resurrection in the literature and the mechanism presented in Section II.2.1. In diboson production, interference resurrection has been studied extensively, both in the triple-W [118–120] and triple-gluon [121] contexts. It has been noted that the operator $\mathcal{O}_{3V}$ does not interfere with the SM in the process $f\bar{f} \to VV$ [128, 129], but interference is restored by considering a larger process where $f\bar{f} \to VV$ is an intermediate stage, VV being off-shell [121, 130, 131]. In density matrix terminology, Ref. [154] discusses resurrection in electroweak boson production. It has also been observed that interference can be artificially canceled if a strict narrow-width approximation is used [118], making a correct quantum treatment of the intermediate VV state crucial. As reviewed, measuring spin polarisation typically requires the decay of the final-state particle. However, our discussion in Section II.2.1 clarifies that the key factor is not decay or the particle being off-shell, but a proper quantum mechanical treatment. Thus, even if we had direct access to the spins of (on-shell) particles at colliders, quantum mechanics would still govern the resurrection phenomenon, independent of the specific method to measure spin.

Having defined the observables needed for the measurement of spin observables, we turn now to their calculation, and to whether they can display resurrection of interference. First, we categorise the SM and SMEFT contributions to $f\bar{f} \to \ell\bar{\ell}$.

II.3.3 Resurrection of the Dipole

We are now ready to discuss the resurrection of dimension-6 operators in 4-fermion scattering. As we noted before, only the left-right operators $\mathcal{O}^1_{\ell equ}, \mathcal{O}^3_{\ell equ}$ and the dipole operators $\mathcal{O}_{V\ell}$ exhibit different helicities structure than the SM. It is clear from the discussion in Section II.2.1 that the contact operators do not interfere with the SM at all, even in the off-diagonal elements of the R matrix, because we sum over (fixed) initial fermion polarisation a, b. So we will not consider them going forward.

We turn now to the dipole operator class. As we just argued, modifying the helicity selection rules for the initial states makes the interference impossible; therefore we focus on final-state dipole operator $\mathcal{O}_{V\ell}$. Just like in the SM, the gauge boson is fixed to be transverse by the vanishing mass of initial fermions, regardless of any helicity selection rules involving the final leptons. The dipole operator imposes the $(T++), (T--)$ configuration in the chiral limit, which means that the full process $f\bar{f} \to V \to \ell\bar{\ell}$ will have the $(+-++), (+--), (-++), (-+--)$ structure in the chiral limit:

$$\mathcal{M}^{\text{Dipole}}_{s_\ell s_{\bar{\ell}}} = 0 + \mathcal{O}(\frac{m_l}{m_{ll}}) \quad \text{if } s_\ell \neq s_{\bar{\ell}}\,. \tag{II.39}$$

Unlike the contact operators, then, the dipole operator interference with the SM populates the off-diagonal entries of the R matrix. The leptonic dipole operators are unique since they are the only class of operators suffering from helicity suppression in the interference, but still contributing an interference term to spin correlations.

II.3.4 Resurrection, Truncation and Unitarity

Before proceeding, it is important to address a subtlety related to the mismatch in large-energy behaviour of the various entries of the R matrix, which arises due to the noninter-

ference and resurrection phenomena: the R matrix, truncated at order Λ^2, violates perturbative unitarity at energies lower than the cutoff. To clarify, let us separate the various contributions to a given observable based on their Λ dependence and energy scaling from NDA. The dipole operator has the NDA scaling of $vm_{\ell\ell}/\Lambda^2$ for interference contributions. However, due to the helicity selection rule only the SMEFT squared scales with energy, while the interference is proportional to the constant chirality-flip factor vm_ℓ/Λ^2 [155]:

$$\frac{d\sigma}{d\Omega} \overset{m_{\ell\ell}\gg m_\ell}{\to} \frac{d\sigma}{d\Omega}^{(0)} + \frac{vm_\ell}{\Lambda^2}\frac{d\sigma}{d\Omega}^{(2)} + \frac{v^2 m_{\ell\ell}^2}{\Lambda^4}\frac{d\sigma}{d\Omega}^{(4)} , \tag{II.40}$$

and similarly we can define $A^{(n)}$ and $R^{(n)}$ by looking at the high-energy behaviour. This means that A receives a small, energy-independent contribution at order Λ^2. However, due to resurrection, the off-diagonal entries of the R matrix, at order Λ^2, have the NDA scaling of $\frac{m_{\ell\ell}v}{\Lambda^2}$ at large energies:

$$\begin{aligned} R_{ii} &\overset{m_{\ell\ell}\gg m_\ell}{\to} R_{ii}^{(0)} + \frac{vm_\ell}{\Lambda^2}R_{ii}^{(2)} + \frac{v^2m_{\ell\ell}^2}{\Lambda^4}R_{ii}^{(4)} , \\ R_{ij} &\overset{m_{\ell\ell}\gg m_\ell}{\to} R_{ij}^{(0)} + \frac{vm_{\ell\ell}}{\Lambda^2}R_{ij}^{(2)} + \frac{v^2m_{\ell\ell}^2}{\Lambda^4}R_{ij}^{(4)} , \; i\neq j . \end{aligned} \tag{II.41}$$

Therefore, if we neglected the SMEFT squared contributions, the off-diagonal terms of the normalised density matrix would also grow like $m_{\ell\ell}$ at large energies:

$$\rho_{ij} = \frac{R_{ij}^{(0)} + \frac{vm_{\ell\ell}}{\Lambda^2}R_{ij}^{(2)}}{A^{(0)} + \frac{vm_\ell}{\Lambda^2}A^{(2)}} \overset{m_{\ell\ell}\gg m_\ell}{\to} \frac{R_{ij}^{(0)} + \frac{vm_{\ell\ell}}{\Lambda^2}R_{ij}^{(2)}}{A^{(0)}} \quad i\neq j . \tag{II.42}$$

If we instead include the order Λ^4 contributions, both the diagonal and off-diagonal entries of R grow like $m_{\ell\ell}^2$ at large energies. Then, the energy dependence asymptotically cancels and the ρ matrix elements approach constant values at large energies.

Truncating at order Λ^2 would result in a violation of perturbative unitarity in the ρ matrix, at energies lower than the nominal cutoff scale Λ. Such a truncation is, however, clearly not permitted, because the SMEFT squared contribution dominates over the interference. Consequently, this affects the entanglement witnesses, causing them to grow over their theoretical maximum of 2 for $\mathfrak{m}_{12}$ and 1 for $\mathcal{C}[\rho]$. The sensitivity of quantum information observables to unitarity violations has been explored in [154] for longitudinal boson scattering. We emphasise that such a violation of perturbative unitarity happens at energies lower than Λ, and as such does not seem directly related to possible violation of unitarity at or past the cutoff; moreover the full R matrix up to order Λ^4 does not exhibit violation of perturbative unitarity at any energy, even past the cutoff.

In order to avoid spurious violations of unitarity while still being able to observe the effect of resurrection of the interference, we define $\rho^{\text{No Int}}$ by ignoring the interference terms:

$$\rho^{\text{No Int}} = \frac{R^{(0)} + (\frac{vm_{\ell\ell}}{\Lambda^2})^2 R^{(4)}}{A^{(0)} + (\frac{vm_{\ell\ell}}{\Lambda^2})^2 A^{(4)}} . \tag{II.43}$$

Another option would be to normalise by the full cross-section A. While at large energies the two choices differ negligibly, at low energies the density matrix would not be properly normalised; thus we find the definition in Eq. (II.43) more appropriate.

In the absence of resurrection, the difference between $\rho^{\text{No Int}}$ and the full spin density matrix is proportional to the small, energy-independent ratio vm_ℓ/Λ^2. On the other hand, resurrection of interference causes the difference between ρ and $\rho^{\text{No Int}}$ to grow linearly

with energy. A successful resurrection should also improve the sensitivity at moderate and low energies.

We now explore the NP reach and resurrection properties of spin correlation, both quantum and not.

II.4 Case Study: τ-Dipoles at Colliders

Having motivated the choice for the class of dipole operators, we will specialise to τ leptons. The motivation is twofold: first, flavour-universal BSM models, as well as loop effects in the SM, give rise to larger contributions to the τ dipole than to the other lighter fermions [156]. [3] Second, unlike the electron and muon $g-2$, which have been measured to incredible precision [162, 163], direct low-energy measurements of $g_\tau - 2$ are precluded by the tiny lifetime of the τ. Current and prospective sensitivity to tau dipoles comes from high-energy collisions: a direct measurement at a fixed-target experiment has been proposed [164, 165], while indirect bounds are extracted from collider experiments such as B-factories [166–171], electron-electron [172, 173], proton-proton [155, 174], or ion-ion [175–177] collisions, by constraining the anomalous τ-lepton coupling to off-shell photons or detecting a radiation zero in radiative τ decays [178, 179]. All these probes suffer from non-interference and, partly as a result, the current sensitivity is orders of magnitude above the precise SM prediction [180]. Moreover, the sign and phase of the Wilson coefficients remain unconstrained.

Therefore, in this chapter we will consider the following lagrangian:

$$\mathcal{L} = \mathcal{L}_{\rm BSM} + \mathcal{L}_{\rm SMEFT}\,, \tag{II.44}$$

$$\mathcal{L}_{\rm SM} \supset eQ_\ell A_\mu \bar{\ell}\gamma^\mu \ell + \frac{e}{s_W c_W}\left(Z_\mu \bar{\ell}\gamma^\mu (Q_{V\ell} + Q_{A\ell}\gamma^5)\ell\right)\,, \tag{II.45}$$

$$\mathcal{L}_{\rm SMEFT} = \frac{c_{\tau B}}{\Lambda^2}\Big(\overline{L}_L \sigma^{\mu\nu}\tau_R\Big) H B_{\mu\nu} + \frac{c_{\tau W}}{\Lambda^2}\Big(\overline{L}_L \sigma^{\mu\nu}\sigma_3\tau_R\Big) H W^3_{\mu\nu} + \text{h.c.}\,, \tag{II.46}$$

where $L_L = (\nu_{\tau L},\, \tau_L)^T$ is the left-handed third-generation lepton doublet, τ_R is the right-handed third generation weak singlet, H is the Higgs boson, and $B^{\mu\nu}$ and $W^3_{\mu\nu}$ stand for the $U(1)_Y$ and the neutral $SU(2)_L$ field-strength tensors, respectively. After electroweak-symmetry breaking, we can rotate the effective couplings by the weak mixing angle,

$$c_\gamma = \cos\theta_W\, c_{\tau B} - \sin\theta_W\, c_{\tau W}\,, \tag{II.47}$$

$$c_Z = \sin\theta_W\, c_{\tau B} + \cos\theta_W\, c_{\tau W}\,. \tag{II.48}$$

We further set the Higgs field to its vev v, which renders the dimension-6 operators a three-point interaction. The rotated couplings in Eq. (II.48) then correspond to the τ-lepton dipole interactions with the photon and the Z-boson. Neglecting higher-order corrections, it is possible to relate the effective coupling c_γ to contributions to the anomalous magnetic and electric moments of the τ-lepton,

$$\Delta a_\tau = \frac{2\sqrt{2}}{e}\frac{m_\tau v}{\Lambda^2}\,\text{Re}(c_\gamma) + \dots\,, \tag{II.49}$$

$$\Delta d_\tau = -\sqrt{2}\frac{v}{\Lambda^2}\,\text{Im}(c_\gamma) + \dots\,, \tag{II.50}$$

[3] Such enhancements can be even larger in scenarios with new bosons coupled to both lepton chiralities, yielding contributions to dipoles $\propto m_\ell m_F/\Lambda^2$, where m_F denotes the mass of the heavy fermion running in the loops [157]. Examples are leptoquark models [158], where F is a heavy quark such as the bottom-quark [159, 160], or scenarios where F is a heavy vector-like lepton [161].

where the dots stand for loop corrections, cf. Ref. [157, 181], and similarly weak magnetic and electric moments can be defined. We will also find it useful to define $C_{\gamma(Z)} = c_{\gamma(Z)}/\Lambda^2$.

In the rest of this section we present our results. We analytically calculate the R-matrix in the EW SM at tree level, as well as with the addition of the SMEFT dipole operators $\mathcal{O}_{\gamma\tau}, \mathcal{O}_{Z\tau}$ with the help of FeynArts and FormCalc [182, 183]. We collect the coefficient of the resulting Fano decomposition in Section II.4.1.

After integrating over z, we calculate, as a function of $m_{\tau\tau}$, the Bell inequality marker $\mathfrak{m}_{12}$, the concurrence $\mathcal{C}[\rho]$, and the local quantum uncertainty LQU. We pick as a benchmark point the current best constraint $|C_\gamma| \leq (1.5 \text{ TeV})^{-2}$ [155] and, since our goal is to compare the reach of different observables to NP, we apply it to $|C_Z|$ as well. We consider 4 possible phases for the Wilson coefficient, to showcase the sensitivity of different observables to the phase of the Wilson coefficients.

Finally, we compare the quantum information observables to single elements of the C matrix, and show how the latter have better sensitivity both at high and low energies to the SMEFT operators, as well as better discrimination power between different phase choices for the Wilson coefficient, hence to the CP properties of the UV theory. We perform this procedure both for ee and pp colliders.

II.4.1 Fano Coefficients

Explicit expression for the R matrix in the electroweak SM, as well as with a parametrisation of the effect of anomalous dipole contributions, first appeared in [184], but they were not calculated in the helicity basis that we adopt here. The Fano coefficients for $f\bar{f} \to \ell\bar{\ell}$ in the EW theory, calculated in the helicity basis, have first appeared in [127]; we agree with their results on most terms, but we find some non-vanishing off-diagonal correlation that were not considered in [127]. These terms are due to the non-zero Z width, and they generate absorptive contributions to the matrix elements, which cannot be generated from the $\Gamma_Z = 0$ expression by the usual substitution $m_Z^2 \to m_Z^2 - im_Z\Gamma_Z$. Of course, contributions linear in Γ_Z are formally one loop and small in the SM due to the small ratio Γ_Z/M_Z, but nonetheless they modify the spin configuration of the final state, and might be relevant for other vector mediators with larger widths. Moreover, we explicitly write down the polarisation vector B, which has not appeared elsewhere.

Following [127] we divide the contributions according to their tensor structure, that is we split the spin production matrix in three parts:

$$R = R^{[0]} + R^{[1]} + R^{[2]}\,, \tag{II.51}$$

where the superscript indicates the number of γ^5 insertions on the τ line. This is because the tensor structure uniquely defines the spin state. Moreover, still following [127], we denote common factors by F. Throughout this section, the coefficients that are not explicitly written are either zero or can be obtained through the known symmetry of the Fano coefficients [143].

We start with the SM. At zero γ^5 insertions, the Fano coefficients are:

$$\begin{cases} A^{[0]} &= F^{[0]}(\beta_\tau^2 z^2 - \beta_\tau^2 + 2) \\ \tilde{B}_r^{[0]} &= F_B^{[0]}\sqrt{1-z^2}\sqrt{1-\beta_\tau^2} \\ \tilde{B}_k^{[0]} &= -F_B^{[0]} z \\ \tilde{C}_{nn}^{[0]} &= -F^{[0]}\beta_\tau^2(1-z^2) \\ \tilde{C}_{rr}^{[0]} &= -F^{[0]}(\beta_\tau^2 - 2)(1-z^2) \\ \tilde{C}_{kk}^{[0]} &= F^{[0]}(\beta_\tau^2 - (\beta_\tau^2-2)z^2) \\ \tilde{C}_{kr}^{[0]} &= 2F^{[0]}\sqrt{1-\beta_\tau^2} z\sqrt{1-z^2} \end{cases}, \tag{II.52}$$

where the common factors are

$$F^{[0]} = 4Ne^4\left(Q_\tau^2 Q_f^2 + 8\,\mathrm{Re}\left(\frac{Q_\tau Q_f Q_{V\tau} Q_{Vf} m_\tau^2}{D_Z}\right) + \frac{16 Q_{V\tau}^2 (Q_{Vf}^2 + Q_{Af}^2) m_\tau^4}{|D_Z|^2}\right), \tag{II.53}$$

$$F_B^{[0]} = 64Ne^4\left(\mathrm{Re}\left(\frac{Q_{Af} Q_{V\tau} Q_f Q_\tau m_\tau^2}{D_Z}\right) + 4\frac{Q_{Af} Q_{Vf} Q_{V\tau}^2 m_\tau^4}{|D_Z|^2}\right), \tag{II.54}$$

with N the normalisation factor in Eq. (II.19), and $D_Z = c_W s_W\left(4m_\tau^2 - (1-\beta_\tau^2)(m_Z^2 - i m_Z \Gamma_Z)\right)$ the boosted propagator of the Z boson, together with the electroweak mixing angles coming from the coupling to fermions. These results agree with Ref. [127].

At one insertion of γ^5, we see the first absorptive contributions, noted by the Γ subscript. They do not share the same common factor with the rest of the coefficients, and disappear as $\Gamma \to 0$:

$$\begin{cases} A^{[1]} &= 2F^{[1]} z \\ \tilde{B}_n^{[1]} &= F_{\Gamma,B}^{[1]}\sqrt{1-\beta_\tau^2}\sqrt{1-z^2} \\ \tilde{B}_r^{[1]} &= F_B^{[1]}\sqrt{1-\beta_\tau^2} z\sqrt{1+z^2} \\ \tilde{B}_k^{[1]} &= F_B^{[1]}(1+z^2) \\ \tilde{C}_{kk}^{[1]} &= 2F^{[1]} z \\ \tilde{C}_{nr}^{[1]} &= F_\Gamma^{[1]}(1-z^2) \\ \tilde{C}_{nk}^{[1]} &= -F_\Gamma^{[1]}\sqrt{1-\beta_\tau^2} z\sqrt{1-z^2} \\ \tilde{C}_{rk}^{[1]} &= F^{[1]}\sqrt{1-\beta_\tau^2}\sqrt{1-z^2} \end{cases}, \tag{II.55}$$

$$F^{[1]} = 16NQ_{A\tau}Q_{Af}Q_{A\tau}\beta_\tau e^4\left(2\,\mathrm{Re}\left(\frac{Q_\tau Q_f m_\tau^2}{D_Z} + \frac{16 Q_{V\tau}^2 Q_{Vf} m_\tau^4}{|D_Z|^2}\right)\right), \tag{II.56}$$

$$F_B^{[1]} = 32Ne^4\beta_\tau Q_{A\tau}\left(\mathrm{Re}\left(\frac{Q_{Vf} Q_f Q_\tau m_\tau^2}{D_Z}\right) + 4\frac{Q_{V\tau}(Q_{Vf}^2 + Q_{Af}^2) m_\tau^4}{|D_Z|^2}\right),$$

$$F_\Gamma^{[1]} = 32Ne^4\beta_\tau\ \mathrm{Im}\left(\frac{Q_{A\tau} Q_{V\tau} Q_f Q_\tau c_W^2 s_W^2 m_\tau^2}{D_Z}\right),$$

$$F_{\Gamma,B}^{[1]} = F_\Gamma^{[1]}\ \text{with}\ (Q_{Vf} \to Q_{Af})\ . \tag{II.57}$$

The contributions from double γ^5 insertions are, in agreement with Ref. [127]:

$$\begin{cases} A^{[2]} &= F^{[2]}(1+z^2) \\ B_k^{[2]} &= F_B^{[2]} z \\ C_{nn}^{[2]} &= F^{[2]}(1-z^2) \\ C_{rr}^{[2]} &= -F^{[2]}(1-z^2) \\ C_{kk}^{[2]} &= F^{[2]}(1+z^2) \end{cases}, \tag{II.58}$$

$$F^{[2]} = 64Ne^4 Q_{A\tau}^2 \beta_\tau^2 \frac{(Q_{Vf}^2 + Q_{Af}^2) m_\tau^4}{|D_Z|^2}, \tag{II.59}$$

$$F_B^{[2]} = -256Ne^4 \,\mathrm{Re}\left(\frac{Q_{Af} Q_{Vf} Q_{A\tau}^2 m_\tau^4}{|D_Z|^2} \right). \tag{II.60}$$

We now pass to the dipole contribution. They were first derived in [185], and similarly to the SM, we find additional absorptive contributions that are linear in Γ_Z; moreover we consider complex couplings, unlike [185] which focused on real couplings only.

At one dipole insertion (*i.e.* one insertion of $\sigma^{\mu\nu}$), only zero or one γ^5 insertions are possible. At zero insertions we get

$$\begin{cases} A^{[6,0]} &= F^{[6,0]} \\ \tilde{B}_r^{[6,0]} &= F_B^{[6,0]} \frac{\beta_\tau^2 - 2}{\sqrt{1-\beta_\tau^2}} \sqrt{1-z^2} - F_{\Gamma,B}^{[6,0]} \frac{z\sqrt{1-z^2}}{\sqrt{1-\beta_\tau^2}} \\ \tilde{B}_n^{[6,0]} &= F_B^{[6,0]} \frac{\beta_\tau}{\sqrt{1-\beta_\tau^2}} \sqrt{1-z^2} - F_{\Gamma,B}^{[6,0]} \frac{z\sqrt{1-z^2}\beta_\tau}{\sqrt{1-\beta_\tau^2}} \text{ with } \left(\mathrm{Re}(c_{\gamma/Z}) \leftrightarrow \mathrm{Im}(c_{\gamma/Z})\right) \\ \tilde{B}_k^{[6,0]} &= 2F_B^{[6,0]} z - F_{\Gamma,B}^{[6,0]}(1-z^2) \\ \tilde{C}_{rr}^{[6,0]} &= F^{[6,0]}(1-z^2) \\ \tilde{C}_{kk}^{[6,0]} &= F^{[6,0]} z^2 \\ \tilde{C}_{rn}^{[6,0]} &= F^{[6,0]} \frac{\beta_\tau}{2}(1-z^2) \text{ with } \left(\mathrm{Re}(c_{\gamma/Z}) \to \mathrm{Im}(c_{\gamma/Z})\right) \\ \tilde{C}_{rk}^{[6,0]} &= F^{[6,0]} \frac{2-\beta_\tau^2}{2\sqrt{1-\beta_\tau^2}} z\sqrt{1-z^2} - F_\Gamma^{[6,0]} \frac{\sqrt{1-z^2}}{\sqrt{1-\beta_\tau^2}} \\ \tilde{C}_{nk}^{[6,0]} &= F^{[6,0]} \frac{\beta_\tau^2\sqrt{1-z^2}}{\sqrt{1-\beta_\tau^2}} + F_\Gamma^{[6,0]} \frac{\beta_\tau z\sqrt{1-z^2}}{2\sqrt{1-\beta_\tau^2}} \text{ with } \left(\mathrm{Re}(c_{\gamma/Z}) \leftrightarrow \mathrm{Im}(c_{\gamma/Z})\right) \end{cases}, \tag{II.61}$$

$$F^{[6,0]} = 16\sqrt{2}Ne^3 \frac{m_\tau v}{\Lambda^2} \Bigg(\mathrm{Re}(c_\gamma) Q_f^2 Q_\tau - \mathrm{Re}(c_Z) \frac{16 c_W s_W Q_{V\tau} (Q_{Af}^2 + Q_{Vf}^2) m_\tau^4}{|D_Z|^2} \tag{II.62}$$
$$+ \left(\mathrm{Re}(c_\gamma) Q_{V\tau} - \mathrm{Re}(c_Z) Q_\tau c_W s_W\right) \mathrm{Re}\left(\frac{4 Q_{Vf} Q_f m_\tau^2}{D_Z} \right) \Bigg),$$

$$F_\Gamma^{[6,0]} = 8\sqrt{2}Ne^3 \beta_\tau \frac{m_\tau v}{\Lambda^2} \,\mathrm{Im}\left(c_\gamma Q_{V\tau} + c_Z Q_\tau c_W s_W\right) \mathrm{Im}\left(\frac{Q_{Af} Q_f m_\tau^2}{D_Z} \right), \tag{II.63}$$

$$F_B^{[6,0]} = 8\sqrt{2}Ne^3 \beta_\tau \frac{m_\tau v}{\Lambda^2} \Bigg(Q_{Af} Q_f \left(\mathrm{Re}\left(c_\gamma\right) Q_{V\tau} + \mathrm{Re}\left(c_Z\right) Q_\tau c_W s_W\right) \mathrm{Re}\left(\frac{m_\tau^2}{D_Z} \right) \tag{II.64}$$
$$+ 8 Q_{Af} Q_{Vf} Q_{V\tau} \,\mathrm{Re}\left(c_Z\right) \frac{m_\tau^4}{|D_Z|^2} \Bigg),$$

$$F^{[6,0]}_{\Gamma,B} = F^{[6,0]}_{\Gamma} \text{ with } (Q_{Af} \to Q_{Vf}) \,. \tag{II.65}$$

At one insertion of both γ^5 and $\sigma^{\mu\nu}$, we obtain:

$$\begin{cases} A^{[6,1]} &= F^{[6,1]} z \\ \tilde{B}^{[6,1]}_r &= F^{[6,1]}_B \dfrac{z\sqrt{1-z^2}}{\sqrt{1-\beta_\tau^2}} + F^{[6,1]}_{\Gamma,B} \dfrac{\beta_\tau}{\sqrt{1-\beta_\tau^2}} \sqrt{1-z^2} \\ \tilde{B}^{[6,1]}_r &= F^{[6,1]}_B \dfrac{z\sqrt{1-z^2}}{\sqrt{1-\beta_\tau^2}} + F^{[6,1]}_{\Gamma,B} \dfrac{1}{\sqrt{1-\beta_\tau^2}} \sqrt{1-z^2} \text{ with } (\mathrm{Re}(c_\gamma) \leftrightarrow \mathrm{Im}(c_\gamma)) \\ \tilde{B}^{[6,1]}_k &= F^{[6,1]}_B (1+z^2) \\ \tilde{C}^{[6,1]}_{kk} &= F^{[6,1]} z \\ \tilde{C}^{[6,1]}_{nr} &= F^{[6,1]}_\Gamma (1-z^2) \\ \tilde{C}^{[6,1]}_{rk} &= F^{[6,1]} \dfrac{\sqrt{1-z^2}}{2\sqrt{1-\beta_\tau^2}} + F^{[6,1]}_\Gamma \dfrac{1}{\sqrt{1-\beta_\tau^2}} z\sqrt{1-z^2} \\ \tilde{C}^{[6,1]}_{nk} &= F^{[6,1]} \dfrac{\beta_\tau\sqrt{1-z^2}}{2\sqrt{1-\beta_\tau^2}} - F^{[6,1]}_\Gamma \dfrac{\beta_\tau}{\sqrt{1-\beta_\tau^2}} z\sqrt{1-z^2} \text{ with } \big(\mathrm{Re}(c_{\gamma/Z}) \to \mathrm{Im}(c_{\gamma/Z})\big) \end{cases} , \tag{II.66}$$

$$F^{[6,1]} = 64\sqrt{2} N e^3 (\frac{m_\tau v}{\Lambda^2}) Q_{A\tau} Q_{Af} \beta_\tau \left(\mathrm{Re}(c_\gamma)\, \mathrm{Re}(\frac{Q_f m_\tau^2}{D_Z}) - \mathrm{Re}(c_Z) \frac{8 c_W s_W Q_{V\tau} m_\tau^4}{|D_Z|^2} \right. \tag{II.67}$$
$$\left. + (\mathrm{Re}(c_\gamma) Q_{V\tau} - \mathrm{Re}(c_Z) Q_\tau c_W s_W)\, \mathrm{Re}\left(\frac{4 Q_{Vf} Q_f m_\tau^2}{D_Z}\right)\right),$$

$$F^{[6,1]}_\Gamma = 32\sqrt{2} N e^3 (\frac{m_\tau v}{\Lambda^2}) Q_{Vf} Q_{A\tau} Q_f \beta_\tau\, \mathrm{Re}(c_\gamma c_W^2 s_W^2)\, \mathrm{Re}(\frac{m_\tau^2}{D_Z}) \,, \tag{II.68}$$

$$F^{[6,1]}_B = 32\sqrt{2} N e^3 Q_{A\tau} (\frac{m_\tau v}{\Lambda^2}) \beta_\tau \left(\mathrm{Re}(c_\gamma Q_f Q_{Vf})\, \mathrm{Re}(\frac{m_\tau^2}{D_Z}) + \mathrm{Re}(c_Z) \frac{4 c_W s_W (Q_{Vf}^2 + Q_{Af}^2) m_\tau^4}{|D_Z|^2} \right), \tag{II.69}$$

$$F^{[6,1]}_{\Gamma,B} = F^{[6,1]}_\Gamma \text{ with } (Q_{Af} \to Q_{Vf}\,, \mathrm{Re}(c_\gamma) \to \mathrm{Im}(c_\gamma)) \,. \tag{II.70}$$

For the double insertion of the dipole operators, we find it useful to split contributions by counting the numbers of factors of $\mathrm{Im}(c_{\gamma/Z})$, keeping the same notation above. Indeed, insertion of the imaginary part of the Wilson coefficient are essentially a γ^5 insertion. At zero insertions we recover the results of Ref. [185]:

$$\begin{cases} A^{[8,0]} &= F^{[8,0]} (-\beta_\tau^2 z^2 - \beta_\tau^2 + 2) \\ \tilde{B}^{[8,0]}_r &= F^{[8,0]}_B \dfrac{\sqrt{1-z^2}}{\sqrt{1-\beta_\tau^2}} \\ \tilde{B}^{[8,0]}_k &= F^{[8,0]}_B z \\ \tilde{C}^{[8,0]}_{rr} &= F^{[8,0]} (2-\beta_\tau^2)(1-z^2) \\ \tilde{C}^{[8,0]}_{nn} &= F^{[8,0]} \beta_\tau^2 (1-z^2) \\ \tilde{C}^{[8,0]}_{kk} &= F^{[8,0]} \left((2-\beta_\tau^2) z^2 - \beta_\tau^2\right) \\ \tilde{C}^{[8,0]}_{rk} &= F^{[8,0]} 2\sqrt{1-\beta_\tau^2} z\sqrt{1-z^2} \end{cases} , \tag{II.71}$$

$$F^{[8,0]} = 32 N e^2 \left(\frac{m_\tau v}{\Lambda}\right)^2 \frac{1}{1-\beta_\tau^2} \left(Q_f^2\, \mathrm{Re}(c_\gamma)^2 - 8\, \mathrm{Re}(c_\gamma)\, \mathrm{Re}(c_Z)\, \mathrm{Re}\left(\frac{Q_f Q_{Vf} m_\tau^2}{D_Z}\right) \right. \tag{II.72}$$

$$+ 16\,\mathrm{Re}(c_\gamma^2)\frac{m_\tau^4 c_W^2 s_W^2 (Q_{Af}^2+Q_{Vf}^2)}{|D_Z|^2}\Big)\,,$$

$$F_B^{[8,0]} = 64Ne^2\left(\frac{m_\tau v}{\Lambda}\right)^2\left(\mathrm{Re}(c_\gamma)\,\mathrm{Re}(c_Z)\,\mathrm{Re}\left(\frac{Q_f Q_{Af} m_\tau^2}{D_Z}\right) + 4\,\mathrm{Re}(c_Z)^2\frac{m_\tau^4 c_W^2 s_W^2 Q_{Af} Q_{Vf}}{|D_Z|^2}\right). \tag{II.73}$$

The imaginary squared contribution is particularly simple; indeed it produces a singlet state $C^{[8,2]} = -A^{[8,2]}\mathbb{1}_3$, with the overall normalisation being

$$A^{[8,2]} = F^{[8,2]} = F^{[8,0]}\beta_\tau^2(1-z^2) \text{ with } \big(\mathrm{Re}(c_{\gamma/Z}) \to \mathrm{Im}(c_{\gamma/Z})\big)\,. \tag{II.74}$$

The pure real and pure imaginary contributions produce then two orthogonal spin configuration, which cannot interfere in the cross section:

$$A^{[8,1]} = 0\,. \tag{II.75}$$

Nonetheless, spin correlations resurrect the interference, and we obtain

$$\begin{cases} \tilde{B}_r^{[8,1]} = F_{\Gamma,B}^{[8,1]}\dfrac{z\sqrt{1-z^2}}{\sqrt{1-\beta_\tau^2}} \\ \tilde{B}_n^{[8,1]} = F^{[8,1]}\dfrac{\sqrt{1-z^2}}{\sqrt{1-\beta_\tau^2}} \\ \tilde{B}_k^{[8,1]} = F_{\Gamma,B}^{[8,1]}1-z^2 \\ \tilde{C}_{rn}^{[8,1]} = F^{[8,1]}\dfrac{1-z^2}{1-\beta_\tau^2} \\ \tilde{C}_{rk}^{[8,1]} = F_\Gamma^{[8,1]}\dfrac{\sqrt{1-z^2}}{\sqrt{1-\beta_\tau^2}} \\ \tilde{C}_{nk}^{[8,1]} = F^{[8,1]}\sqrt{1-\beta_\tau^2}z\sqrt{1-z^2} \end{cases}, \tag{II.76}$$

$$F^{[8,1]} = 64Ne^2\left(\frac{m_\tau v}{\Lambda}\right)^2\frac{\beta_\tau}{1-\beta_\tau^2}\Big(Q_f^2\,\mathrm{Re}(c_\gamma)\,\mathrm{Im}(c_\gamma) \tag{II.77}$$

$$+ 4Q_f Q_{Vf}\left(\mathrm{Re}(c_\gamma)\,\mathrm{Im}(c_Z) + \mathrm{Re}(c_Z)\,\mathrm{Im}(c_\gamma)\,\mathrm{Re}(\frac{c_W s_W m_\tau^2}{D_Z})\right)$$

$$+ 16\frac{c_W^4 s_W^4 (Q_{Vf}^2+Q_{Af}^2)\,\mathrm{Re}(c_Z)\,\mathrm{Im}(c_Z) m_\tau^4}{|D_Z|^2}\Big),$$

$$F_\Gamma^{[8,1]} = 128Ne^2\left(\frac{m_\tau v}{\Lambda}\right)^2\beta_\tau\left(Q_f Q_{Af}\,\mathrm{Re}(c_\gamma)\,\mathrm{Im}(c_Z) - \mathrm{Re}(c_Z)\,\mathrm{Im}(c_\gamma)\,\mathrm{Im}(\frac{c_W^3 s_W^3 m_\tau^2}{D_Z})\right) \tag{II.78}$$

$$F_B^{[8,1]} = 256Ne^2\left(\frac{m_\tau v}{\Lambda}\right)^2\beta_\tau\Big(Q_f Q_{Af}\left(\mathrm{Re}(c_Z)\,\mathrm{Im}(c_\gamma) - \mathrm{Re}(c_\gamma)\,\mathrm{Im}(c_Z)\right)\mathrm{Re}(\frac{c_W s_W m_\tau^2}{D_Z}) \tag{II.79}$$

$$+ 4\frac{\mathrm{Re}(c_Z)\,\mathrm{Im}(c_w^4 s_w^4 c_Z) Q_{Af} Q_{Vf} m_\tau^4}{|D_Z|^2}\Big),$$

$$F_{\Gamma,B}^{[8,1]} = F_\Gamma^{[8,1]} \text{ with } (Q_{Af} \to Q_{Vf})\,. \tag{II.80}$$

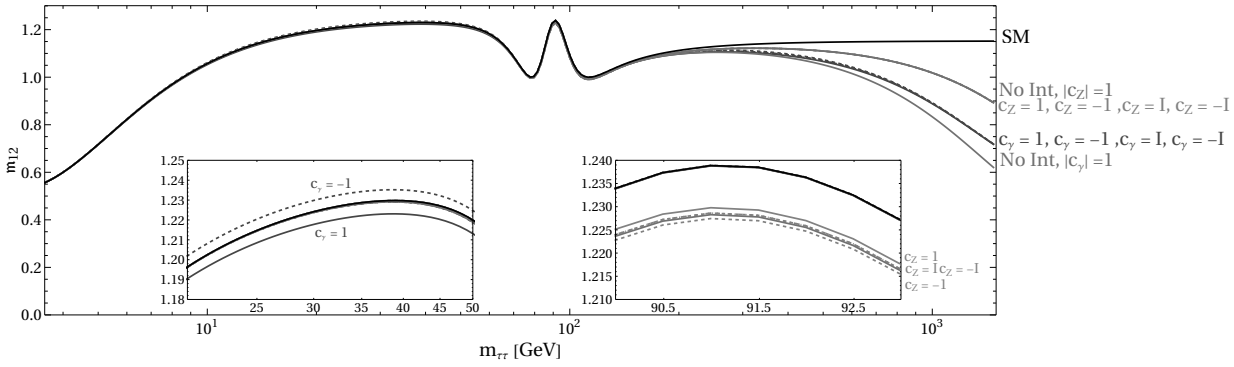

Figure II.1: The $\mathfrak{m}_{12}$ Bell inequality marker for $ee \to \tau\tau$, $C_{\gamma/Z} = 1/1.5\,\text{TeV}^{-2}$. The insets show the local maxima of entanglement to appreciate the deviations due to the photon dipole operator (around $m_{\tau\tau} = 40$ GeV) and Z dipole operator (around $m_{\tau\tau} = m_Z$). For $m_{\ell\ell} \gg m_Z$, the SM approaches a constant value, while the SMEFT operators bring down the entanglement of the τ pair state. Resurrection of interference of the photon dipole can be observed, but the interference and SMEFT squared contributions partially cancel each other. Moreover, while at the local maxima the $c = 1$ and $c = -1$ contributions can be distinguished, this is not true for $m_{\ell\ell} \gg m_Z$; imaginary Wilson coefficients, on the other hand, contribute negligibly at low energies and cannot be distinguished from real coefficients at large energies.

II.4.2 Quantum Observables and Spin Correlations

II.4.2.1 Lepton Colliders

In Figs. II.1 to II.4 we show the spin correlation observables for $ee \to \tau\tau$, at energies relevant for both past (LEP), current (Belle II), and proposed lepton colliders (FCC-ee, CLIC and ILC). Of course, while we refer to an ee collider, the results for a $\mu\mu$ collider would be exactly the same at the energies we consider here, because in both cases the mass of the initial leptons can be neglected.

In the SM, the maximum amount of entanglement can be observed at energies close to $30 - 50$ GeV, where the photon exchange dominates and the external fermions can be considered as massless, and around the Z pole, where the Z-exchange dominates. As a result, around these energies one can observe the largest deviations in the spin correlation observables: adding the γ dipole operator changes the correlation pattern around the first maximum, while it has negligible effect at the Z pole, and vice versa adding the Z dipole has a clearly observable effect at the Z pole, being a resonant contribution there.

Observing Fig. II.1, one can notice how resurrection is successful in the Bell inequality marker $\mathfrak{m}_{12}$, in the sense that the interference has a non-negligible effect at large energies, but unfortunately the effect is to reduce the deviation from the SM, making the observable less sensitive compared to if resurrection did not occur. Moreover, at large energies the phase of the Wilson coefficient does not make any significant difference in the Bell inequality violation. Around the first maximum, however, the phase does play a role, with the pure imaginary coupling (hence CP-violating) benchmark increasing the amount of Bell inequality violation, and the opposite happening for pure real couplings (CP-conserving).

We show the concurrence in Fig. II.2. We have a similar situation regarding the phase of the Wilson coefficient, but unlike the case of $\mathfrak{m}_{12}$, here the interference contribution are

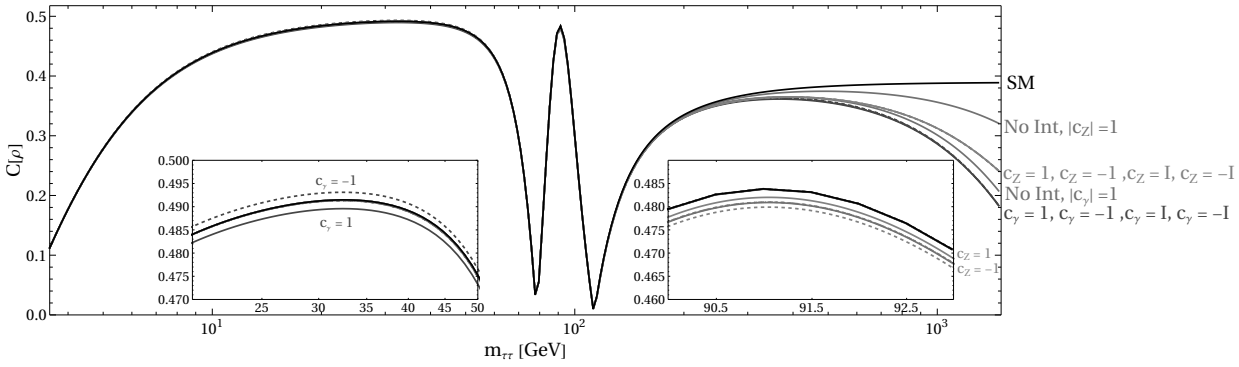

Figure II.2: Same as Fig. II.1, but here the Concurrence $C[\rho]$, which quantifies entanglement directly, is plotted. In this case, resurrection of interference can be observed for both the photon and Z dipole operators, and the interference and SMEFT squared contributions both decrease entanglement. However, at large energies the sign and phase of the Wilson coefficient cannot be determined, and at low energies there is limited sensitivity to the imaginary part of the Wilson coefficients.

actually of the same sign as the SMEFT squared, allowing for increased sensitivity thanks to resurrection.

Since the concurrence is a finer discriminant of quantum correlation than Bell inequality violation, one might imagine that the quantum discord, being an even finer discriminant, might fare even better as a NP probe. This is not the case, as can be seen in Fig. II.3: just like the case of $\mathfrak{m}_{12}$, the interference contributions for the LQU have opposite sign as the SMEFT squared contributions. It is interesting to note how the LQU features a maximum at small energies that is absent from the entanglement markers, as well as the fact that there is an increase in LQU when the SMEFT operators are added, while entanglement and Bell inequality violation fall off.

Finally, we consider the elements of the C matrix. In Fig. II.4, we plot the (nk) element of the C matrix. In the SM, this entry receives only a contribution proportional to the imaginary part of the Z propagator, which is small with respect to A anywhere but around the Z resonance. Moreover, no contribution from SMEFT squared is present, except in the interference between CP conserving and CP violating dipole moments, and thus C_{nk} is a perfect candidate to measure the sign and phase of the Wilson coefficients. Only the real part of the Wilson coefficients contributes in the high-energy limit and indeed the lines for pure imaginary coupling deviate negligibly from the SM except around the Z pole. It should be noted that, at high energy, information about the sign of the Wilson coefficient is lost, partially explaining the similar phenomenon in the quantum information observables. However, unlike the quantum observables, sizable deviations from the SM can be observed at lower energies, as well as separation between the lines belonging to different sign. It should be noted that, if we considered the (nr) element instead, the roles of the imaginary and real part of the Wilson coefficient would be switched. This makes it straightforward to experimentally disentangle the phase of the Wilson coefficient, as real and imaginary part contribute to different entries of the spin correlation matrix. On the other hand, the quantum observables, being a combination of all the spin observables, lose differentiating power between the different scenarios for the phase of the Wilson coefficient.

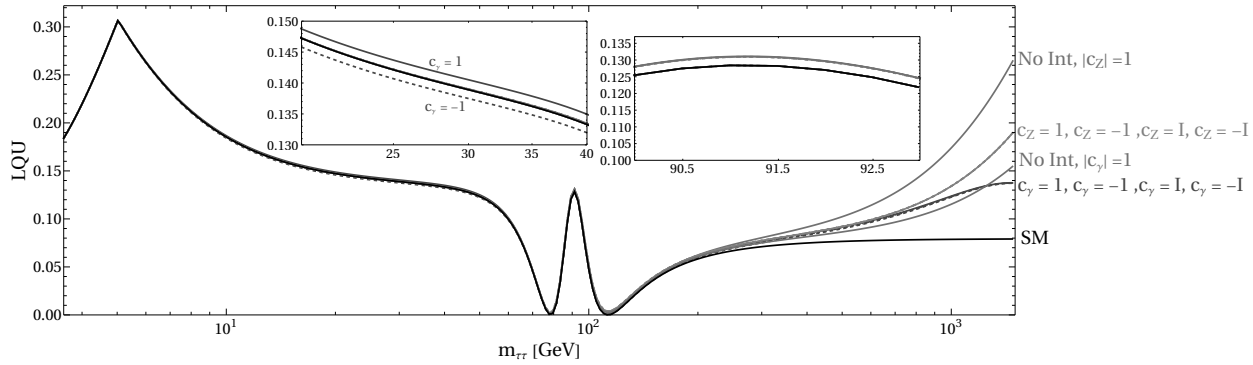

Figure II.3: Same as Fig. II.1, but for the LQU, which quantifies quantum discord. The conclusions are mostly similar as in Fig. II.1, but resurrection of interference can be observed for the Z dipole, as well.

II.4.2.2 SMEFT Sensitivity

To compare the different observables as NP probes, we show in Fig. II.5 their sensitivity at three benchmark energies, namely $m_{\ell\ell} = 10.56\,\text{GeV}, m_Z, 500$ GeV. The first energy is the $\Upsilon(4S)$ resonance at which Belle II operates, while the other two are relevant for a TeraZ machine and one of the proposed future lepton colliders, respectively. For Belle II, we use the uncertainties derived from Monte Carlo simulations in Ref. [151], which considered 200 million events. For the TeraZ machine, we rescale the uncertainties estimated in [186] by a factor $10\sqrt{50}$ to reach the expected 100 million events. Finally, for the lepton collider at 500 GeV we rescale the TeraZ uncertainty by the square root of cross section, as suggested in [185]. For the spin correlation matrix, we consider at each benchmark point only the element that provides the greatest deviation from the SM. At all benchmark energies, we also show the reach of the total cross section σ, taking into consideration only statistical uncertainty.

It is clear from Fig. II.5 that, at energies high enough to be sensitive to the CP violation in the EW theory, the quantum information observables diminish the sensitivity with no advantage. At Belle II energies, the concurrence has a slightly better sensitivity for real couplings compared to the spin correlations, but at the price of significantly worse sensitivity for imaginary couplings. Moreover, the bounds are derived from one single element of the C matrix; the sensitivity can be enhanced by considering more than one entry, as well as the polarisation vectors B. Thus, we argue that the quantum observables perform worse in resurrections scenarios, and the strongest bounds are instead provided by the spin correlation matrix directly.

Quantum information observables do not display increased sensitivity to the phase of the Wilson coefficient, and are unable to distinguish CP conserving and violating scenarios. Due to their definition, which involves taking the eigenvalues of a 3×3 matrix, understanding analytically the reason behind these facts is challenging. The C matrix coefficients, instead, can be easily calculated and interpreted. Experimentally, measuring the C matrix is needed to reconstruct the density matrix, so there seems to be no advantage in using quantum information observables in this scenario.

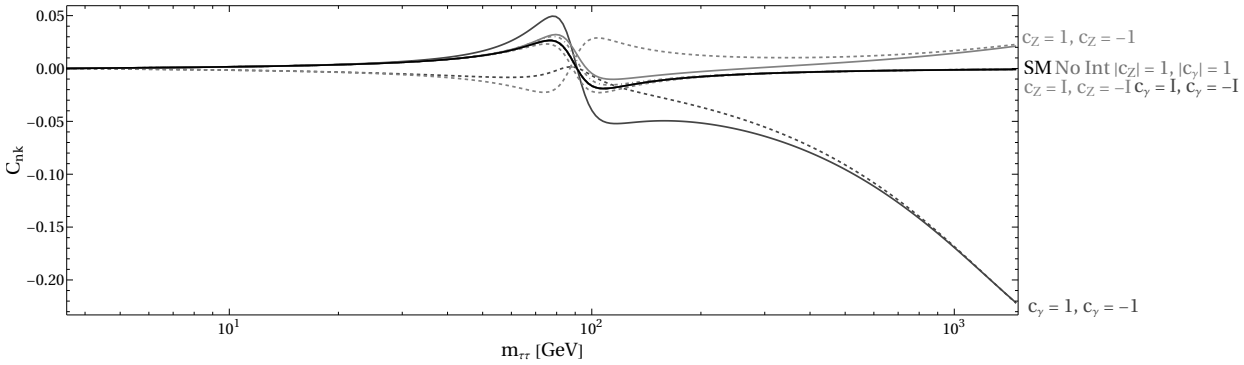

Figure II.4: Same as Fig. II.1, but for the (nk) element of the spin correlation matrix. Unlike the quantum information observables, here the SMEFT squared contribution is negligible, and the interference gives the leading deviation from the SM. Moreover, the sign of the real part of the Wilson coefficient changes dramatically the shape of the curve, everywhere but near the NP scale Λ. Note that the imaginary part of the Wilson coefficient contributes modestly to negligibly, but the roles of imaginary and real parts are exchanged in the (nr) element, such that the phase of the Wilson coefficient can be obtained by examining all the elements of the C matrix.

II.4.2.3 Hadron Colliders

At hadron colliders, the LO prediction at partonic level has to be weighted by the PDF of the partons, as explained in Section II.3. Figures II.6 to II.9 are the analogue of Figs. II.1 to II.4, and the same patterns can be seen regarding resurrection of interference. Namely, the net effect of the resurrection phenomenon in the Bell inequality marker $\mathfrak{m}_{12}$ and the local quantum uncertainty LQU is to decrease the sensitivity to the NP scale Λ. For the concurrence $C[\rho]$ the resurrection phenomenon improves the sensitivity, but only for real Wilson coefficients. In the spin correlation matrix elements, instead resurrection improves the sensitivity, both for real and imaginary Wilson coefficients.

As mentioned in Section II.3.2, the measurement of spin correlations at hadron colliders is much more involved than at lepton colliders. Indeed, while at lepton colliders the ambiguity due to the non-measurement of neutrinos can be resolved using impact parameters [153], the same task is made more difficult at hadron colliders by the lack of knowledge of the c.o.m. frame. Measurements at resonances, such as $m_{\ell\ell} = m_Z(m_H)$ can partially circumvent this difficulty by assuming the process predominantly occurs via on-shell $Z(H)$ decay [187]. Indeed, a measurement of the τ polarisation has recently been performed at the CMS experiment, using a sample with an integrated luminosity of 36.3 fb^{-1} [188]. Different strategies have been devised to boost the reconstruction efficiency for the τ momentum, including matrix element [189] and machine learning [190–192] techniques, and a dedicated algorithm to calculate the spin correlation coefficients at hadron collider exists [193].

Given the difficulties posed by a measurement of polarisations at collider, we do not try here to estimate the experimental uncertainty on the spin correlation coefficients. Instead, we report the uncertainty that a Z-pole measurement should have to reach the benchmark bound $C_\gamma \lesssim 1/1.5\,\text{TeV}^2$, obtained from high-energy measurement of the cross section. That is, to be competitive with the limit reported in Ref. [155] at 95%CL, the uncertainty

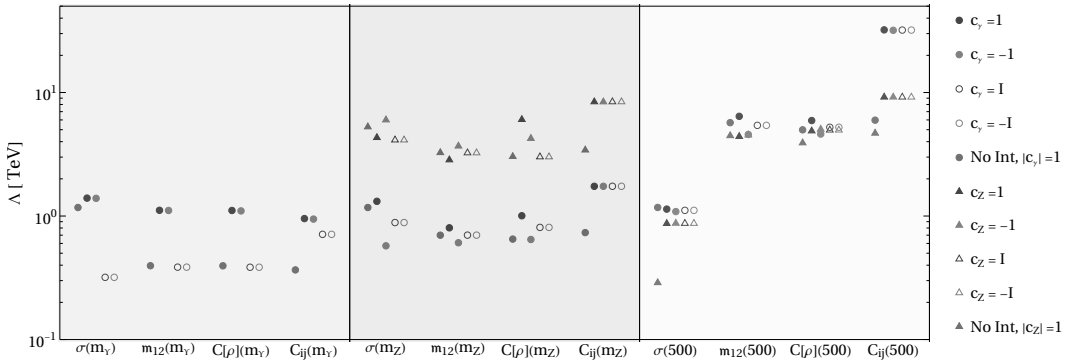

Figure II.5: 95% CL (confidence level) sensitivity on the new physics scale Λ for the $\mathcal{O}_{V\tau}$ operators, derived from measurements of the total cross section, as well as different spin correlation observables at three benchmark energies. Quantum information observables perform similarly or better than the single coefficient of the C matrix at Belle-II energies, where the photon dominates and there is no CP violation, but become progressively less effective at higher energies, performing poorly compared to the spin correlation coefficient. NP scales lower than the EW scale are not plotted.

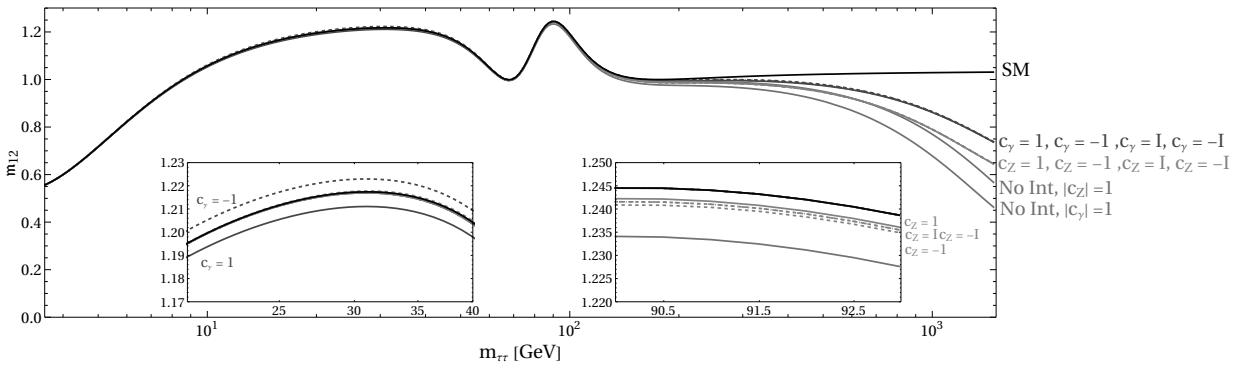

Figure II.6: Same as Fig. II.1, but for pp initial state.

$\delta C(\delta B)$ on the entries of $C(B)$ need to satisfy

$$\begin{aligned} \delta B &< 0.0005\,, \\ \delta C &< 0.008\,, \end{aligned} \tag{II.81}$$

to be contrasted with the current uncertainty of $\delta B_{\rm CMS} = 0.015$ [188]. Similarly to the ee case, the phase of the Wilson coefficient can be determined by measuring all the entries of B and C. For the weak dipole, an exclusion of $C_Z \lesssim 1/1.5\,\text{TeV}^{-2}$ is expected if the following experimental uncertainties can be reached

$$\begin{aligned} \delta B &< 0.003\,, \\ \delta C &< 0.03\,. \end{aligned} \tag{II.82}$$

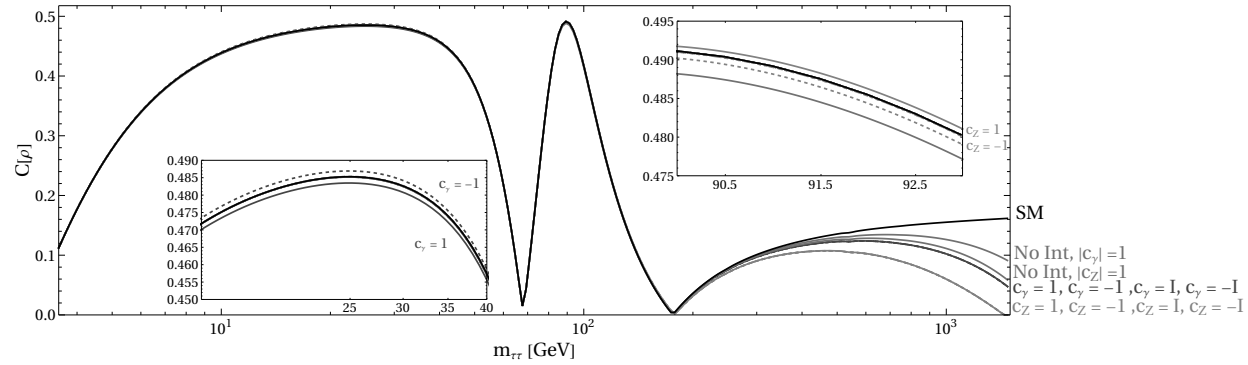

Figure II.7: Same as Fig. II.2, but for *pp* initial state.

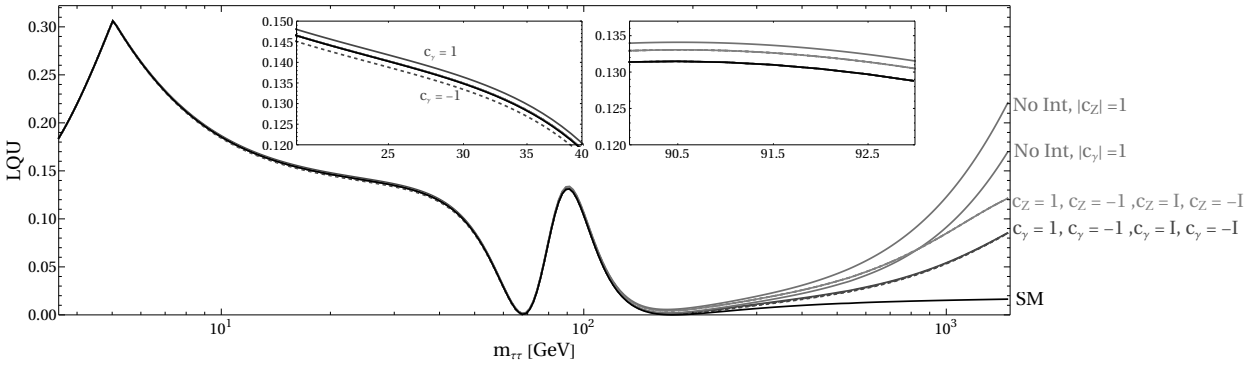

Figure II.8: Same as Fig. II.3, but for *pp* initial state.

II.5 Conclusions and Outlook

In this section we explored interference resurrection in 4-fermion scattering by measuring the final-state angular correlations, and the resulting improvement in sensitivity to SMEFT operators. We find that, at moderate and large energies compared to the EW scale, spin observables greatly outperform the cross section in sensitivity. We also consider quantum information observables, which have obtained considerable attention lately in the top sector, and have been shown to outperform other angular observables as a probe of SMEFT operators [127]. We compare the sensitivity on the new physics scale Λ for γ or Z dipole operators, in Fig. II.5, and find that there is no advantage in employing quantum observables like the concurrence $C[\rho]$, the Bell inequality violation marker $\mathfrak{m}_{12}$ or the local quantum uncertainty LQU. Indeed, classical spin correlations significantly improve the sensitivity in comparison to both cross-section measurement and quantum information observables. As we show in Figs. II.1 to II.4 for the *ee* case and Figs. II.6 to II.9 for the *pp* case, the resurrection is only partially successful in the quantum information observables, because phase information is lost, and in some cases the interference partially cancels against the SMEFT squared contribution.

We believe that these results in the $\tau\tau$ case differ from the top pair case because top pair production respects CP, C and P parities to a good approximation [122], which imposes

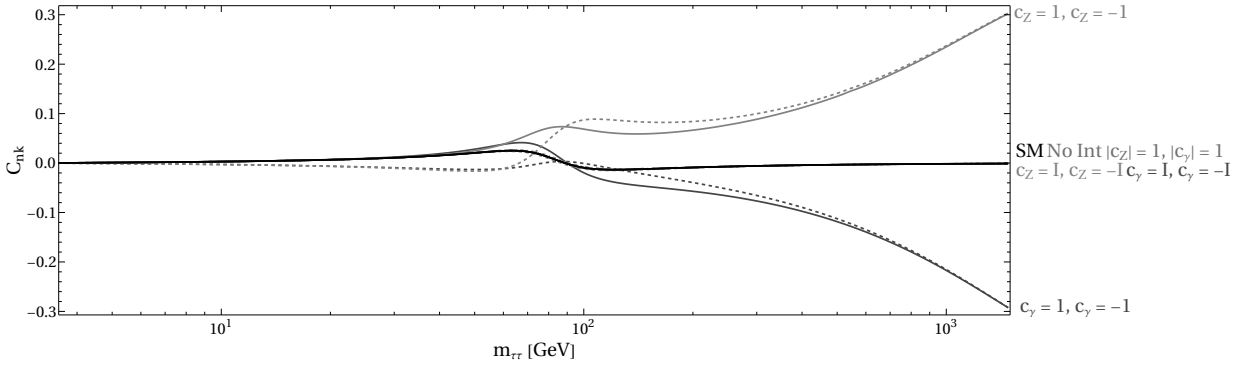

Figure II.9: Same as Fig. II.4, but for pp initial state.

a quite simple spin state. In this case, entanglement can be directly extracted from the diagonal entries of the spin correlation matrix C. However, as we observed in Section II.2.1, resurrection of interference only involves the off-diagonal entries of the C matrix, so the simplified entanglement markers do not participate in resurrection. Moreover, the violation of P and C symmetries makes the simplified criterion for entanglement used in [127] only a sufficient, but not necessary, condition for entanglement. More appropriate entanglement markers are $\mathfrak{m}_{12}$ and $C[\rho]$, that distill the R matrix to a single number, thus losing the ability to differentiate the different off-diagonal components of the C matrix. In addition, the relatively complicated expressions of $\mathfrak{m}_{12}$ and $C[\rho]$, involving the eigenvalues of a 3×3 matrix, hinder an analytical understanding of how exactly the quantum information observables relate to the underlying spin coefficients. We can nonetheless observe in Figs. II.1 to II.4 and II.6 to II.9 that CP information is mostly lost in the quantum information observables at high energies, while the spin correlation coefficients retain it. This support the hypothesis that CP violation is why QCD top pair production is different from EW $\tau\tau$ production. Since the spin correlation coefficients are anyway the building blocks for any quantum information study, they seem like a much more appropriate choice as NP probes. We again stress the difference with top quark pair production, where the Peres-Horodecki criterion allows direct measurement of entanglement, without necessarily measuring the C matrix elements [123].

In summary, in the context of this thesis, the results of this section are both encouraging and discouraging. The understanding of the phenomenon of resurrection as a restoring of coherence between diagrams by a judicious choice of observable is a step ahead in understanding the interplay between fundamental quantum mechanics and the search of new physics. On the other hand, the existence of a direct counterexample dampens our hopes that probing the true quantum nature of the theory, via the measurement of entanglement, would afford us a better sensitivity. That is, while angular correlation resurrect interference, restoring a purely quantum phenomenon, the intrinsically quantum Bell inequality do not seem to better our probes of BSM physics. In addition, it was already known from the literature [125, 126, 194] that tests of Bell's inequality suffer from a loophole distinct from low-energy experiments which, from the point of view of the author, is fatal in trying to establish quantum mechanics at high energies.

With this half-victory of quantum thinking, we move to the next section, where we study the interplay of kinetic and mass mixing for Abelian gauge bosons. As we will see, the interpretation of the phenomenology will lead us to a purely quantum phenomenon, the

quantum Zeno effect described in Section I.1.2.

Part II

Large Mixing in Nearly Degenerate Vector Bosons

CHAPTER III

Large Mixing in Nearly-Degenerate Vector Bosons

III.1 Introduction

New Z' gauge bosons are a ubiquitous feature of many BSM theories, including new $U(1)'$ gauge symmetry extensions of the SM [195–205], models with a vector or axial-vector portal to dark matter or dark sectors [206–214], and models with light vector dark matter [215–220]. Typically, these new Z' vectors are assumed to be well-separated in mass from existing neutral vector states in the SM, including both the Z boson of electroweak symmetry as well as vector mesons from QCD. Correspondingly, for weakly-coupled Z' bosons, the narrow-width approximation affords an intuitive factorisation of the BSM signal phenomenology from the SM background.

Importantly, the narrow-width approximation and subsequent factorisation can be improved by increasing theoretical precision, as in the well-studied case of the Z-γ mixing calculation necessary to extract Z-pole observables at the LEP (Large Electron-Positron collider) experiments [221, 222]. Specifically, the large mass difference between the Z and the photon affords a sound Dyson resummation of the 1-particle irreducible two-point correlation function, given the inverse of the fractional mass separation is much smaller than α, so that interference effects can be treated as subleading at each order in perturbation theory.

In the context of a $U(1)'$ gauge symmetry extension to the SM, the Z' mass parameter and a kinetic mixing coupling [223] between the Z' field strength and the SM hypercharge field strength control the vector boson mass spectrum. Given that the Z width is measured to be 2.4952 ± 0.0023 GeV [224], there is an approximate 5 GeV window for input Z' masses where a cross section factorisation according to the Breit-Wigner prescription [225] breaks down. In this mass range, large kinetic mixing between the Z' and Z boson is expected to be completely excluded given that the Z' properties are expected to wildly disrupt Z-pole observables. This intuition is imprecise, however, since there must exist a decoupled regime where kinetic mixing becomes negligible and Z' bosons avoid exclusion from LEP data.

Here, we employ the required framework to address this oversight, which enables us to calculate the collider phenomenology of Z' bosons in a mass range close to the Z boson and to rigorously extract limits on the kinetic mixing and other Z' properties. Clearly, this framework is highly relevant for interpreting correctly the existing LEP data. Our work is also motivated by the possibility of future Z-pole factories, such as FCC-ee [226] and CEPC [227], which will test the SM electroweak parameters to unprecedented precision

and can offer singular sensitivity in the kinetic mixing vs. Z' mass plane. Moreover, studies of other Z' masses degenerate with SM vector mesons are then also tractable with our framework.

Our calculation is based on the work developed in Refs. [228, 229]. This treatment of 1-loop mixing and oscillation has been adapted to constrain extra Higgs scalars [229] as well as right-handed neutrinos [230, 231]. In hindsight, this formalism also addresses standard studies of K_L, K_S mixing and oscillation as well as neutrino mixing and oscillation [224, 232]. Earlier work on particle mixing in the context of resonant CP violation for strongly mixed scalar or fermion states includes Ref. [233]. The collider phenomenology of two BSM vector bosons with nearly degenerate masses has been considered in Refs. [234, 235]; in this section, we instead consider adding one single vector boson to the SM, and letting it be nearly degenerate with the SM Z resonance.

We will specifically focus on Z, Z', and γ vector boson mixing with the Z and Z' bosons being closely spaced in mass. Since we are motivated to understand very weakly-coupled Z' bosons, we will remain agnostic about the explicit current mediated by the Z' boson and treat the kinetic mixing parameter independently of the Z' gauge coupling. In practice, this is afforded by a hierarchical structure of heavy fermions coupled to the Z' boson that satisfy a trace condition which renders the kinetic mixing parameter to be logarithmic and suppressed by a loop factor [236]. We also recognise that interacting massive Z' bosons are generally restricted to a limited energy range of validity from unitarity unless the $U(1)'$ symmetry is Higgsed [237], but the $U(1)'$ Higgs sector plays no role in our discussion and will also be neglected.

In comparison to earlier treatments of both mixing and oscillation in quantum field theory observables as well as earlier treatments of kinetic mixing for vector bosons, here we will emphasise the mathematical necessity for non-unitary transformations needed to diagonalise the kinetic mixing as well as the independent diagonalisation of the two-point correlation functions and their corresponding impact on phenomenology. This will illustrate fundamental properties of $U(1)$ gauge theories in relation to the optical theorem and the required non-Hermiticity of unstable state masses.

Previous work studying the effects of Z' bosons on electroweak observables include Refs. [198, 238–242]. Notably, only Refs. [198] and [242] explicitly consider the complications of strong Z-Z' mixing in the quasi-degenerate regime, and a related recent discussion of large Z' mixing with the ρ meson was presented in [243].

Our main goal in this work is to present consistent constraints on kinetic mixing in the quasi-degenerate region around the Z pole, calculated from three primary observables: the W boson mass, the Z boson width and the Bhabha scattering rate. We emphasise the importance of avoided level crossing in interpreting the available parameter space, as well as the correct assignment of 1-loop widths that display the quantum Zeno effect [244], which reflects the decoupling of the Z' boson in the double limit of both vanishing kinetic mixing and mass splitting. Unfortunately, previous work did not correctly calculate the physics of the double limit and hence consistent limits on kinetic mixing in the quasi-degenerate regime are presented here for the first time. We critique the earlier literature in Section III.6. The novelty of our results stemming from the phenomena of avoided crossing and the quantum Zeno effect offers a fresh view of the physics of global symmetries, since these phenomena are a characteristic feature of the quantum physics of two-level systems.

In Section III.2, we review gauged $U(1)$ extensions of the SM, as well as kinetic mixing. In Section III.3, we present the formalism for deriving the collider phenomenology of the

Z, γ and a new Z' boson. We derive the improved Breit-Wigner propagators, which reflect the correct pole structure of the massive vector states at 1-loop order. In Section III.4, we discuss the essential features of our Z' model and the canonical diagonalisation of kinetic mixing. We then expand on the quasi-degenerate regime, explaining highly-mixed but decoupled properties of the Z' boson via the quantum Zeno effect and review the feature of avoided crossing. In Section III.5, we present the collider constraints of a quasi-degenerate Z' boson in the kinetic mixing vs. mass plane. We conclude in Section III.7. In Section III.6, we present the physics of the double limit and critically evaluate the previous literature that analysed the quasi-degenerate regime.

III.2 U(1) extensions of the Standard Model

A Z' is a new spin-1 particle that carries a force other than the ones of the SM, and is neutral under the SM gauge group, which implies that it also is its own antiparticle [245]. Many extensions of the SM, tailored to explain phenomena as varied as DM, the apparent unification of gauge couplings (so-called grand-unification theories, or GUT), the origin of electroweak symmetry breaking [246], as well as present and past anomalies in scattering data, have been formulated, see [247] for a classic review. Indeed, adding a Z' to the SM is, both conceptually and as a model building practice, among the easiest extensions one can imagine. Another way in which Z' models arise naturally is by gauging the global symmetries of the SM, in particular gauging the accidental symmetries of the SM is an economical way to explain the absence of violation by higher-dimensional operators [248–250]. Adding a new $U(1)$ gauge boson K to the SM allows for new terms of the form $\epsilon F^{\mu\nu}K_{\mu\nu}$, so-called "kinetic mixing". This term is gauge invariant, since the field-strength tensor of an Abelian gauge boson is invariant by itself, and it is dimension four, so by the "totalitarian principle" [251] it should be added whenever a theory features multiple $U(1)$ gauge symmetries. Moreover, even if it is set to zero at a given scale, loop effects can generate, so long as there is no symmetry that forbids it. If there are fermions charged under both $U(1)$s, for instance, no such symmetry is present, and at 1-loop a non-zero ϵ is generated [223]:

$$\epsilon = -\frac{g' g_K}{16\pi^2} q \ln \frac{M^2}{\mu^2} \,, \tag{III.1}$$

with g_K the gauge couplings of the new gauge group, q and M the charge and mass of the fermions, and μ the renormalisation scale. Given the logarithmic dependence on the fermion mass, one can naively estimate $\epsilon \sim (10^{-2} - 10^{-1}) g_K$ at a low scale [223]. It should be emphasised that this mechanism is only one among many possibilities to generate kinetic mixing in a concrete UV model and indeed even gravitational interactions alone can generate kinetic mixing [252]. In this thesis we will adopt the position that kinetic mixing is an almost inescapable consequence of adding new Abelian gauge bosons, and treat the kinetic mixing parameter as a free parameter of the theory.

Kinetic mixing is studied in the context of so-called "dark sectors", where DM is part of a larger sector that, just like the SM, is composed of matter and force carriers. Then, if DM is not directly charged under the SM gauge symmetries, but it is charged under an Abelian gauge group that mixes via kinetic mixing with $U(1)_Y$, this can act as a "portal" between baryons and dark matter [253–255], explaining in the process the reason why DM interacts so feebly with baryons.

We now introduced the improved Breit-Wigner propagators that we will employ in this study.

III.3 Modified Breit-Wigner Propagators for the Quasi-Degenerate Case

The 1-loop mixing between the SM Z and γ is a canonical example where extraction of constraints on new physics from LEP Z-pole observables using the simple tree-level factorisation by the Z mass and its branching fractions [256] does not lead to the desired level of precision. Indeed, especially when considering new physics affecting electroweak parameters [257, 258], $\gamma - Z$ mixing, which arises at 1-loop, has to be included. When particles have flavour interactions that are misaligned with the mass basis, as for the case of the active neutrinos in the SM, the phenomenon of oscillation is also observed. Mixing and oscillation phenomena simultaneously occur in neutral kaon propagation, where the 1-loop mixing in the mass eigenstates K_L and K_S and their oscillating decay amplitudes gave the first direct evidence for CP violation in weak interactions [259]. In the Z, Z', and γ case, however, since the Z boson's lifetime is $\sim 10^{-25}$ s, oscillation phenomena are completely unobservable at present and future colliders. Hence, we will focus on the modification of the Z propagator and decay rates. Whether oscillation might be phenomenologically relevant for realistic BSM vector bosons nearly degenerate with QCD vector resonances with larger lifetimes, such as the Υ, is left for future work.

Following the analyses of Refs. [228, 229], we provide a modified Breit-Wigner approach to the 1-loop mixing of quasi-degenerate vector bosons. We begin by remarking that since we will be focused on contributions of massive vector bosons near their poles, we can safely neglect the longitudinal parts of the vector boson propagators. This is justified since near the pole, only the pole mass and width, both gauge-invariant quantities, contribute non-negligibly to observables [234]. We remark this consideration also side-steps questions of gauge invariance and unitarity in the renormalisation of gauge bosons [260–264].[1]

Compared to the standard BW (Breit-Wigner) approximation, the main complication in our scenario is that we study mass splittings that are parametrically comparable or smaller than the leading order widths of the involved particles. As a result, it is not possible to assign unequivocally a given field to a pole of the 2-pt. Green's function. Moreover, the standard approach of resumming 1-particle irreducible diagrams into a single propagator presumes large mass splitting from other asymptotic states, and trying to recover a $\delta m \to 0$ limit leads to off-diagonal mixing contributions that are beyond perturbative control, such that a modification of the BW prescription is needed: an early construction is found in Ref. [265].

Separately, propagators of unstable particles treated in an on-shell formalism should mix orders of perturbation theory, as required by the optical theorem. In a BW approximation, only a subset of diagrams is retained in the Dyson series resummation, which generally sacrifices gauge invariance and also unitarity of the theory at high energies [260–262, 264]. One of the advantages of the 1-loop treatment of Ref. [229] is the inclusion of interference diagrams in the Dyson resummation, which improves the treatment of gauge invariance

[1] In particular, the full propagator of a vector boson, in R_ξ gauge, is expressed as

$$i\Delta_{\mu\nu} = \left(g_{\mu\nu} - \frac{p_\mu p_\nu}{p^2}\right) \frac{-i}{p^2 - m^2 + \Pi_T} + \frac{p_\mu p_\nu}{p^2} \frac{-i\xi}{p^2 - \xi(m^2 - \Pi_T - p^2\Pi_L)} \ ,$$

where Π_T and Π_L are defined via $\Pi_{\mu\nu} = \Pi_T g_{\mu\nu} + \Pi_L \, p_\mu p_\nu$, with $\Pi_{\mu\nu}$ denoting the self-energy at momentum p [234]. We remark that both the gauge-dependent term – which will anyway cancel against the ghost contributions in observables [221] – and the gauge-independent term contributing to the longitudinal propagator are numerically negligible, since they are suppressed by the small ratio $m_f/\sqrt{p^2}$, with m_f (typically the electron mass) as the smaller of the initial and final fermion masses, after contracting the propagator with the incoming and outgoing fermions.

and hence ameliorates unitarity issues. As a result, since only gauge invariant quantities are used in the calculation, we retain good accuracy in a wide regime around the pole masses.

We begin with the renormalised irreducible 2-pt. vertex function matrix as a function of the Mandelstam variable s. Denoting the vector fields as Z, A, and K for the SM Z boson, photon, and new physics gauge boson, respectively, we have

$$\mathbf{\Gamma} = i(s\mathbb{1} - \mathbf{M}(s)) = i \begin{pmatrix} s - m_Z^2 - \Pi_{ZZ}^T(s) & -\Pi_{ZA}^T(s) & -\Pi_{ZK}^T(s) \\ -\Pi_{ZA}^T(s) & s - \Pi_{AA}^T(s) & -\Pi_{AK}^T(s) \\ -\Pi_{ZK}^T(s) & -\Pi_{AK}^T(s) & s - m_K^2 - \Pi_{KK}^T(s) \end{pmatrix} \tag{III.2}$$

where $\mathbf{M}(s)$ is the 1-loop improved mass squared matrix that contains the renormalised self-energies. The propagator matrix is the negative inverse of $\mathbf{\Gamma}$: $\mathbf{\Delta}(s) = -(\mathbf{\Gamma})^{-1}$.

As mentioned previously, we only retain the transverse part of the propagator as we are only interested at the region near the pole where the (gauge-dependent) longitudinal part of the propagator is numerically negligible. Furthermore, from now on, we will not write down the s dependence or the T superscript for the self energies Π_{ij}, keeping them implicit.

We first consider the diagonal entries of the propagator matrix $\mathbf{\Delta}$, which are constructed from $\mathbf{\Gamma}$ entries as [2]

$$\Delta_{ii}(s) = \frac{\Gamma_{jj}\Gamma_{kk} - \Gamma_{jk}^2}{\Gamma_{ii}\Gamma_{jk}^2 + \Gamma_{jj}\Gamma_{ki}^2 + \Gamma_{kk}\Gamma_{ij}^2 - \Gamma_{ii}\Gamma_{jj}\Gamma_{kk} - 2\Gamma_{ij}\Gamma_{jk}\Gamma_{ki}} \equiv \frac{i}{s - m_i^2 + \Pi_i^{\text{eff}}} , \tag{III.3}$$

where Γ_{ij} is the (ij) entry of $\mathbf{\Gamma}$, $i = 1, 2, 3$; $j, k \neq i$, and we introduced the effective self-energy

$$\Pi_i^{\text{eff}} = \Pi_i - i\frac{\Gamma_{ij}\Gamma_{jk}\Gamma_{ki} - \Gamma_{ki}^2\Gamma_{jj} - \Gamma_{ij}^2\Gamma_{kk}}{\Gamma_{jj}\Gamma_{kk} + \Gamma_{jk}^2} , \tag{III.4}$$

which preserves the form of an unmixed propagator while including 3×3 mixing contributions, with $\Pi_1 = \Pi_{ZZ}$, $\Pi_2 = \Pi_{AA}$, and $\Pi_3 = \Pi_{KK}$. Note that only the first term of Eq. (III.4) survives in the zero mixing limit.

Next, the off-diagonal entries of $\mathbf{\Delta}$ are

$$\Delta_{ij}(s) = \frac{\Gamma_{ij}\Gamma_{kk} - \Gamma_{jk}\Gamma_{ki}}{\Gamma_{ii}\Gamma_{jj}\Gamma_{kk} + 2\Gamma_{ij}\Gamma_{jk}\Gamma_{ki} - \Gamma_{ii}\Gamma_{jk}^2 - \Gamma_{jj}\Gamma_{ki}^2 - \Gamma_{kk}\Gamma_{ij}^2} . \tag{III.5}$$

The poles of the characteristic polynomial of $\mathbf{\Delta}$ are by definition zeros of $\det(\mathbf{\Gamma})$. This observation allows us to rewrite the elements of $\mathbf{\Delta}$ as

$$\Delta_{ii} = \frac{(s - m_j^2 + \Pi_{jj})(s - m_k^2 + \Pi_{kk}) - \Pi_{jk}^2}{\det(\mathbf{\Gamma})} , \quad \Delta_{ij} = \frac{\Pi_{jk}\Pi_{ki} - \Pi_{ij}(s - m_k^2 + \Pi_{kk})}{\det(\mathbf{\Gamma})} . \tag{III.6}$$

This form makes it clear that *each* of the elements of the propagator matrix has as many poles as zeros of $\det(\mathbf{\Gamma})$, *i.e.* three. This suggests to approximate the propagators as the sum of three Breit-Wigner propagators,

$$\Delta_{ij} \approx \sum_{a=I}^{III} \mathbf{Z}^{ai}\mathbf{Z}^{aj}\frac{i}{s - \mathcal{M}_a^2} \equiv \sum_{a=I}^{III} \mathbf{Z}^{ai}\mathbf{Z}^{aj}\Delta_a^{\text{BW}} , \text{ for } i, j = 1, 2, 3 , \tag{III.7}$$

[2] In this and following expressions, repeated indices are not summed over.

in order to maintain the correct pole structure, where $\mathbf{Z}_{ai}, \mathbf{Z}_{aj}$ are constant coefficients to be determined and the poles are at $\mathcal{M}_a^2$, which can be found by solving $\det(\mathbf{\Gamma}) = 0$.

The coefficients in Eq. (III.7) are determined by imposing the renormalisation conditions of unit residue and vanishing mixing on-shell, *i*.e. we construct a matrix $\mathbf{Z}$ such that

$$\begin{aligned} \lim_{s\to\mathcal{M}_I^2} \frac{-i}{s-\mathcal{M}_I^2} \left(\mathbf{Z}\Gamma\mathbf{Z}^T\right)_{11} &= 1 \ , \\ \lim_{s\to\mathcal{M}_{II}^2} \frac{-i}{s-\mathcal{M}_{II}^2} \left(\mathbf{Z}\Gamma\mathbf{Z}^T\right)_{22} &= 1 \ , \\ \lim_{s\to\mathcal{M}_{III}^2} \frac{-i}{s-\mathcal{M}_{III}^2} \left(\mathbf{Z}\Gamma\mathbf{Z}^T\right)_{33} &= 1 \ , \end{aligned} \tag{III.8}$$

and

$$\lim_{s\to\mathcal{M}_a^2} \frac{-i}{s-\mathcal{M}_a^2} \left(\mathbf{Z}\Gamma\mathbf{Z}^T\right)_{ij} = 0 \ , \tag{III.9}$$

for every $a = I, II, III, i \neq j$.

For example, by expanding the diagonal entry propagator Δ_{11} around the pole $s = \mathcal{M}_I^2$, we obtain

$$\Delta_{11} \approx \frac{i}{s-\mathcal{M}_I^2} \frac{1}{1+\partial_s \Pi_i^{\text{eff}}(s=\mathcal{M}_I^2)} \equiv \Delta_I^{\text{BW}} Z_{I1}^2 \ , \tag{III.10}$$

where the entry

$$Z_{I1} = \frac{1}{\sqrt{1+\partial_s \Pi_1^{\text{eff}}(s=\mathcal{M}_I^2)}} \ . \tag{III.11}$$

On the other hand, for the off-diagonal entry Δ_{12}, expanding around $s = \mathcal{M}_I^2$ gives

$$\Delta_{12} = \Delta_{11}\frac{\Delta_{12}}{\Delta_{11}} \approx (Z_{I1})^2 \Delta_I^{\text{BW}} \left.\frac{\Delta_{12}}{\Delta_{11}}\right|_{s=\mathcal{M}_I^2} \equiv (Z_{I1})^2 R_{I2} \Delta_I^{\text{BW}} \ . \tag{III.12}$$

The $\mathbf{Z}$ matrix then is

$$\mathbf{Z} = \begin{pmatrix} Z_{I1} & Z_{I1}R_{I2} & Z_{I1}R_{I3} \\ Z_{II\,2}R_{II\,1} & Z_{II\,2} & Z_{II\,2}R_{II\,3} \\ Z_{III\,3}R_{III\,1} & Z_{III\,3}R_{III\,2} & Z_{III\,3} \end{pmatrix} \ , \tag{III.13}$$

with elements defined in analogy with Eqs. (III.11) and (III.12). Note that the entries of the $\mathbf{Z}$ matrix can also be interpreted as the finite wave-function renormalisation factors required by the LSZ formalism to be able to employ propagators for external particles [229, 266].[3]

We can now write the momentum-space amplitude for a process $X \to Y$ mediated by *s*-channel exchange of mixing gauge bosons [229]

$$\begin{aligned} \mathcal{A}(X\to Y) &= \sum_{i,j=1,2,3} V_i^X \Delta_{ij}(s) V_j^Y \approx \sum_{i,j=1,2,3} V_i^X \left(\sum_{a=I}^{III} \mathbf{Z}_{ai}\Delta_a^{\text{BW}}(s)\mathbf{Z}_{aj}\right) V_j^Y \\ &= \sum_{a=I}^{III} V_{\text{eff},\,a}^X \Delta_a^{\text{BW}}(s) V_{\text{eff},a}^Y \ , \end{aligned} \tag{III.14}$$

[3]The LSZ formalism for mixed states has been analysed in detail in Refs. [267, 268].

where we defined the effective vertex functions V_{eff} as the sum of the vertex functions of the flavour eigenstates weighted by the Z factors, that is

$$V^X_{\text{eff},\,a} = \sum_{i=1,2,3} \mathbf{Z}_{ai} V_i^X \ , \tag{III.15}$$

and V_i^X is the vertex function of the given in-state in momentum space, *i*.e. the Feynman rule.

If the BSM couplings are kept small, they mostly affect the vertex functions, as expected. However, the off-diagonal propagators in Eq. (III.7) can be comparable with the diagonal propagators for any BSM coupling, if the mass splitting is small enough.

Armed with Eq. (III.15), in Section III.5 we will study the collider phenomenology of the general kinetic mixing that we introduce in the next section. We should stress that we only consider the 1-loop contributions to the propagator of the vector bosons, and ignore the 1-loop vertex renormalisation, as we are interested in the phenomenology near the Z pole, where non-resonant contributions are heavily suppressed.

III.4 Quasi-Degenerate Vector Bosons with Kinetic Mixing, the Quantum Zeno Effect and Avoided Crossing

In this section, we review the procedure to analyse the spectrum and couplings of a $U(1)'$ gauge symmetry that is kinetically mixed with SM hypercharge, initially following Ref. [207]. As mentioned in the Introduction, we will not need to consider Higgs mixing effects in regard to the treatment at the poles of the degenerate Z and Z' bosons. We will also treat the Z' current as generic but leave all SM matter fields uncharged under $U(1)'$. After outlining the standard solution for solving the kinetic mixing, we analyse the case when the Z and Z' bosons are quasi-degenerate. The phenomenological consequence of the propagator treatment of the Z and Z' boson presented in Section III.3 results in a quantum Zeno effect, which is introduced in Section III.4.1 and applied in Section III.4.2, that drives the widths apart and, counter to the naive expectation that the Z and Z' bosons are highly mixed when quasi-degenerate, implies decoupling of the Z' from the SM. The phenomenon of avoided crossing is also reviewed. In Section III.6, we critically evaluate the previous literature discussing the quasi-degenerate Z-Z' regime and point out a flaw in previous work that led to incorrect calculations of the bounds in the kinetic mixing vs. Z' mass plane.

We denote the *g*auge basis field K for the new $U(1)'$ symmetry gauge boson when the Lagrangian includes the kinetic mixing between the hypercharge and K field strength tensors, reserving the Z' notation when discussing the *m*ass basis new physics vector field.

We start with the relevant terms of the Lagrangian after spontaneous symmetry breaking $SU(2)_L \times U(1)_Y \times U(1)' \to U(1)_{\text{EM}}$,

$$\mathcal{L} \supset -\frac{1}{4} B_{\mu\nu} B^{\mu\nu} - \frac{1}{4} W^i_{\mu\nu} W^{i\,\mu\nu} - \frac{1}{4} K_{\mu\nu} K^{\mu\nu} + \frac{\chi}{2\cos(\theta_W)} B_{\mu\nu} K^{\mu\nu} + \frac{1}{2} \begin{pmatrix} W^{3\,\mu} & B^\mu & K^\mu \end{pmatrix} \mathbf{M} \begin{pmatrix} W^3_\mu \\ B_\mu \\ K_\mu \end{pmatrix} , \tag{III.16}$$

where $\mathbf{M}$ is the tree-level mass squared matrix of the vector fields in the gauge basis, χ is the kinetic mixing parameter, and $\theta_W = \arctan(g'/g)$ is the SM weak mixing angle. As detailed in Ref. [207], we perform a weak angle rotation R_W which diagonalises the mass matrix but apportions the hypercharge kinetic mixing between the SM Z and γ states.

The diagonalisation of the kinetic mixing is accomplished by subsequent transformations U_1 and U_2, which diagonalise the kinetic mixing but reintroduce mass mixing between the Z and K vector states. A final mass matrix rotation R_M is performed to diagonalise the vector masses. The corresponding matrices are

$$R_W = \begin{pmatrix} c_W & s_W & 0 \\ -s_W & c_W & 0 \\ 0 & 0 & 1 \end{pmatrix} \,,\; U_1 = \begin{pmatrix} 1 & 0 & 0 \\ -\chi^2 t_W & 1 & \chi \\ -\chi t_W & 0 & 1 \end{pmatrix} \,,\; U_2 = \begin{pmatrix} \sqrt{\frac{1-\chi^2}{1-\chi^2 c_W^{-2}}} & 0 & 0 \\ 0 & 1 & 0 \\ \frac{-\chi^3 t_w}{\sqrt{(1-\chi^2)(1-\chi^2 c_W^{-2})}} & 0 & \frac{1}{\sqrt{1-\chi^2}} \end{pmatrix} \,, \tag{III.17}$$

$$R_M = \begin{pmatrix} c_M & 0 & s_M \\ 0 & 1 & 0 \\ -s_M & 0 & c_M \end{pmatrix} \,,\; \tan\theta_M = \frac{1}{\beta \pm \sqrt{\beta^2+1}} \,,\; \beta \equiv \frac{m_{Z,\,\mathrm{SM}}^2(1-\chi^2)^2 - m_K^2(1-\chi^2\,c_W^{-2} - \chi^2\,t_W^2)}{2m_K^2\,\chi\,t_W\sqrt{1-\chi^2\,c_W^{-2}}} \,,$$

where the upper (lower) sign in the definition of θ_M corresponds to $m_{Z,\,\mathrm{SM}} > m_K$ ($m_{Z,\,\mathrm{SM}} < m_K$).

After diagonalisation, this tree-level vector boson mass squared matrix reads

$$\mathrm{diag}\left(\frac{m_{Z,\,\mathrm{SM}}^2 + m_K^2 - \chi^2\,m_{Z,\,\mathrm{SM}}^2 + \Delta_\chi}{2(1-\chi^2\,c_W^{-2})},\; 0,\; \frac{m_{Z,\,\mathrm{SM}}^2 + m_K^2 - \chi^2\,m_{Z,\,\mathrm{SM}}^2 - \Delta_\chi}{2(1-\chi^2\,c_W^{-2})} \right) \,, \tag{III.18}$$

with

$$\Delta_\chi = \sqrt{(m_{Z,\,\mathrm{SM}}^2\,(1-\chi^2) - m_K^2)^2 + 4m_{Z,\,\mathrm{SM}}^2 m_K^2\,\chi^2\,t_W^2} \,. \tag{III.19}$$

We remark that the massive gauge bosons exhibit avoided crossing already at tree-level, since Δ_χ always causes the mass eigenvalues to move further apart compared to the diagonal entries before the θ_M rotation. In summary, the new mass basis for the neutral gauge bosons is

$$\begin{pmatrix} \tilde{Z}_\mu \\ \tilde{A}_\mu \\ Z'_\mu \end{pmatrix} = R_M^T U_2^{-1} U_1^{-1} \begin{pmatrix} Z_{\mathrm{SM},\,\mu} \\ A_\mu \\ K_\mu \end{pmatrix} \,. \tag{III.20}$$

As a result of the basis change, Z'_μ now couples to SM fermions at tree level, while the coupling of the photon $\tilde{A}_\mu$ remains untouched due to the unbroken $U(1)_{EM}$ gauge symmetry.

Moving beyond Ref. [207], we are particularly interested in the double limit where the fractional mass splitting $\delta m \equiv (m_{Z,\,\mathrm{SM}} - m_K)/m_{Z,\,\mathrm{SM}}$ and kinetic mixing χ both approach 0. As evidenced by Eq. (III.17), these limits do not commute, meaning the order in which the limits are taken is crucial. If we first hold χ fixed and finite and take $\delta m \to 0$, then we arrive at a degenerate Z-Z' system that has a maximal mixing with $\theta_M \to \pi/4$. If we instead keep δm fixed and finite and take $\chi \to 0$, then we obtain $\theta_M \to 0$ and the Z-Z' system is again quasi-degenerate for small δm but the Z' boson is decoupled from SM currents. The incompatibility of these limits demonstrates that the typical naive factorisation of resonances fails in the degenerate regime, and more puzzling, approaching a Z_2 symmetric limit seems ill-defined.

The primary pitfall in this line of reasoning is that a consistent 1-loop treatment of the propagator matrix, as presented in Section III.3 will introduce 1-loop contributions to the mass matrix that will void the θ_M definition. As a result, the inclusion of the pole masses extracted from the improved Breit-Wigner treatment also repackages the large

mixing, shifting the interaction dominantly into one of the mass eigenstates. Therefore, we justify the decoupling of the Z' boson even when it is quasi-degenerate with the Z boson. Importantly, there is a regime in the kinetic mixing vs. Z' mass plane that is inaccessible because of avoided crossing in the tree-level Z-Z' masses. The derivation of the physics of the double limit is detailed in Appendix III.6, where we also critically evaluate earlier literature that addressed the quasi-degenerate Z-Z' regime.

We are studying the competition of the explicit breaking of the Z_2 symmetry from 1-loop shifts in the pole masses versus the possible soft breaking from a tree-level mass splitting. To understand the decoupling, we recognise that the mass squared matrix is symmetric but not Hermitian, and that the imaginary terms in the eigenvalues of the mass squared matrix will mark the degree of decoupling. As similar observation in the context of scalar mixing with the Higgs boson was made in Ref. [269], where the authors connected an observed reduction in a particle's width due to mixing with another shorter-lived particle to the phenomenon of the quantum Zeno effect. To that end, we can formalise these subtleties about decoupling and mixing in the quasi-degenerate regime using the language of the quantum Zeno effect.

III.4.1 A Toy Model to Illustrate the Quantum Zeno Effect

The quantum Zeno effect is a feature of quantum systems that allows the time evolution of a given system to be arbitrarily slowed down by repeated measurements [244]. That is, the act of frequent measurement (or any other non-unitary "*observations*") can disturb the unitary evolution of a quantum system by effectively acting as a projection operator.

To understand the mechanism, consider the 2×2 matrix

$$\mathbf{M} = \mathbf{M}_{\text{tree}} + \mathbf{M}_{1\,\text{loop}} = \begin{pmatrix} M^2 - iM\Gamma & -i\epsilon M\Gamma \\ -i\epsilon M\Gamma & M^2 + \Delta_{\text{tree}} - i\epsilon^2 M\Gamma \end{pmatrix} \tag{III.21}$$

as a toy model of two particles of mass M (*i.e.* $\mathbf{M}_{\text{tree}} = \text{ diag}\left(M^2,\, M^2 + \Delta_{\text{tree}}\right)$) having identical interactions, but with the second particle's coupling constant different by a factor ϵ w.r.t the first. We neglect the real part of the 1-loop self-energy because we are only interested in understanding the behavior of the imaginary part of the pole masses. By the optical theorem, the imaginary piece of each entry of $\mathbf{M}$ is related to a tree-level scattering process, but because of mixing, the identification of an imaginary term in the self-energy with the width of any physical eigenstate is incorrect, as we will see below. The absence of an imaginary piece is a self-consistency requirement for the corresponding vector to decouple.

First, if we assume $\Delta_{\text{tree}} \gg M\Gamma$, *i*.e. large mass splitting, the eigenvalues are

$$M_1^2 = M^2 - iM\Gamma + \mathcal{O}\left(M\Gamma/\Delta_{\text{tree}}\right) \;, \quad M_2^2 = M^2 + \Delta_{\text{tree}} - i\epsilon^2 M\Gamma + \mathcal{O}\left(M\Gamma/\Delta_{\text{tree}}\right) \;, \tag{III.22}$$

and we see that the second particle's width is equal to the first one but rescaled by ϵ^2. In this regime, the usual Breit-Wigner approximation and factorisation of resonances is completely justified.

However, if we assume perfect degeneracy, *i*.e. $\Delta_{\text{tree}} = 0$, the exact eigenvalues of this matrix are

$$M_1^2 = M^2 - i(1+\epsilon^2)M\Gamma \;, \quad M_2^2 = M^2 \;. \tag{III.23}$$

We see that one of the particles absorbs all the 1-loop effects, where the imaginary part of its two-point correlation function is the typical $-iM\Gamma$ plus an extra ϵ^2 amount due to

mixing. The other particle, however, is left untouched by 1-loop renormalisation, and in particular develops no width and remains stable, just like in the $\epsilon \to 0$ limit. The key point here is that for $\Delta_{\text{tree}} = 0$, the tree-level mass matrix enjoys a Z_2 symmetry that is broken at 1-loop. But the breaking is saturated, in the sense that only one particle shows the breaking and the other remains at the previously Z_2 conserving value.

Finally, we analyse Eq. (III.21) for $\Delta_{\text{tree}} \ll M\Gamma$, where we have competition between the explicit soft breaking of the Z_2 symmetry by Δ_{tree} and the 1-loop Z_2 breaking from interactions. The eigenvalues of $\mathbf{M}$ are now

$$M_1^2 = M^2 - i(1+\epsilon^2)M\Gamma + \frac{\epsilon^2}{1+\epsilon^2}\left(\Delta_{\text{tree}} + \Delta_{\text{tree}}^2 \frac{-iM\Gamma}{(1+\epsilon^2)^2\,(M\Gamma)^2}\right) + \mathcal{O}\left(\frac{\Delta_{\text{tree}}^3}{(M\Gamma)^2}\right) ,$$
$$M_2^2 = M^2 + \frac{1}{1+\epsilon^2}\left(\Delta_{\text{tree}} - \Delta_{\text{tree}}^2 \frac{-i\epsilon^2 M\Gamma}{(1+\epsilon^2)^2\,(M\Gamma)^2}\right) + \mathcal{O}\left(\frac{\Delta_{\text{tree}}^3}{(M\Gamma)^2}\right) . \tag{III.24}$$

Importantly, the imaginary part of M_2^2 is now suppressed by $(\Delta_{\text{tree}}/M\Gamma)^2$ with respect to the large mass splitting case in Eq. (III.22), and moreover, the first particle still acquires the dominant $(1+\epsilon^2)M\Gamma$ imaginary term as in Eq. (III.23). Indeed, the width of the second particle is

$$\Gamma_2 = -\frac{\text{Im}(M_2^2)}{M} \approx \epsilon^2\,\Gamma\left(\frac{\Delta_{\text{tree}}}{M\Gamma}\right)^2 \ll \epsilon^2\,\Gamma\,, \tag{III.25}$$

where we further assumed $\epsilon \ll 1$, demonstrating explicit agreement with Ref. [269].

We now apply the features of the quantum Zeno effect and the aforementioned avoided crossing behavior from Eq. (III.19) to our quasi-degenerate Z' study.

III.4.2 Applying the quantum Zeno effect to the quasi-degenerate Z' regime

In our Z-Z'-γ scenario with kinetic mixing χ and fractional mass splitting δm between gauge basis vectors $Z_{\text{SM},\,\mu}$ and K_μ, the width of the $\tilde{Z}_\mu$ mass eigenstate changes from $\cos^2\theta_M \Gamma_{Z,\,\text{SM}}$ to $\Gamma_{Z,\,\text{SM}}\left(1 + \left(\tan\theta_M m_{\tilde{Z}}\,\delta m^{\text{Phys}}/\Gamma_{Z,\,\text{SM}}\right)^2\right)$ after diagonalizing the 1-loop mixing, where we defined the fractional mass splitting of the physical eigenstates $\tilde{Z}$ and Z', $\delta m^{\text{Phys}} = (m_{\tilde{Z}} - m_{Z'})/m_{\tilde{Z}}$ and θ_M is the final rotation angle of Eq. (III.17). On the other hand, the width of the $\tilde{K}_\mu$ mass eigenstate changes from $\sin^2\theta_M\,\Gamma_{Z,\,\text{SM}}$ to $\tan^2\theta_M\,\Gamma_{Z,\,\text{SM}}\left(m_{\tilde{Z}}\,\delta m^{\text{Phys}}/\Gamma_{Z,\,\text{SM}}\right)^2$, as a consequence of the quantum Zeno effect. Given $m_{\tilde{Z}}\,\delta m^{\text{Phys}} \ll \Gamma_{Z,\,\text{SM}}$, the $\tilde{K}_\mu$ vector exhibits decoupling, since its contribution to Z-like scattering processes is suppressed by $\tan^2\theta_M (m_{\tilde{Z}}\,\delta m^{\text{Phys}}/\Gamma_{Z,\,\text{SM}})^2$. Again, this arises because the diagonalisation of the 1-loop propagator matrix has removed the χ-induced mixing between the vector states and shifted the leading $\tan^2\theta_M\,\Gamma_{Z,\,\text{SM}}$ effect into the $\tilde{Z}$ propagator.

We remark that the reverse logic self-consistently describes the effect of a possible $\tilde{Z}$ contribution to K-like amplitudes, where we can introduce a dark current and Γ_K width for the K_μ vector. Here, the kinetic mixing leads to a quantum Zeno effect on the Γ_K width correction to the imaginary piece of the $\tilde{Z}$ two-point correlation function, which will exhibit the same $\tan^2\theta_M (m_{Z'}\,\delta m^{\text{Phys}}/\Gamma_K)^2$ suppression.

We stress that, because of avoided crossing, the tree-level eigenvalues from Eq. (III.19) are never the same for any non-vanishing χ, and hence including the 1-loop correction will always induce a small but suppressed width for the Z' boson. The avoided crossing also dictates that the kinetic mixing χ and the physical mass splitting between the $\tilde{Z}$ and Z'

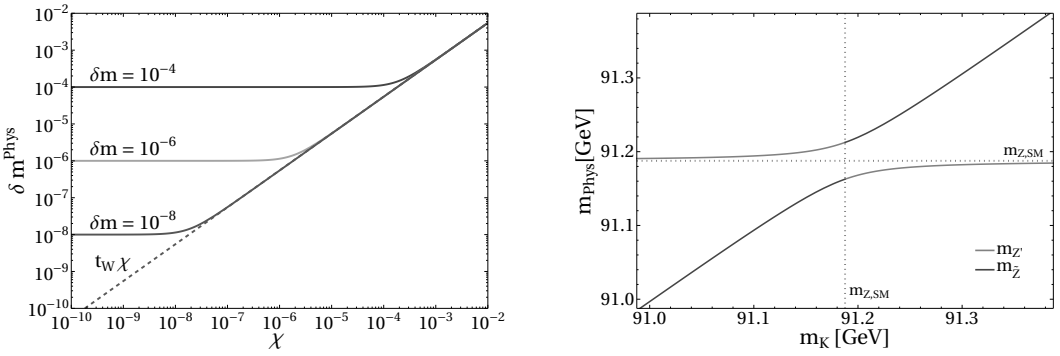

Figure III.1: Left panel: Physical mass splitting as a function of the kinetic mixing χ for three different values of the input fractional mass splitting δm. When $\chi \ll |\delta m|$, the physical mass splitting is equal to the input one, while for $\chi \gg |\delta m|$, the physical mass splitting follows a universal linear scaling with slope t_W. Right panel: Avoided crossing of the mass eigenvalues for fixed $\chi = 10^{-3}$ as a function of input mass m_K.

bosons are not independent, as shown in Fig. III.1. Namely, for a fixed χ, $\delta m^{\rm Phys}$ has two asymptotic limits:

$$\begin{cases} \delta m^{\rm Phys} = t_W \chi & \text{for} \quad |\delta m| \ll \chi \ , \\ \delta m^{\rm Phys} = \delta m & \text{for} \quad \chi \ll |\delta m| \ll 1 \ . \end{cases} \tag{III.26}$$

Hence, for fixed χ, the physical mass $m_{Z'}$ cannot be arbitrarily close to $m_{Z,\,\rm SM}$, and instead we always retain $t_W\chi$ as a dimensionless order parameter of the mass splitting, This is illustrated in the right panel of Fig. III.1 for $\chi = 10^{-3}$, where varying the input m_K parameter smoothly through $m_{Z,\,\rm SM}$ retains a nonzero $\delta m^{\rm Phys}$ for the entire range.

The following approximation is valid in the $\chi \ll |\delta m| \ll 1$ limit:

$$m_{Z'} \approx m_{Z,\rm SM}(1 \pm t_W\chi/2) \ , \tag{III.27}$$

the upper (lower) sign corresponding to $\delta m > 0$ ($\delta m < 0$).

Moreover, as applied to the Z pole, a given χ dictates a minimum $\Delta_{\rm tree}$, and therefore, the width suppression from the quantum Zeno effect Eq. (III.25) cannot completely decouple the Z' boson.

III.5 Collider Constraints on Kinetic Mixing

In this section, we apply the formalism presented in Section III.3 to the Z' model discussed in Section III.4, to derive collider constraints on the kinetic mixing parameter χ in the mass region where the Z' boson is quasi-degenerate with the Z boson.

We eschew performing a full fit to electroweak precision data and instead focus on three observables that would dominate such a fit: the mass of the W boson, the width of the Z boson, and the lineshape for Bhabha scattering ($e^+e^- \to \mu^+\mu^-$) measured by the LEP experiments [222]. These observables are calculated using the six model parameters $m_{Z,\,\rm SM}$, m_K, s_W, χ, $\Gamma_{Z,\,\rm SM}$ and a possible Γ_K. As noted in [238], s_W in the on-shell scheme admits a flat direction in the $(m_{Z,\,\rm SM}, s_W)$ direction of the global electroweak fit, so we set s_W self-consistently with the $m_{\tilde{Z}}$ output of our calculations.

We use the W boson mass instead of the Z boson mass as our observable because the standard global electroweak fit treats the Z mass as an input, testing consistency to the SM electroweak parameters by allowing the input Z mass parameter to float within its ~ 2 MeV uncertainty. For our purposes, it is more tractable to use the aforementioned model parameters and test the consistency with the measured W mass, which is defined in the global SM electroweak fit as [224]

$$m_W = m_Z \, c_W(m_Z) \, \rho^{1/2} \, , \tag{III.28}$$

$$\rho^{1/2} = 1.01019 \pm 0.00009 \, , \tag{III.29}$$

where the running of the weak angle has been absorbed into the measured values of the Fermi constant G_F and cosine of the weak mixing angle at m_Z, $c_W(m_Z)$, while the ρ parameter absorbs the remaining dependence on the relatively poorly-measured top and Higgs masses.

By employing this definition, we assume there is no tension in the observed values of the electroweak precision observables and the observed m_W, so we will employ the world average of $m_W = 80.377 \pm 0.012$ GeV [224], which does not include the recent CDF Run-II result [270]. The better precision of the new CDF result would not appreciably change the magnitude of the constraints on χ. Following our framework, we calculate the Z-like mass eigenvalue from the real part of the pole of the Breit-Wigner propagator, and use Eq. (III.28) to test consistency with the experimental m_W value. This is shown as the Δm_W line in Fig. III.2.

The second major effect from the Z' model would be a modification of the observed total Z width, $\Gamma_{\tilde{Z}}$, from the imaginary part of the pole of the Breit-Wigner propagator. The constraints coming from $\Gamma_{\tilde{Z}}$ moderately depend on the Γ_K parameter that would characterise the effect of a dark vector current coupling for the K boson. As noted in Section III.4, the modification of the observed Z width by finite Γ_K is suppressed by the quantum Zeno effect, a feature which has been missed in previous literature, as described in Section III.6. The constraints from the modification of the Z width are shown as $\Delta\Gamma_{Z,\,\mathrm{SM}}$ lines in Fig. III.2 for given choices of $\Gamma_K/\Gamma_{Z,\,\mathrm{SM}} = 0$, 0.1, 0.5, and 1. We advocate that a modern global fit focusing on kinetic mixing constraints in the quasi-degenerate regime should use a propagator matrix structure as described in Section III.3, since the one-particle Breit-Wigner propagator form would miss essential features of the physics of the double resonance.

This last point also justifies the importance of considering the discretised lineshape of Bhabha scattering as measured by the LEP experiments [222]. We adopt the specific $\sqrt{s}$ center of mass (c.o.m.) energies used in Run 1 of the LEP collider to deconvolute the extracted Z resonance lineshape from a possible sharp resonance feature from a Z' boson. This is illustrated in Fig. III.3, which shows the comparison between the continuous versus discrete $m_{\mu\mu}$ distribution of a Z' boson with $m_{Z'} = 90.5$ GeV and $\chi = 5 \times 10^{-3}$ and $\Gamma_K = 0$ or $\Gamma_K = \Gamma_{Z,\,\mathrm{SM}}$. Clearly, the sharp feature is missed by the discrete scan in $\sqrt{s}$, especially given the beam energy resolution of 0.15% at LEP Run 1 [271], and the resulting discretised points only show a relatively small deviation from the SM expectation. Importantly, the lineshape of Bhabha scattering deviates more strongly for $\Gamma_K = \Gamma_{Z,\,\mathrm{SM}}$, since the Z' feature is distributed over a larger energy range and hence illustrates the importance of calculating the lineshape dependence on Γ_K accurately.

To calculate the constraints on $m_{Z'}$ and χ, we compute the Bhabha scattering cross section on a grid of parameter points for the kinetic mixing model as well as the $\chi \to 0$ and $m_K \to \infty$ decoupled limit that corresponds to the SM. We sample the cross section

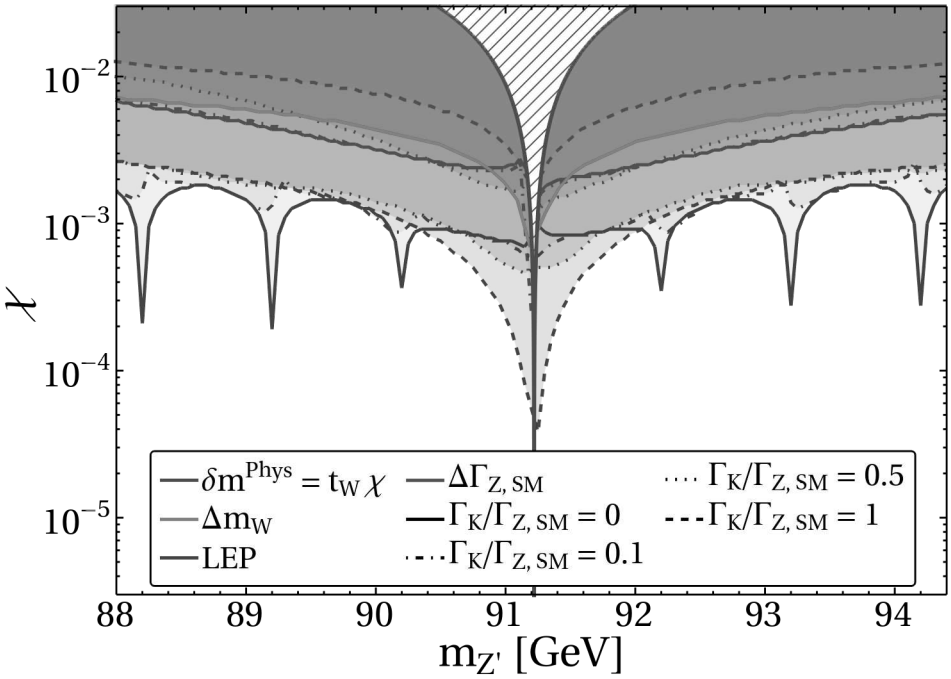

Figure III.2: Constraints in the ($m_{Z'}$, χ) plane arising from excluded shifts in the W mass (red line) and Z-like width (brown lines), as well as Bhabha scattering (blue lines) from LEP Run 1 [222]. The gray hatched region labeled "$\delta m^{\rm Phys} = t_W\,\chi$" shows the ($m_{Z'}$, χ) forbidden region from avoided crossing.

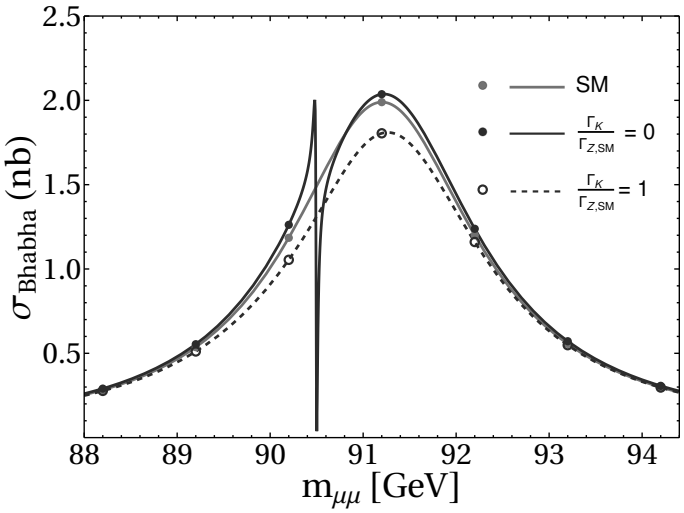

Figure III.3: Cross section rates showing the Z' resonance peak on top of the Z peak in Bhabha scattering for $m_{Z'} = 90.5$ GeV, $\chi = 5 \times 10^{-3}$, and either $\Gamma_K = 0$ (solid blue, filled blue circles) or $\Gamma_K = \Gamma_{Z,\rm SM}$ (dashed blue, hollow blue circles). The SM prediction is also shown (brown line, filled brown circles). The circles indicate the LEP $\sqrt{s}$ energies used in Run 1.

rate with the LEP $\sqrt{s}$ scan points for a total of 10^6 Bhabha events using a Gaussian beam energy spread 0.15% [271]. We then consider the absolute sum of the relative residual defined by these rates,

$$\Delta_{\rm Bhabha} = \sum_{\sqrt{s} \in \text{ LEP scan}} \left| \frac{\sigma^{\rm SM+Z'}_{\rm Bhabha}(\sqrt{s}) - \sigma^{\rm SM}_{\rm Bhabha}(\sqrt{s})}{\sigma^{\rm SM}_{\rm Bhabha}(\sqrt{s})} \right| , \tag{III.30}$$

and compare $\Delta_{\rm Bhabha}$ to the combined statistical and systematic uncertainty from the LEP experiments: this combined uncertainty is estimated from the peak rate of Bhabha scattering,

$$\sigma^{\rm SM}_{\rm Bhabha}(\sqrt{s} = m_{Z,\,\rm SM}) = \frac{12\pi}{m^2_{Z,\,\rm SM}} \frac{\Gamma^{ee}_{Z,\,\rm SM} \Gamma^{\mu\mu}_{Z,\,\rm SM}}{\Gamma^2_{Z,\,\rm SM}} , \tag{III.31}$$

where $\Gamma^{ee}_{Z,\,\rm SM}(\Gamma^{\mu\mu}_{Z,\,\rm SM})$ is the partial width of the SM Z to $e^+e^-(\mu^+\mu^-)$. Hence the experimental uncertainties on the values of the global SM electroweak fit combine to give the aggregate uncertainty for the Bhabha cross section. After including the correlations between the quantities in Eq. (III.31), we impose, at 90% C.L.,

$$\Delta_{\rm Bhabha} < 0.76\% \ . \tag{III.32}$$

The resulting constraints are shown as the blue lines in Fig. III.2 for various choices of Γ_K. As seen in Fig. III.2, the larger Γ_K choices typically lead to stronger constraints, with the notable exception of the spikes for $\Gamma_K = 0$. Here, the fortunate coincidence between the Z' mass and the $\sqrt{s}$ energy from LEP Run 1 lead to enhanced constraints.

In Fig. III.2, we also show a gray hatched region to indicate the forbidden quasi-degenerate regime arising from avoided crossing, which was illustrated in Fig. III.1. For a

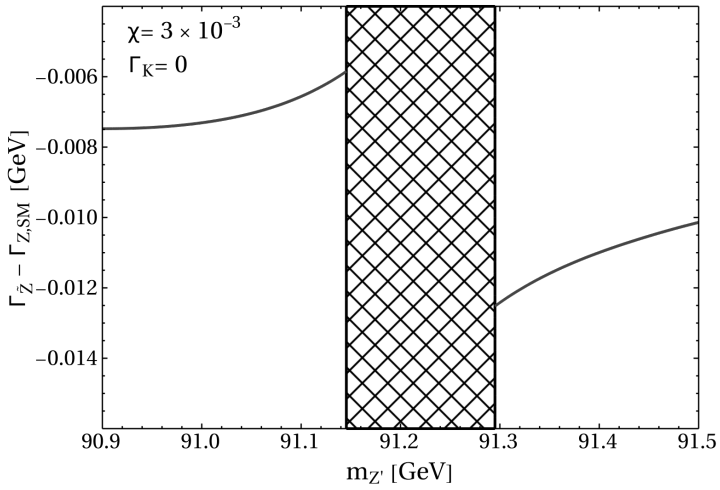

Figure III.4: Shift in the SM-like $\tilde{Z}$ width, for an illustrative parameter point of $\chi = 3 \times 10^{-3}$, $\Gamma_K = 0$, as a function of the physical mass $m_{Z'}$. The discontinuous jump of the width around $m_{Z'} = m_{Z,\,\mathrm{SM}}$ is evident.

given χ, the avoided crossing forces the physical $m_{Z'}$ to deviate from $m_{Z,\,\mathrm{SM}}$ by a minimum amount, see Eq. (III.26).

We remark that the asymmetry in the constraints around the $m_{Z,\,\mathrm{SM}}$ line is a physical effect of the fact that the imaginary part of the pole masses are discontinuous around $m_{Z'} = m_{Z,\,\mathrm{SM}}$.

This is shown in Fig. III.4 for $\chi = 3 \times 10^{-3}$ and $\Gamma_K = 0$.

This discontinuity is caused by the appearance of a mass threshold at $m_{\tilde{Z}}$: as $m_{Z'}$ is dialed to be larger than $m_{\tilde{Z}}$, the $Z' \to \tilde{Z}$ transition gets enhanced resulting in a larger width for the Z' bosons, and a smaller width for the $\tilde{Z}$ boson, because the $\tilde{Z} \to Z'$ process is now classically forbidden. Farther from the degenerate point but still in the $m_{Z'} - m_{Z,\,\mathrm{SM}} \lesssim \Gamma_{Z,\,\mathrm{SM}}$ region, this mass threshold is almost negligible and the constraints are approximately symmetrical around $m_{Z,\,\mathrm{SM}}$. We note here that this effect, which can only be captured if the energy dependence of the self-energies, is not displayed by the effective Hamiltonian treatment of Section III.4.1.

Having emphasised the importance of the $\sqrt{s}$ collider parameter choices and the beam energy resolution in testing for a possible second resonance near the Z pole, we estimate the projected sensitivity improvement in the χ vs. $m_{Z'}$ plane from a GigaZ factory in Fig. III.5. For the GigaZ machine, we assume a finer energy scan, with twice the number of $\sqrt{s}$ choices as LEP Run 1, as well as an effective sensitivity reflecting the higher luminosity and assumed systematic uncertainties improving over the LEP experiments by two orders of magnitude. We reserve a dedicated sensitivity study of the different future e^+e^- machines operating at the Z pole, such as FCC-ee [226] and CEPC [227], for future work.

We also reserve a complete evaluation of the electroweak global fit adding the effects of the quasi-degenerate Z' boson for future work, which would include observables such as forward-backward asymmetries and modifications of α_{EM}. One important aspect of such a global fit would be fixing the normalisation of the observed Z peak in comparison to the

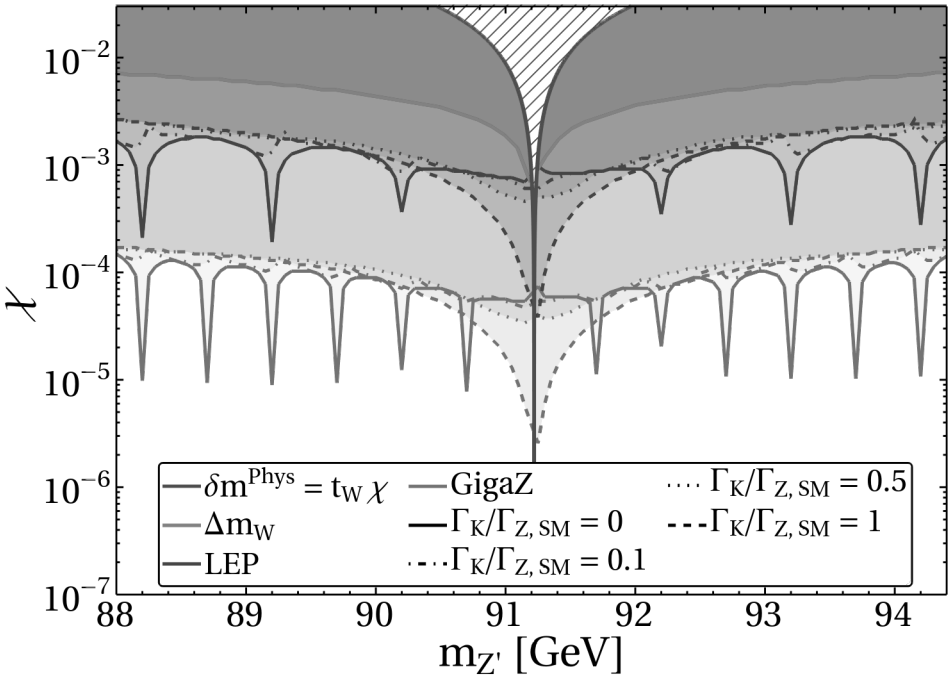

Figure III.5: The same constraints in the $(m_{Z'}, \chi)$ plane from Fig. III.2, with the projection for a Giga-Z factory (light brown lines) running over twice as many $\sqrt{s}$ scan points compared to LEP Run 1.

off-shell region, to avoid theoretical biases about additional resonances or other lineshape distortions. This global fit would also give a robust result for the increase in the quoted Z mass uncertainty of ~ 2 MeV when a quasi-degenerate Z' boson is added to the theory.

III.6 The Double Limit of Vanishing Mass Difference and Kinetic Mixing

In this section, we discuss the physics of the double limit for Z' bosons that are kinetically mixed with hypercharge and also quasi-degenerate with the Z boson. The corresponding $\chi \to 0$ and $\delta m = (m_{Z,\,\mathrm{SM}} - m_K)/m_{Z,\,\mathrm{SM}} \to 0$ limits do not commute, which we demonstrate using the definition of β and $\tan\theta_M$ in Eq. (III.17).

If we first keep χ finite and send $\delta m \to 0$, then $\beta \propto \chi$ and sending $\chi \to 0$ will give $\theta_M \to \pi/4$, leading to a degenerate $Z - Z'$ system that is maximally mixed. On the other hand, if we keep δm finite and take $\chi \to 0$, then $\beta \to \infty$ and $\theta_M \to 0$, which causes the Z' boson to decouple completely from the SM.

We remark that, unfortunately, previous work [198] did not correctly analyse the physics of this double limit. Concretely, Ref. [198] uses the definition of the $Z - Z'$ mixing angle from Ref. [272], which we express in our notation as

$$\tan\theta_M = \frac{2m_{Z,\,\mathrm{SM}}^2 t_W \dfrac{\chi}{\sqrt{1-\chi^2 c_W^{-2}}}\left(m_{Z'}^2 - m_{Z,\,\mathrm{SM}}^2\right)}{\left(m_{Z'}^2 - m_{Z,\,\mathrm{SM}}^2\right)^2 - \left(m_{Z,\,\mathrm{SM}}^2 t_W \dfrac{\chi}{\sqrt{1-\chi^2 c_W^{-2}}}\right)^2} \,. \tag{III.33}$$

Unlike Eq. (III.17), this definition of $\tan\theta_M$ uses the physical Z' mass instead of the input m_K parameter. If this distinction is neglected and we incorrectly replace $m_{Z'}^2$ above by m_K^2, then the mixing angle appears to cross zero at $m_K = m_{Z,\,\mathrm{SM}}$, leading to the conclusion that the exactly mass-degenerate limit generates no shift in the mass. The appearance of a zero in the mass shift expression by [198] is contrary to the phenomenon of avoided crossing.

We remark that the $\Gamma_{\tilde{Z}}$ constraints in [198] are also inconsistent as a result of using the large mass-splitting approximation for the invisible width of the $\tilde{Z}$ boson, $\Gamma_{\tilde{Z},\,\mathrm{inv}} \approx \tan^2\theta_M \frac{m_{Z,\,\mathrm{SM}}}{m_{Z'}}\Gamma_K$. As we explain in Section III.4, while this rescaling of widths is appropriate for large mass-splitting, the qualitatively different behavior of the quantum Zeno effect takes over for the quasi-degenerate regime, where the Γ_K width gives a highly suppressed contribution to the invisible width of the $\tilde{Z}$ boson. Our results from the change in the Z width are calculated using the 1-loop improved BW prescription, and are shown Fig. III.2.

Another feature of the treatment in [198] is a saw-tooth shape of the kinetic mixing constraints in the quasi-degenerate region, where collider experiments are used to give constraints on Z' masses continuously across the Z pole. Although our consistent constraints also exhibit a sawtooth shape, this shape arises because of avoided crossing. Hence, for a given χ, we cannot populate Z' masses continuously across the Z pole, which is another aspect of the physics of the quasi-degenerate regime absent in Ref. [198].

III.7 Conclusions

We have derived consistent collider constraints on a kinetically mixed Z' boson that is nearly degenerate with the SM Z boson, emphasizing the use of an improved Breit-Wigner prescription to avoid an uncontrolled perturbative expansion. We analyse both model-independent constraints, characterised by the kinetic mixing parameter χ, and model-dependent constraints, such as Z' width effects arising from a possible coupling of the Z' boson to a dark sector. Our main results are shown in Fig. III.2, where we show the constraints from the LEP measurements in the χ vs. $m_{Z'}$ plane for the quasi-degenerate regime.

To explain the features seen in Fig. III.2, we needed to consider a double limit of vanishing mass splitting and kinetic mixing and how this limit is calculated using the 1-loop improved Breit-Wigner framework from Section III.3. This motivated a natural explanation of the phenomenology in terms of the quantum Zeno effect and avoided level crossing, which govern the imaginary and real parts of the poles of the Breit-Wigner propagators, respectively. We also remarked in Section III.6 how these phenomena were missed in previous work, leading to wrong conclusions in the nearly degenerate region. Although our treatment via the 1-loop improved Breit-Wigner prescription allows us to derive the correct widths and to derive the quantum Zeno effect, a prescription where the leading order width already approximates the 1-loop improved widths would be useful. In the current framework, the leading order widths undergo an order one correction by the 1-loop improvement. This issue has been partially addressed in Ref. [273], in the context of an effective action for scalar mixing, as well as the very recent Ref. [274], in the context of vector boson mixing. Compared to Ref. [274], we explicitly calculate and show the collider constraints in the χ vs. $m_{Z'}$ plane. We highlight that our results show that the real and imaginary parts of the pole masses are discontinuous at $m_K \simeq m_{Z,\,\mathrm{SM}}$, in contrast to the claim in Ref. [274] that the imaginary part remains continuous.

In this part, we have seen how the interference can become an $\mathcal{O}(1)$ correction to the incoherent cross section, by having two resonances sit closely to each other. In interpreting the phenomenology, the quantum Zeno effect has proven to govern the imaginary part of the Breit-wigner propagators. Thus, a purely quantum mechanical phenomenon, with no classical analogue, was truly relevant to assess the sensitivity to NP. In the next part, we will switch gears, considering nonperturbative effects in quantum mechanics, motivated by analogous effects postulated to happen in the electroweak theory.

Part III

The Quantum Imprint

CHAPTER IV

The Quantum Imprint

IV.1 Introduction

A central puzzle in the study of quantum phenomena is the possible emergence of a classical limit. Empirically, of course, classical physics dominates everyday interactions while the fundamental quantumness of Nature has been established to extraordinary precision [275]. The simplest explanation for this disparate behavior is that the separation of energy or length scales affords an appropriate effective field theory description, upon which a perturbative calculation can accurately capture the dynamics of the relevant degrees of freedom. Exemplars of the success of perturbation theory include the anomalous magnetic moment of the electron and perturbative quantum chromodynamics for jet processes at the Large Hadron Collider [162, 276–278].

Perturbation theory based on Feynman diagrams suffers, however, from factorial growth in the number of diagrams [279, 280]. This makes the possibility of performing a realistic calculation in a quantum theory describing everyday interactions quite remote. Moreover, in absence of precise cancellations, the resulting power series is expected to be divergent [36]. This phenomenon is present also in classical or tree-level computations, so that predictions of the classical limit of a perturbative QFT do not seem possible, even if we were afforded infinite experimental precision and computational power. Namely, the divergent asymptotic nature of perturbative expansions in QFT prohibits solving quantum amplitudes to arbitrarily high order in coupling constants.

Nevertheless, some quantum systems are amenable to resummation methods, such as Borel-Laplace resummation, which characterises and captures the asymptotic nature of the perturbative expansion, as reviewed in Ref. [281]. As the name suggests, the resummation proceeds in two steps, Borel transformation and Laplace transformation. The former turns a divergent series in a variable g into a series, expressed in a new variable z, with nonzero radius of convergence. The resulting series can be analytically continued in the "Borel plane", viz. the complex-z plane. The result of Borel transformation is in turn Laplace-transformed into a *function* valid for any value of g. That is, Borel-Laplace resummation turns an all-order result in perturbation theory from a divergent series into a well-defined function. This process can fail if the Borel-transformed series has poles on the positive real axis, *i.e.* in the domain of integration of the Laplace transform (see, *e.g.*, Refs. [282–284] for more details). Physically, this failure is due to phenomena that lie beyond perturbation theory, such as instantons. Quantum theories with classically degenerate vacua are a good example of this, as they suffer from the lack of Borel-Laplace summability. In turn, the location of the poles in the Borel plane gives precise information about instantons, such as their action and relative importance [285–290].

Far from a failure of the program of extracting exact results from perturbation theory, theories that cannot be Borel-Laplace resummed are, from a modern perspective, studied for the connection they provide between perturbative and nonperturbative data. Indeed, the specific way in which the resummation procedure can fail encodes nonperturbative effects. A general theory of such encodings was developed under the term "resurgence" [32–34]. Aspects of resurgence in QFT and QM have been widely investigated (see, *e.g.*, [291–306]). Applied to high-energy physics, resurgence aims to include nonperturbative effects in the calculation of observables by leveraging its connection to perturbative data. The latter is typically amenable to a systematic computation in practice.

An asymptotic divergent series in a small parameter g and its resummed counterpart approximately agree for the first $\sim 1/g$ orders [21]. This explains the practical success of perturbation theory and redirects studies of its shortcomings to "theory laboratories", *i.e.* questions of internal consistency. Traditionally, QM has provided an ideal environment for such studies [298, 305, 307–313]. Most of these investigations, however, have focused on the vacuum state, or low-lying excitations of the spectrum. Here, instead, along the lines of other notable exceptions [37, 40, 100, 314–319], we are interested in highly excited quantum states, *i.e.* states with energy E_n, where n is large. This is because in the limit $n \to \infty$ and $\hbar \to 0$ we expect all quantum effects to be strongly suppressed, letting us address the aforementioned puzzle of the emergence of classical physics from a quantum world.

The quantum anharmonic oscillator features a single or double well potential, depending on the sign of the quadratic potential term. For highly energetic quantum states, where the quartic term dominates, the general expectation is that the two sign choices give approximately equal results. In this sense the classical limits of these two different theories are then expected to be one and the same. This intuition contrasts with the fact that, at a purely classical level, the theories have different vacuum structure, which should distinguish the two. In this chapter we use techniques of resurgence to study the classical limit of the anharmonic oscillator and straighten this apparent contradiction. Resurgent asymptotics give us the practical bonus of constructing observables from perturbation theory and at the same time removing divergent series from our calculation, which would cast doubts on the validity of any classical limit. Indeed, this has lead to an *exact* quantisation condition for anharmonic oscillators, interpreted as a self-consistency condition on the energy eigenvalues [320]. In particular, we use the method of exact WKB to quantise the anharmonic oscillator. Based on the Balian-Bloch formalism [321], this method quantises the theory by considering all classical paths in a *complex* phase space. The latter drastically contrasts with conventional WKB computations, which only consider classical paths that lie entirely on the real axis. Paths off the real axis, being classically inaccessible, are then interpreted as purely quantum, typically describing tunneling solutions (instantons).

We anticipate here our findings: even in the classical limit, the amplitudes of the theory contain information on the quantum nature of the system. We prove this explicitly for the anharmonic oscillator for the case of amplitudes of the type $\langle \nu \,|\, x \,|\, 0 \rangle$, whose classical limit has been calculated to all orders in Refs. [40, 319]. We show that they match exactly the action of the imaginary classical path that enters the quantisation condition. We believe this result – which we coin the "quantum imprint rule" – to hold in any quantum theory, possibly with modifications due to different structure of the vacuum, as we elaborate in the main text.

This chapter is arranged as follows. In Section IV.2 we briefly review the WKB method and how it is related to the quantisation of a classical theory. Then, in Section IV.3, we apply this to the quantum mechanical anharmonic oscillator featuring a symmetric dou-

ble well potential. In particular, we revisit its exact quantisation condition by including instantons everywhere in the complex plane. Section IV.4 contains a derivation of the quantum imprint rule, the key result of our work. We then interpret and discuss the universality and possible extensions of our result to QFT. Finally, conclusions and prospects for future studies are contained in Section IV.5.

IV.2 The Exact WKB Method and Quantisation of Periods

We review the exact WKB method and its application in QM, with an emphasis on the quantisation condition from perturbative and nonperturbative cycles. We begin, as usual, by constructing wave function solutions to the Schrödinger equation as a formal power series in $\hbar$ [322], giving asymptotic series expansions of quantised energy level eigenvalues. Our discussion closely follows Ref. [323], and a more pedagogical introduction can be found in Ref. [284].

IV.2.1 The WKB Approach

The general idea behind the WKB method is that the quantum action, controlled by the expansion parameter $\hbar$, is small compared to the classical action associated to the particle's motion. That is, $\hbar$ is small compared to the classical phase-space volume occupied by the particle, and as such, the WKB ansatz is a semiclassical expansion. Quantum mechanically, this corresponds to particle states at large quantum numbers, occupying many quanta of the available phase space.

In QM, the dynamics of a particle moving in a potential $V(x)$ are governed by the Schrödinger equation,

$$\hbar^2\psi''(x) + p^2(x)\psi(x) = 0\,, \tag{IV.1}$$

where $\psi(x)$ denotes the particle's wave function, the prime denotes a derivative with respect to x, the mass has been set to unity, and p is the momentum associated to the energy E of the particle,

$$p(x) = \sqrt{2\,(E - V(x))}\,. \tag{IV.2}$$

Using the WKB approach, we write $\psi(x)$ as

$$\psi(x) = \exp\left(\frac{i}{\hbar}\int^x \mathrm{d}y\, Q(y)\right)\,, \tag{IV.3}$$

where $Q(x)$ is an unknown function. The WKB ansatz transforms Eq. (IV.1) into a Riccati equation on $Q(x)$,

$$Q^2 - i\hbar Q' = p^2(x) = 2\,(E - V(x))\,. \tag{IV.4}$$

At this level, we are simply rewriting the Schrödinger equation, but the chosen form for $\psi(x)$ is particularly apt for a semiclassical expansion. In the limit in which $\hbar$ is small, the wave function becomes highly oscillatory, *i.e.* its de Broglie wavelength becomes unobservably small. Since analytic solutions to Eq. (IV.4) for general $V(x)$ are lacking, we expand $Q(x)$ as a power series in $\hbar$,

$$Q(x) = \sum_{k=0}^{\infty} Q_k(x)\hbar^k\,, \tag{IV.5}$$

which, according to Eq. (IV.4), dictates a recursion relation of the series coefficients of $Q(x)$,

$$Q_{k+1}(x) = \frac{1}{2Q_0(x)} \left(iQ'_k(x) - \sum_{i=1}^{k} Q_i(x) Q_{k+1-i}(x) \right) , \tag{IV.6}$$

with $Q_0(x) = \pm p(x)$. Here, the two sign choices generate two independent solutions of Eq. (IV.4). This recursion relation enables us to reconstruct the wave function to arbitrary order in $\hbar$, in principle.

We can now notice that not all terms of the series expansion (IV.5) carry relevant information. If we split the series expansion into contributions of even and odd powers of $\hbar$,

$$Q(x) = \sum_{k=0}^{\infty} Q_{2k}(x)\hbar^{2k} + \sum_{k=0}^{\infty} Q_{2k+1}(x)\hbar^{2k+1} \equiv P(x) + Q_{\text{odd}}(x) , \tag{IV.7}$$

we find that the odd contributions are a total derivative,

$$Q_{\text{odd}}(x) = \frac{i\hbar}{2} \frac{P'(x)}{P(x)} = \frac{i\hbar}{2} \frac{\mathrm{d}}{\mathrm{d}x} \log P(x) . \tag{IV.8}$$

Therefore, we can drop the odd contribution and write

$$\psi^{\pm}(x) = \frac{1}{\sqrt{P(x)}} \exp\left(\pm \frac{i}{\hbar} \int^x \mathrm{d}y\, P(y) \right) , \tag{IV.9}$$

where the sign corresponds to the sign choice made on Q_0. Strictly speaking, we have only rewritten a solution of the Schrödinger equation in terms of a formal power series expansion in the quantum action. We have not yet made a step towards describing true *quantum* solutions of the system, in the sense that the eigenfunctions of the Hamiltonian have to span a Hilbert space, which is only true if the particle's energy is quantised according to $\hbar$. In the WKB framework, the necessary condition is implemented via the quantisation of so-called quantum periods, which we discuss next.

IV.2.2 Connection Problems, Quantum Periods, and Quantisation

The linearity of the Schrödinger equation, together with the two possible sign choices in Eq. (IV.9), implies that the most general form of the wave function is

$$\psi(x) = a^+\psi^+(x) + a^-\psi^-(x) . \tag{IV.10}$$

Asymptotic boundary conditions then determine the coefficients $a^{\pm}$, since the sign of the imaginary part of $p(x)$ dictates whether a solution grows without bounds ("dominant") or vanishes ("recessive") at infinity. Due to the normalisability of the wave function, only a recessive solution is viable at infinity and the behavior of its coefficient can be uniquely established. That is, asymptotic boundary conditions at infinity only specify the recessive solution, leaving the dominant contribution unspecified [324]. The recessive solution is then analytically continued from infinity. However, if a point is encountered where $p(x)$ vanishes along this process, either of the solutions changes discontinuously, since the integration region of the exponent in Eq. (IV.9) now includes a branch point of the integrand. Beyond the branch point, a different linear combination of $\psi(x)^+$ and $\psi(x)^-$ is employed, such that requiring continuity of the wave function casts the WKB method into a "connection problem", *i.e.* the problem of finding the coefficients $a^{\pm}$ in one region given a set of known coefficients in another region. A complete solution of this

connection problem requires analytical control over exponentially suppressed quantities around the branch points of $p(x)$ [325]. Indeed, if such a solution can be found, it is expressed in terms of a connection formula.

The points where $p(x)$ vanishes are called "turning points", because in a classical theory they are the points where kinetic energy vanishes and the particle reverses its motion. Due to conservation of energy, they are given by

$$p(x)^2 = E - V(x) = 0\,. \tag{IV.11}$$

A region where $p(x) > 0$ is then classically allowed, while a region where $p(x) < 0$ is classically forbidden. As a simple example, let us consider a confining potential $V(x)$ that features exactly two turning points, x_- and x_+. In the quantum theory, we expect the wave function of the particle to be highly oscillating in the classically allowed region inside the well and exponentially decaying outside of it. This behavior has to be mimicked by the WKB ansatz (IV.9) and, as explained before, the two different behaviors have to match at the turning points of the potential. Crucially, in a scenario involving only two turning points, solving this connection problem leads to the quantisation condition (see, *e.g.*, Ref. [284])

$$\int_{x_-}^{x_+} \mathrm{d}x\, P(x) = \pi\hbar \left(n + \frac{1}{2}\right)\,, \tag{IV.12}$$

where n is an integer. We stress that this expression is *exact*. At the same time, the LHS is given as a formal power series in $\hbar$. An approximation of the latter by its leading order term leads to the well-known Bohr-Sommerfeld quantisation,

$$\int_{x_-}^{x_+} \mathrm{d}x\, p(x) = \pi\hbar \left(n + \frac{1}{2}\right)\,. \tag{IV.13}$$

This can be thought of as a quantisation of the phase space volume that is occupied by the particle of energy E, as given by the LHS of this relation. The solutions to this equation finally give the quantised energy levels, $E = E_n$. In this sense, the exact quantisation condition (IV.12) incorporates higher order corrections to the Bohr-Sommerfeld formula.

In more geometric terms, the integral between the two turning points can be written as an integral along a contour $\mathcal{A}$ in the complex plane, which encircles the allowed classical motion of the particle at the corresponding energy,

$$\int_{x_-}^{x_+} \mathrm{d}x\, P(x) = \frac{1}{2} \oint_{\mathcal{A}} \mathrm{d}x\, P(x)\,. \tag{IV.14}$$

Closing the contour in the complex plane regularises the integral on the LHS, which otherwise would suffer from divergences at the turning points, because these are branch points of the integrands (see, *e.g.*, Ref. [284]). The RHS of Eq. (IV.14) is typically referred to as a "quantum" or "WKB period".[1] Using the formal series expansion of $P(x)$ in powers of $\hbar$, the exact quantisation condition can be written as

$$\oint_{\mathcal{A}} \mathrm{d}x\, P(x) = \sum_{k=0}^{\infty} \mathrm{vol}_k(E)\hbar^{2k} = 2\pi\hbar \left(n + \frac{1}{2}\right)\,, \tag{IV.15}$$

where we have defined the quantum coefficients of the occupied phase space volume,

$$\mathrm{vol}_k(E) = \oint_{\mathcal{A}} \mathrm{d}x\, Q_{2k}(x)\,. \tag{IV.16}$$

[1] The name is chosen in analogy to integrals that appear in the calculation of planetary orbits.

These volumes substantially enter connection formulas, as we have already seen for the case of a potential with two turning points. Implementing them in practice, however, is not straightforward. Generically, the series expansion in Eq. (IV.15) is factorially divergent, $\mathrm{vol}_k(E) \sim (2k)!$. The situation is even more dire, as it is typically not even Borel-Laplace resummable. Therefore, we have to consider exponentially suppressed corrections to the formal power series responsible for lifting the ambiguities that lead to the failure of Borel-Laplace summability.

The problem is even more pronounced in QM systems involving more than two classical turning points. The pairwise matching of turning points to build quantum periods must also be tessellated to cover the entire Borel plane [320], since a consistent connection formula needs to take into account all possible periods [326]. As a blessing in disguise, the inclusion of these periods in turn corresponds to the aforementioned exponentially small corrections that enable unambiguous resummation. We already provided a concise introduction to the theory of asymptotic series and Borel-Laplace resummation in Section I.1.5, but a more detailed introductory account can be found in Refs. [282–284].

IV.3 The Exact Quantisation Condition in the Symmetric Double Well

Applying the exact WKB method in practice requires analyzing situations with multiple turning points, which can be associated with perturbative or nonperturbative phenomena in the quantum theory. We will study these details in the context of the double well potential following Ref. [284].

IV.3.1 Classical Turning Points and their Structure

The symmetric double well is a prime example from QM where nonperturbative effects play a crucial role, since the instanton solutions breaks the classical denegeracy of equivalent vacua. Said degeneracy is conserved in the energy levels derived from perturbation theory and only broken nonperturbatively (see, *e.g.*, Refs. [298, 299]). We remark that QM models with smooth potentials cannot undergo spontaneous symmetry breaking, because instantons explicitly break the classical symmetry enjoyed by degenerate vacua. Thus, their effect in understanding the physics of QM systems is irreducible. The exact WKB method systematically accounts for instanton effects and results in a recipe to unambiguously calculate observables whose series expansion is otherwise not Borel-Laplace resummable.

We parameterise the symmetric double well potential as

$$V_{\mathrm{DW}}(x) = \frac{1}{32g^2}\left(1 - 4g^2x^2\right)^2 . \tag{IV.17}$$

The classical vacua are located at $v_\pm = \pm 1/(2g)$, with an energy barrier of height $\Lambda = 1/(32g^2)$ separating them. The potential has four classical turning points. Due to the $\mathbb{Z}_2$ symmetry of the theory, the turning points come in pairs and, for given E, are

$$a^2 = \frac{1 + 4\sqrt{2Eg^2}}{4g^2}\,, \quad b^2 = \frac{1 - 4\sqrt{2Eg^2}}{4g^2}\,. \tag{IV.18}$$

Note that b becomes imaginary if the particle's energy exceeds the potential barrier, $E > \Lambda$. Thus, the turning point structure of the double well characterises classically allowed and forbidden regions.

Intuitively, a particle with energy less than Λ will oscillate around one of the two minima between the turning points $x \in (-a, -b)$ or $x \in (b, a)$. Quantum mechanically, of course, the particle can tunnel through the classically forbidden region $(-b, b)$ to the other well. The classically allowed (forbidden) region is associated to the WKB contour $\mathcal{A}$ ($\mathcal{B}$) from Eq. (IV.14), lying on the real axis and encircling the corresponding turning points.

We now consider $E > \Lambda$, such that the particle can cross over the barrier to the second well. The classically allowed region, characterised by the cycle $\mathcal{A}$, now extends from $x = -a$ to $x = a$, while the formerly forbidden region with $x \in (-b, b)$ has moved to the imaginary axis in the complex plane. In this case, the contour $\mathcal{B}$ does not describe below-the-barrier tunneling any more, instead corresponding to above-the-barrier reflection. Nevertheless, it contains crucial physical information such as level splitting.

IV.3.2 Quantum Periods of the Double Well

As we have outlined in Section IV.2, wave function continuity everywhere in the complex plane is essential for quantisation, and it can be expressed in the form of a connection formula. In terms of resurgent language, the Voros-Silverstone connection formulae [327, 328] provide the solution to this problem as well as the conceptual basis for the complex WKB framework. For the symmetric double well, the Voros-Silverstone connection formula is translated into the exact quantisation condition [324]

$$1 + \mathrm{e}^{\pm 2\pi i \nu} = \pm \epsilon i f(\nu)\,, \tag{IV.19}$$

where

$$\nu = \frac{1}{2\pi\hbar} \oint_{\mathcal{A}} \mathrm{d}x\, P(x)\,, \quad f(\nu) = \exp\left(\frac{i}{2\hbar} \oint_{\mathcal{B}} \mathrm{d}x\, P(x) \right)\,. \tag{IV.20}$$

Both sides of Eq. (IV.19) depend on the energy of the particle via the definitions of the contours $\mathcal{A}$ and $\mathcal{B}$ following Eqs. (IV.14) and (IV.18) and prescribe the exact solutions and energies of the quantum theory.

IV.3.3 Perturbative Quantum Periods

If we momentarily neglect the nonperturbative cycle and set $f(\nu) = 0$, the quantisation condition simplifies to the well-known Bohr-Sommerfeld quantisation presented in Section IV.2,

$$\nu = n + \frac{1}{2}\,, \tag{IV.21}$$

where n is a positive integer, such that the perturbative cycle satisfies

$$\oint_{\mathcal{A}} \mathrm{d}x\, P(x) = 2\pi\hbar \left(n + \frac{1}{2} \right)\,. \tag{IV.22}$$

To obtain energy eigenvalue solutions that satisfy Eq. (IV.22), we adopt the systematic approach of [329] and first expand the left hand side in $\hbar$ as $\oint_{\mathcal{A}} \mathrm{d}x\, P(x) = \sum_{k=0}^{\infty} \mathrm{vol}_k(E) \hbar^{2k}$.

Geometrically, for the symmetric double well, the kinetic energy of the particle $p^2(x)$ describes an elliptic curve of genus one in the complex plane of x. This implies that the different quantum corrections to the phase space volume, $\mathrm{vol}_k(E)$, can be generated from a differential operator of at most second order acting on $\mathrm{vol}_0(E)$ [329, 330],

$$\mathrm{vol}_k(E) = \left(f_k^{(0)} + f_k^{(1)} \frac{\mathrm{d}}{\mathrm{d}E} + f_k^{(2)} \frac{\mathrm{d}^2}{\mathrm{d}E^2} \right) \mathrm{vol}_0(E)\,, \tag{IV.23}$$

where the coefficients are functions of the energy, $f_k^{(i)}(E)$.

Recalling that $\mathrm{vol}_k(E) = \oint_{\mathcal{A}} \mathrm{d}x\, Q_{2k}(x)$, and $Q_{2k}(x)$ are known via the recursion relation (IV.6), we can adapt the recursion relation to identify the $f_k^{(i)}$ functions using the ansatz [329]

$$\sum_{i=0}^{2} f_k^{(i)} \frac{\mathrm{d}^i}{\mathrm{d}E^i} Q_0(x) = Q_{2k}(x) + \sum_{j=0}^{j_{\max}} \frac{\partial}{\partial x}\left(\alpha_j(E) \frac{x^j}{p^{3k-3+2r}(x)}\right) , \tag{IV.24}$$

for suitable coefficients $\alpha_j(E)$ and integer r, and $j_{\max}$ large enough. More precisely, as any choice of r and $j_{\max}$ fixes a set of solutions α_j and $f_k^{(i)}$, the former has to be chosen large enough such that the recursion ansatz (IV.24) closes. This recasting of the recursion relation from the Riccati equation into geometric language is guaranteed by arguments based on cohomology [329, 331].

For illustration, we present the first coefficient functions $f_1^{(i)}(E)$ for the symmetric double well. As a starting point, the leading-order volume reads [332]

$$\mathrm{vol}_0(E) = \oint_{\mathcal{A}} p(x) = 2\int_b^a p(x) = \frac{2}{3} g a \left[\left(a^2+b^2\right) E\left(1-\frac{b^2}{a^2}\right) - 2b^2 K\left(1-\frac{b^2}{a^2}\right)\right] , \tag{IV.25}$$

where K and E denote the complete elliptic integral of the first and second kind, respectively, and the turning points a and b are given by Eq. (IV.18). The ansatz (IV.24) then gives a prescription to compute the first quantum correction to the classical period,

$$\mathrm{vol}_1(E) = \left(-\frac{g^2\left(48Eg^2-1\right)}{4E\left(32Eg^2-1\right)} + \frac{g^2}{2}\frac{\mathrm{d}}{\mathrm{d}E}\right) \mathrm{vol}_0(E) . \tag{IV.26}$$

We remark that this operator is not unique, as we could have replaced the constant term $f_1^{(0)}(E)$ by a second-derivative term $f_1^{(2)}(E)$.

Including the first quantum correction $\mathrm{vol}_1(E)$, we obtain the series expansion of Eq. (IV.22) in terms of the energy and coupling,

$$\oint_{\mathcal{A}} \mathrm{d}x\, P(x) = 2\pi E + \left(6\pi E^2 + \frac{1}{2}\pi\hbar^2\right) g^2 + \left(70\pi E^3 + \frac{25}{2}\pi E\hbar^2\right) g^4 + \dots . \tag{IV.27}$$

After including more orders of the quantum corrections to the perturbative cycle, we invert the series expansion (IV.27) and obtain the standard result of Rayleigh-Schrödinger perturbation theory for the energy levels,

$$E(\nu) = \hbar\nu - \left(3\nu^2 + \frac{1}{4}\right)\hbar^2 g^2 - \left(17\nu^3 + \frac{19}{4}\nu\right)\hbar^3 g^4 + \mathcal{O}\left(\hbar^4 g^6\right) , \tag{IV.28}$$

as presented in the seminal work by Bender and Wu [307, 308], whose methodology has been implemented in Ref. [310]. We remark that the non-alternating signs of the leading-ν coefficients indicate that the series is not Borel-Laplace resummable, ultimately due to having neglected instanton contributions.

Before we close this discussion, we note that the leading-order terms of the form $\nu^j\hbar^j g^{2(j-1)}$ in Eq. (IV.28) are generated by the leading-order period $\mathrm{vol}_0(E)$ upon series inversion. Indeed, this reflects that textbook WKB is a semiclassical expansion, suitable for quantum states at large ν. However, terms subleading in ν at each order of the expansion can be obtained from higher order corrections to the quantum period, $\mathrm{vol}_{k\geq 1}(E)$. In this way, the all-order (perturbative) result obtained via WKB reproduces Rayleigh-Schrödinger perturbation theory for arbitrary quantum numbers ν. What is still lacking is an account of the nonperturbative corrections that arise when $f(\nu) \neq 0$.

IV.3.4 Nonperturbative Quantum Periods

To systematically account for the nonperturbative quantum effects, we now have to include the function $f(\nu)$ in Eq. (IV.19). We first compute its exponent, *i.e.* the nonperturbative quantum period associated to the cycle $\mathcal{B}$. Therefore, we expand

$$-i \oint_{\mathcal{B}} \mathrm{d}x\, P(x) = \sum_{k=0}^{\infty} \mathrm{vol}_k^{\mathrm{np}}(E) \hbar^{2k}\,, \tag{IV.29}$$

where we have defined the coefficients of the nonperturbative quantum period as

$$\mathrm{vol}_k^{\mathrm{np}}(E) = -i \oint_{\mathcal{B}} \mathrm{d}x\, Q_{2k}(x)\,. \tag{IV.30}$$

These coefficients can be computed in the same manner as the coefficients of the perturbative quantum period presented previously. Starting at leading order we get [332]

$$\mathrm{vol}_0^{\mathrm{np}}(E) = -i \oint_{\mathcal{B}} p(x) = -2i \int_{-b}^{b} p(x) = \frac{4}{3} g a \left[\left(a^2+b^2\right) E\left(\frac{b^2}{a^2}\right) - \left(a^2-b^2\right) K\left(\frac{b^2}{a^2}\right)\right]. \tag{IV.31}$$

This is indeed explicitly related to the corresponding perturbative cycle, $\mathrm{vol}_0(E)$, as prescribed by the geometry of genus-one curves (see Ref. [330] and references therein). Moreover, the differential operator that generates $\mathrm{vol}_k^{\mathrm{np}}(E)$ exactly coincides with the one that generates $\mathrm{vol}_k(E)$, essentially because they are expressed as closed contour integrals in the complex plane and their differential operators may be taken outside the integral. For instance, the first quantum correction to the nonperturbative period is, similar to Eq. (IV.26),

$$\mathrm{vol}_1^{\mathrm{np}}(E) = \left(-\frac{g^2\left(48Eg^2-1\right)}{4E\left(32Eg^2-1\right)} + \frac{g^2}{2}\frac{\mathrm{d}}{\mathrm{d}E}\right) \mathrm{vol}_0^{\mathrm{np}}(E)\,, \tag{IV.32}$$

with all higher orders working similarly.

Next, closely following [284], we plug the perturbative series expression for the energy $E(\nu)$, shown in Eq. (IV.28), into the nonperturbative quantum period via the turning points. We reproduce a series expansion of the form

$$\begin{aligned} -\frac{i}{\hbar} \oint_{\mathcal{B}} \mathrm{d}x\, P(x) =& \frac{1}{3g^2\hbar} \\ &+ \frac{1}{\hbar}\left(2\left(\log\left(\frac{g^2\nu\hbar}{2}\right)-1\right)\nu\hbar + 17g^2\nu^2\hbar^2 + 125g^4\nu^3\hbar^3 + \frac{17815}{12}g^6\nu^4\hbar^4 + \dots\right) \\ &+ \hbar\left(-\frac{1}{12\nu\hbar} + \frac{19}{12}g^2 + \dots\right) \\ &+ \hbar^3\left(\frac{7}{1440\nu^3\hbar^3} + \frac{22709}{576}g^6 + \dots\right) + \mathcal{O}\left(\hbar^5\right)\,. \end{aligned} \tag{IV.33}$$

The organisation of terms according to $\hbar$ allows us to identify the different contributions from each quantum volume correction. For example, in the RHS of Eq. (IV.33), terms proportional to $1/\hbar$ (with powers of $\nu\hbar$ fixed) originate from the leading order period, $\mathrm{vol}_0^{\mathrm{np}}(E)$, and in general the terms proportional to $\hbar^{2k-1}$ correspond to $\mathrm{vol}_k^{\mathrm{np}}(E)$.

Recalling that $f(\nu) = \exp\left[i \oint_{\mathcal{B}} \mathrm{d}x\, P(x)/(2\hbar)\right]$, we see that the leading contribution of $f(\nu)$ to the quantisation condition is an exponentially small shift of n away from half-integers,

$$f(\nu) \propto \exp\left(-\frac{1}{6g^2\hbar} + \dots\right) . \tag{IV.34}$$

This contribution can be recognised as the instanton action, confirming that $f(\nu)$ encodes the quantum effects of tunneling between the wells of the potential. In fact, the inclusion of nonperturbative effects through $f(\nu)$ lifts the vacuum degeneracy between the energy levels $E_\nu^\pm$ of opposite parity, as we review now.

IV.3.5 Nonperturbative Corrections to the Energy Levels

Following the exact quantisation condition, the energy levels can be expressed in terms of the perturbative energy levels E_ν^{pert} as well as the nonperturbative contribution $f(\nu)$, as a series in the latter. Again following closely [284], we regard the perturbative quantisation as a definition of the relation between ν and E, and the full quantisation condition to instead define the relation between ν and n, which solves the Bohr-Sommerfeld quantisation condition for given energy E. We will find that $f(\nu)$ performs an exponentially small shift of (ν) away from half-integers, which accounts for tunnelling. To begin, we write the solution to the full quantisation condition as

$$\nu = n + \Delta\nu\,, \tag{IV.35}$$

where $\Delta\nu$ is defined as a formal power series in an auxiliary parameter λ, that we will only need to separate orders in $f(\nu)$ and will set equal to 1 at the end of the computation:

$$\Delta\nu = \sum_k \Delta\nu^{(k)}\lambda^k. \tag{IV.36}$$

The quantisation condition can be rewritten as [284]

$$\Delta\nu = \frac{i}{2\pi}\log\left(1 + i\epsilon\lambda f(n+\Delta\nu)\right), \tag{IV.37}$$

And then plugging in the ansatz Eq. (IV.36), one can obtain the non-perturbative energy levels, again as a power series in the auxiliary parameter λ:

$$E = \sum_k E^{(k)}\lambda^k \tag{IV.38}$$

where the first three orders read [284]:

$$E^{(0)} = E(\nu) \equiv E(n)\,, \tag{IV.39}$$

$$E^{(1)} = -\frac{\epsilon}{2\pi} f(\nu)\frac{\mathrm{d}E(\nu)}{\mathrm{d}\nu}\,, \tag{IV.40}$$

$$E^{(2)} = -\frac{i}{4\pi} f(\nu)^2\frac{\mathrm{d}E(\nu)}{\mathrm{d}\nu} + \frac{\hbar^2}{8\pi^2}\frac{\mathrm{d}}{\mathrm{d}\nu}\left(f(\nu)^2\frac{\mathrm{d}E(\nu)}{\mathrm{d}\nu}\right) . \tag{IV.41}$$

A few interesting things can be seen from these coefficients: the one-instanton contribution $E^{(1)}$, which we associate with a single tunnelling event, breaks the degeneracy between $\epsilon = +, -$ that is otherwise present in the perturbative energy level. Moreover, at the two instanton level, an imaginary contribution appears, which seems in contrast with the fact that the eigenvalues of the anharmonic oscillator all need to be real and positive. On

the contrary, this imaginary contribution *restores* the reality of the energy eigenstates. As anticipated, the perturbative series is asymptotic, and moreover it is non-alternating, meaning that the late coefficient all have the same sign. Then, just like the example in Eq. (I.46), the Borel-Laplace transform has an exponentially small imaginary ambiguity. Given that the ambiguity in the resummation enters explicitly the quantisation condition, the sign of the ambiguity is related to the sign appearing in front of $f(\nu)$, and indeed the two contributions are equal and opposite [282]. This is the so-called BZJ (Bogomolny–Zinn-Justin) mechanism [287,291], which has been shown to persist at all orders for genus-one potentials [305], and there are hints of its validity in certain QFTs see *e.g.* [333, 334]. Indeed, $E^{(1)}$, being proportional to the derivative of an asymptotic series, is itself asymptotic, so it needs to be resummed, and it turns out that the resulting ambiguity is cancelled against an imaginary piece in the three-instanton contribution $E^{(3)}$, and so on, with the ambiguities cancelling separately in each topological sector, such that the exact answer is unambiguous and real. The all-orders BZJ mechanism, then, allows for arbitrary exponential precision by matching the imaginary ambiguities, resolving the question of how non Borel-Laplace resummable quantities can give rise to meaningful results.

Besides the explicit calculable correction to energy levels and the resolution of the $\mathbb{Z}_2$ parity breaking and Borel-Laplace summability questions, the nonzero nature of $f(\nu)$ is evident in all physical quantities, even when evaluating amplitudes corresponding to a classical limit of the theory. In the next section, we justify this claim, which is the main result of this chapter.

IV.4 Quantum Imprints at Large Quantum Number

In this section, we demonstrate a novel correspondence between the tunneling action in the anharmonic oscillator and the amplitude of multiparticle production in scalar QFT. We are particularly focused on the expression from Eq. (IV.33), which admits two different scaling regimes as a formal series expansion in $\hbar$.

The common approach [284] is to consider ν fixed, and send $\hbar \to 0$ to approach a classical regime. For fixed ν being small, however, it is doubtful that semiclassical behavior is obtained given that energy eigenstates are nonclassical. Naïvely, the semiclassical limit is obtained for large ν, where the action is large with respect to $\hbar$. As a result, simultaneously considering $\nu \to \infty$ and $\hbar \to 0$ suppresses quantum behavior. Moreover, the correct states to consider in the semiclassical limit are coherent states, *i.e.* states with minimal uncertainty. In particular, coherent states, by virtue of saturating the Heisenberg uncertainty principle, become classical in the $\hbar \to 0$ limit. On the other hand, coherent states do not have a well-defined occupation number ν, but instead follow a Poisson distribution centered around a given ν with a width of $\sqrt{\nu}$. At large ν, the width divided by the mean occupation number approaches zero, and so does the distinction between $|\nu\rangle$ and $|\nu+1\rangle$. Hence, in the $\nu \to \infty$ and $\hbar \to 0$ double scaling limit, using coherent or energy eigenstates gives the same amplitude.

We are thus motivated to define the 't Hooft-like coupling parameter

$$\lambda = \hbar\nu\,, \tag{IV.42}$$

which stays fixed in the double scaling limit $\nu \to \infty$ and $\hbar \to 0$. In this double scaling limit, terms proportional to $1/\hbar$ in Eq. (IV.33) are the only relevant contribution to the

nonperturbative quantum period, and its exponent takes the form

$$-\frac{i}{\hbar}\oint_{\mathcal{B}} \mathrm{d}x\, P(x)\Big|_{\frac{1}{\hbar}} \simeq \frac{1}{3g^2\hbar} + \frac{\lambda}{\hbar}\left[2\left(\log\left(\frac{g^2\lambda}{2}\right)-1\right)+17g^2\lambda+125g^4\lambda^2+\frac{17815}{12}g^6\lambda^3+\mathcal{O}\left(g^8\lambda^4\right)\right]. \tag{IV.43}$$

We remark that Eq. (IV.43), as well as Eq. (IV.28) depend on the perturbation coupling g^2 via powers of $g^2\hbar$. This affords a possible rescaling in the anharmonic oscillator [335] to absorb $\hbar$ into g^2. Here, we do not perform this substitution because we are interested in a semiclassical limit, which is made more explicit by keeping g^2 fixed and sending $\hbar \to 0$.

IV.4.1 The Quantum Imprint Rule

We now demonstrate that the double scaling limit shown in Eq. (IV.43) is remarkably related to the multiparticle production amplitudes at very high energies in QFT. In particular, in ϕ^4 theory, the amplitude of a highly-excited scalar decaying to a high multiplicity final state of n on-shell scalars, $\phi^* \to n\phi$, provides an example of nonperturbative UV dynamics in QFTs. As the effective expansion parameter $g^2 n$ is no longer small, the process becomes nonperturbative in the large n regime given n is proportional to the energy [38, 39, 92, 99–108]. In this scenario, it is believed that the multiparticle amplitude is of exponential form, which could either be decaying or even growing as n becomes large [101,105,336–340] (see also Ref. [341] for a review). A quantum mechanical analogue to this amplitude is given by the matrix element $\langle \nu \,|\, x \,|\, 0\rangle$ of the anharmonic oscillator with a quartic coupling. Such matrix elements were shown to be generically of exponential form inversely proportional to the anharmonic coupling g^2 [40, 319],

$$\langle \nu \,|\, x \,|\, 0\rangle = \exp\left(\frac{F}{g^2}\right), \tag{IV.44}$$

where the "holy grail function" F is a function of the coupling g^2 and the energy level ν. For the double well potential (IV.17) at large ν, the function F reads [319],[2]

$$\frac{F}{g^2} = \frac{1}{2}\left(\log\left(\frac{g^2\lambda}{2}\right)-1\right)\frac{\lambda}{\hbar}+\frac{17}{4}\frac{g^2\lambda^2}{\hbar}+\frac{125}{4}\frac{g^4\lambda^3}{\hbar}+\frac{17815}{48}\frac{g^6\lambda^4}{\hbar}+\ldots+\mathcal{O}\left(\frac{1}{\nu}\right). \tag{IV.45}$$

Remarkably, up to an overall numerical factor of four, all but the first term $1/(3g^2\hbar)$ of the nonperturbative quantum period in Eq. (IV.43) can be read off from F.

Therefore, in the double scaling limit with fixed 't Hooft coupling λ, we find the curious relation

$$\lim_{\substack{\nu\to\infty \\ \hbar\to 0}} \langle \nu \,|\, x \,|\, 0\rangle^2 f(\nu) = \exp\left(-\frac{1}{6g^2\hbar}\right), \tag{IV.46}$$

for any fixed λ. Here, the RHS of Eq. (IV.46) corresponds to the instanton action associated to the tunneling of the quantum theory and is, in particular, independent of the quantum number ν. In other words, we see that in the limit of large ν, the transition amplitude from the vacuum to a highly excited state, driven by the operator x, multiplied by the nonperturbative quantum period is an exact one-instanton amplitude. We have verified this explicitly for the first 15 terms of both Eq. (IV.43) and Eq. (IV.45). In the following, we refer to Eq. (IV.46), the key result of this chapter, as the "quantum imprint rule".

[2] Here, we adopt a different normalisation for the mass and coupling in the Schrödinger equation compared to Ref. [319], and we explicitly keep track of factors of $\hbar$.

IV.4.2 Discussion of the Quantum Imprint Rule

To fully appreciate the physical insights provided by Eq. (IV.46), we first revisit the exact quantisation condition (IV.19) for the symmetric double well potential. The RHS, $f(\nu)$, measures the tunneling through the barrier that separates the wells. It solely corresponds to the quantum contribution to the wave function continuity, or in other words, setting $f(\nu) = 0$ resembles a classical theory. Thus, Eq. (IV.19) can be understood as a quantisation condition for standing waves where the boundary conditions specify the spectrum of modes.

This is equivalent to the perturbative quantisation of the latter via Eq. (IV.22), which would, for instance, ignore the splitting of the energy levels through instanton effects.

And yet, only a nonvanishing $f(\nu)$ can provide information about the intrinsic quantum nature of the theory, which cannot be absent according to Eq. (IV.46). That is, for physical observables such as the transition amplitude $\langle \nu \,|\, x \,|\, 0 \rangle$ in the semiclassical regime $\nu \to \infty$ and $\hbar \to 0$, the leading instanton contribution on the RHS of Eq. (IV.46) prevails: the amplitude is asymptotically given by the nonperturbative cycle, *i.e.* a solely quantum contribution to the theory, multiplied by the one-instanton amplitude,

$$\langle \nu \,|\, x \,|\, 0 \rangle^2 \sim \exp\left(-\frac{1}{6g^2\hbar}\right) \exp\left(-\frac{i}{2\hbar}\oint_{\mathcal{B}} \mathrm{d}x\, P(x)\right) \quad \text{for} \quad \nu \to \infty\,,\, \hbar \to 0\,. \tag{IV.47}$$

This leading deviation from classical behavior is always present for all finite coupling values, and formally "gaps" amplitudes in the quantum theory from amplitudes in a classical analogue.

Moreover, the quantum imprint rule is an exact result in the coupling expansion by construction, since it involves both the all-order perturbative result of $\langle \nu \,|\, x \,|\, 0 \rangle$ as well as the nonperturbative quantum period entering the function $f(\nu)$, precluding any further quantum corrections. We carefully note, however, that this only holds in the limits $\nu \to \infty$ and $\hbar \to 0$.

Indeed, both $\langle \nu \,|\, x \,|\, 0 \rangle$ and $f(\nu)$ receive corrections in powers of $1/\nu$ (or equivalently in $\hbar/\lambda$), that do not obey the relationship observed in Eq. (IV.46). Explicitly, the first correction to the nonperturbative quantum period in the double scaling limit involves terms proportional to $\hbar$,

$$-\frac{i}{\hbar}\oint_{\mathcal{B}} \mathrm{d}x\, P(x)\bigg|_{\hbar} \simeq g^2\hbar\left(\frac{19}{12} + \frac{153}{4}g^2\lambda + \frac{23405}{24}g^4\lambda^2 + \mathcal{O}\left(g^6\lambda^3\right)\right). \tag{IV.48}$$

Similarly, the holy grail function F was shown to enter the multiparticle amplitude $\langle \nu \,|\, x \,|\, 0 \rangle$ in the form [40, 319]

$$\langle \nu \,|\, x \,|\, 0 \rangle = \exp\left(\frac{F}{g^2}\right) = \exp\left[\frac{1}{g^2}\left(F_0 + \frac{F_1}{\nu} + \frac{F_2}{\nu^2} + \ldots\right)\right]. \tag{IV.49}$$

Upon reintroducing factors of $\hbar$, the first quantum correction to the exponent in our notation reads

$$\frac{1}{g^2}\frac{F_1}{\nu} = \frac{5}{16}g^2\lambda + \frac{99}{128}g^4\lambda^2 + \frac{4279}{1536}g^6\lambda^3 + \ldots\,. \tag{IV.50}$$

Recalling that $\lambda = \hbar\nu$, we find that the correction to $f(\nu)$ given in Eq. (IV.48) is $1/\nu$-suppressed with respect to the quantum correction (IV.50). Therefore, the two expressions do not match, as they come with different powers of $1/\nu$. Moreover, this pattern continues beyond the leading quantum $1/\nu$ (or $\hbar$) corrections to the quantum imprint rule. In

particular, the holy grail function F involves terms with combinations of powers that do not appear in $f(\nu)$ and vice versa. We reluctantly conclude that the quantum imprint rule is an exact result strictly in the limit $\nu \to \infty$ and $\hbar \to 0$. Nevertheless, as an exact result, the quantum imprint rule can be interpreted as a quantum anomaly, similar to the Adler-Bell-Jackiw anomaly [83, 342] for axial $U(1)$ symmetries. Specifically, the classical $\mathbb{Z}_2$ symmetry of the theory is broken by $f(\nu)$ upon quantisation, and the breaking enters the matrix elements of the theory by means of the quantum imprint. In other words, the quantum imprint violates the semiclassical limit in a qualitatively similar way that instantons explicitly violate amplitudes that measure classical conservation laws [343].

We remark that the need of a double scaling limit to uncover the quantum imprint rule coincides with general arguments against strict reductionism [11, 344]. Indeed, the limit $\hbar \to 0$ is singular, and thus the naive correspondence principle fails, allowing the possibility of emergent phenomena.[3]

IV.4.3 Other Quantum Imprint Examples

Thus far, we have derived the quantum imprint rule for the anharmonic oscillator featuring a symmetric double well potential. We note that our arguments can be repeated almost verbatim for the anharmonic single well potential,

$$V_{\mathrm{SW}}(x) = \frac{1}{32g^2}\left(1 + 4g^2x^2\right)^2 , \tag{IV.51}$$

albeit with a different explicit form of $f(\nu)$ and $\langle \nu \,|\, x \,|\, 0 \rangle$. In this case, the classically forbidden region characterised by the complex contour $\mathcal{B}$ is found on the imaginary axis for any positive value of the energy.

Here, in contrast to the double well, the perturbative series expansion of the energy levels is tractable and Borel-Laplace resummable to the exact result [335, 345].[4] Nonetheless, an exact WKB treatment of the theory is also interesting to consider, and must include both real and imaginary instantons, since the corresponding perturbative quantum period is unfortunately not Borel-Laplace summable [326, 348]. We have performed this exact WKB calculation explicitly and our results indeed show that Eq. (IV.46) also holds for the anharmonic oscillator featuring a single well potential and hence reinforce the quantum imprint rule.

Beyond this example, we can outline possible avenues to explore how to generalise the quantum imprint rule (IV.46). One crucial aspect to analyse is the classical vacuum structure of the theory, which is $\mathbb{Z}_2$ symmetric in the anharmonic double well potential and hence possesses four turning points, *i.e.* two independent cycles. The underlying geometry is thus that of a genus-one surface, which allowed us in Section IV.3.3 to use *e.g.* powerful cohomology results [329, 331]. As an aside, it is worth noting that the geometry of higher genera surfaces is still poorly understood, and thus theories with more complicated vacuum structures are likely intractable to calculate at present. Nevertheless, we conjecture that a modified version of Eq. (IV.46) may still hold in theories with more complicated vacuum degeneracies, where the modification tallies the leading instanton amplitudes.

[3] For another striking example where the correspondence principle fails, consider two on-phase particles of de Broglie wavelength λ_{DB} colliding along the x-axis. By linearity, the total intensity is proportional to $\cos^2(x/\lambda_{\mathrm{DB}})$. In this case, the correspondence principle limit $\lambda_{\mathrm{DB}} \to 0$ is singular and does not approach the classical result, which is simply twice the intensity of either particle.

[4] In some cases, summability to an exact result also applies to higher-dimensional QFTs [346, 347]. A more general, systematic assessment of Borel-Laplace summability can be found in [311].

We end this discussion by noting the quantum imprint rule is a concrete realisation of a perturbative-nonperturbative connection as predicted by resurgence theory (see, *e.g.*, Refs. [298–300, 305]). Indeed, the amplitude $\langle \nu \,|\, x \,|\, 0 \rangle$ was calculated using perturbation theory alone, while $f(\nu)$ is a purely nonperturbative quantity. In this sense, Eq. (IV.46) furnishes an explicit breaking of the factorisation between the perturbative and nonperturbative sectors.

IV.5 Conclusions and Outlook

In this chapter, we have employed an exact WKB analysis to identify purely perturbative and nonperturbative sectors of the anharmonic oscillator featuring a symmetric double well potential. The nonperturbative contribution to the quantisation condition can be entirely characterised by the function $f(\nu)$, which measures the tunneling through the classically forbidden potential barrier that separates the minima and also generates energy splitting between classically degenerate levels. Remarkably, at large quantum numbers, or more precisely in the classical double scaling limit $\nu \to \infty$ and $\hbar \to 0$ with $\hbar\nu$ fixed, we have found that $f(\nu)$ is precisely given by transition amplitudes to highly excited states, $\langle \nu \,|\, x \,|\, 0 \rangle$, as shown in Eq. (IV.46). The transition amplitude is the quantum mechanical analogue of multiparticle production in scalar QFTs at high energies, which becomes nonperturbative in the limit of a large number of final state particles.

Naïvely, the quantum states at large ν are so energetic that they should not feel the potential barrier of the double well. Nevertheless, the RHS of Eq. (IV.46) is given by the instanton action. We interpret this as the irreducibility of the quantum nature of the theory, even in the correspondence principle limit. In other words, the instanton characterises the leading deviation of the theory from classical behavior. Being an all-orders result, it gaps the quantum theory, as there is no value of the coupling where this contributions vanishes entirely. Therefore, strictly speaking, the classical limit is hindered by an essential singularity at $\hbar = 0$, and we hence dub Eq. (IV.46) the quantum imprint rule.

Furthermore, we have found that the same quantum imprint rule also holds in the case of an anharmonic oscillator with a single well potential. This leads us to speculate that a general version of the quantum imprint rule can be derived in any quantum mechanical theory, provided the RHS is modified to account for different vacuum structures, which we plan to address in future work. We also conjecture that a more general form of Eq. (IV.46) can be used to define universality classes of different theories via the quantitative measure that gaps the theory from its classical behavior. In this sense, we can highlight that the double well and the single well anharmonic oscillators, while maintaing superficial differences in the explicit form of $f(\nu)$ and $\langle \nu \,|\, x \,|\, 0 \rangle$, are similar to each other in the semiclassical limit because they belong to the same universality class governed by Eq. (IV.46).

CHAPTER V

Conclusion and Outlook

Following the discussion in Section I.1.7, we can slightly reword Leggett's question as: "What evidence do we have that quantum mechanics works at subatomic energies?". Just like the original question, the naive answer to this one would be "a lot". Every time a loop correction is needed to match experimental precision, every time interference between diagrams cannot be neglected, we are using principles of quantum mechanics, taking into account contributions would vanish in the $\hbar \to 0$ limit. Similarly, oscillations are a purely quantum mechanical phenomenon and they have been observed in both neutrinos [349] and neutral mesons [350–353]. However, other aspects of quantum mechanics are yet to be verified at high energies: no loophole-free test of Bell inequality has been performed yet [194, 354], although many loophole-prone versions have [123, 355–358]. Tunneling has never been observed at high energies: the theta vacuum of the strong sector is responsible for the mass of the η' meson, but the direct effect of nonzero topological susceptibility of the vacuum, that is strong CP violation, has notoriously not been detected yet [359] and recent research even puts in doubt its physical relevance [360]. Similarly, vacuum decay through tunnelling would lead to observable gravitational waves signatures [361–363] that have so far not been detected (see however [364]). It is safe to assume, then, that any discovery of previously unobserved quantum effects in QFT will bring with it a large amount of information about BSM physics. The work in this thesis tries to answer the question in three disparate yet connected ways, which we now summarise. We then proceed to outline exciting lines of research for the future.

V.1 Summary

In the first part, we studied entanglement at colliders, and in particular how it can improve sensitivity to SMEFT operators by restoring ("resurrecting") coherence between SM and SMEFT-induced processes in the process $f\bar{f} \to \ell\bar{\ell}$. Angular correlations have been shown to resurrect the interference of operators inducing dipole moments for leptons, thus improving the sensitivity to these operators with respect to cross-section measurements. Building on previous proposals, measures of quantum correlations of the spins of the outcoming leptons were calculated. The impact of the resurrection was determined to be, in certain cases, actually negative for BSM sensitivity. In general, we concluded that angular correlations, which are the proxies to measure spin correlations, are more sensitive than quantum correlation measures such as measures of entanglement. This contrasts with previous studies that suggested that the study of quantum correlation would by itself bring greater sensitivity to NP.

In the second part, we looked at the impact of interference by studying the interplay

between mass and kinetic mixing between the SM Z and a NP Z' in the mass range $[88, 95]$ GeV. We found that previous work, working in the NWA, failed to capture important aspects of the phenomenology, namely the avoided crossing in both the real and imaginary part of the pole masses of the two bosons, as well as the quantum Zeno effect which governs the visible width of the Z' as well as the invisible width of the Z. Thus we showed the importance of quantum effect in the phenomenology of Z' bosons, and more generally of nearly degenerate particles.

In the third and last part, we uncovered an intriguing relation between large-multiplicity amplitudes and the vacuum structure of the quantum mechanical anharmonic oscillator. To do so, we used the resurgent methods of exact WKB, together with the all-order perturbative formula for large-multiplicity amplitude $\langle 0| x |\nu\rangle$ that was derived in [40]. The two turn out to be exactly related to one another in the semiclassical limit $\hbar \to 0$, $\nu \to \infty$ with $\lambda = \nu\hbar$ kept fixed. Aside from a novel exact relation in quantum mechanics, this finding leads itself to possible generalisations in QFT, relating two nonperturbative quantities that have received much attention since the 1980s due to their appearance in calculation involving electroweak sphalerons, which are the only breaking of $B + L$ in the SM and might play a role in the generation of matter-antimatter asymmetry [97].

The results of this thesis fit into the broader effort to explore quantum effects as tools for uncovering new physics, aligning with the vision laid out by A. J. Leggett in his seminal paper [42]. Leggett's work, which questioned the limits of quantum mechanics at macroscopic scales, emphasised the importance of probing quantum phenomena beyond the well-tested microscopic realm. Similarly, this thesis extends the search for quantum mechanical signatures, but at high-energy scales in particle physics. The recent announcement by two LHC collaborations [123, 358] of the detection of quantum correlations in top-pairs prompted intense theoretical activity to ascertain the sensitivity of quantum correlations to NP [124]. While the result of Part I seem to indicate that the quantum nature of the observable is not a prerequisite for enhanced sensitivity, we still believe that particle physics can be advanced by studying the effect of purely quantum phenomena. Indeed, the correct phenomenology of nearly degenerate particle, uncovered in Part II, requires quantum and not classical reasoning. Moreover, a key result in this work is the newly uncovered link between large-multiplicity scattering amplitudes and the vacuum structure of the quantum anharmonic oscillator. This connection, found using nonperturbative methods, bridges semiclassical and purely quantum phenomena in a novel way. It suggests that even in the high-energy limit, quantum mechanics reveals deeper structures that were previously hidden. This insight offers a fresh perspective on the interplay between quantum corrections and semiclassical physics, showing that large-multiplicity amplitudes could be a gateway to understanding nonperturbative effects in quantum field theory, including potential links to cosmology.

We now conclude this thesis with speculation regarding future research.

V.2 Outlook

The distillation of the ideas written in this thesis to the language of effective field theories is an interesting future project that would make calculations of quantum effects in NP more transparent. For instance, an effective field theory for unstable particles has been developed in refs. [365, 366] as an extension of heavy quark effective field theory [68]. Recently, mixing in the presence of a medium has also been treated with effective field theory tools [367]. Further developing these tools might in future lead to a proper quantum description of the thermal evolution of particles in the primordial plasma, as advocated

in [368]. This is also related to studies of resonant leptogenesis [369].

All the calculations performed in Part I are at tree-level, given that the effect of NLO (next-to-lowest order) is expected to be small, as spin correlations are ratios of cross sections. Nonetheless, it would be interesting to understand the effect of soft radiation and loop effects. Interestingly, one expects the properly resummed tree-level answer, corresponding a classical field theory, not to exhibit entanglement at all. Thus, if the LO calculation is to be close to the exact one, it seems like quantum corrections, on their own, would work to increase entanglement. The interplay of quantum corrections and soft radiation merits further discussion.

Entanglement has also been proposed as a guiding principle for parameter selection through the emergence of global symmetries via a sort of stationary principle for entanglement [185, 354, 370–373]. While enticing, most of these proposals either rely on specific angular configurations or additional assumptions, so at the current state it is hard to establish a general principle and more information is needed. Refs. [374, 375], indeed, have shown how no clear guidance can be reached from a minimal entanglement principle for the two-higgs-doublet model, once more general configurations than the one used in [373] are studied. In Part I, we add another piece to the puzzle by studying the LQU, a discord-like measure for non-classical correlation [148]. As can be seen in Figs. II.3 and II.8, the LQU has a local maximum that is absent in the entanglement markers, and cannot be easily explained by the presence of a symmetry or resonance. While other measures of quantum discord have already been considered in the literature [147], their simplified definition used so far can only be applied to the simple spin state of the top, and the complete case involves a complicated minimisation procedure. In contrast, the LQU has an explicit formula that is applicable to any bipartite qubit [148], so its use facilitates studies of non-classical correlations beyond entanglement. It will be interesting to study the robustness of the principles proposed in [370–372] on measures of non-classicality that go beyond entanglement using the LQU.

Another interesting avenue for the mixture of quantum information and the search of new physics, which goes beyond simply assessing the sensitivity to SMEFT operators, is the search for violation of spacetime symmetries, which would change the pattern of correlations of spin in a more dramatic way. A first step in this direction was performed in [376], but there is still much to do, for instance a classification in the style of [377] of violations of Lorentz in entanglement would be a useful tool. On an even more speculative side, inspiration could be found in the field of beyond-quantum correlations, which have gained considerable popularity in nonrelativistic quantum mechanics [378, 379], and a strategy to detect them has been proposed at relativistic energies too [380].

As previously mentioned, it would be of prime interest to derive an analogous identity to the quantum imprint rule Eq. (IV.46) in QFT. Namely, the analogy between quantum anomalies and Eq. (IV.46) is striking since the latter violates the classical limit in a qualitatively similar way as amplitudes measuring anomalous classical conservation laws. We can also offer Eq. (IV.46) as a measure to distinguish universality classes of QFTs apart from their respective classical limits. In the event that the quantum imprint rule is realised as an exact relation in QFT, its application as an operative equation to derive perturbative or nonperturbative physics amplitudes would be highly effective. For instance, if the quantum imprint rule, or a direct generalisation thereof, holds for scalar field theory, making use of the Goldstone boson equivalence theorem [381–383] one can then formulate a quantum imprint for longitudinal electroweak bosons. As underlined several times, both the large-multiplicity scattering of electroweak bosons and the tunneling action at high energies are object of intense scrutiny, as reviewed in Sections I.1.6 and I.2.4, so

relating them is sure to advance our knowledge of purely quantum phenomena, in the SM and beyond. The link between semiclassical expansion and large charge, which has been employed in [109] and subsequent works, could turn the quantum imprint into an interesting window into CFT physics, especially given the indications that the large-charge expansion might be resurgent [384].

List of Figures

List of Tables

Acronyms

1PI 1-particle irreducible 23

BSM beyond the Standard Model 30, 41, 53, 57, 58, 60, 63, 93
BW Breit-Wigner 60, 73
BZJ Bogomolny–Zinn-Justin 87

CFT conformal field theory 25, 96
CHSH Clauser-Horne-Shimony-Holt 37
CL confidence level 50, 51, 98

DM dark matter 20, 59

EFT effective field theory 21, 22, 29, 31
EOM equations of motion 15, 22
EW electroweak 29, 37, 42, 49, 51–53, 98

HEFT higgs EFT 22

LEP Large Electron-Positron collider 47, 57, 60, 67–72, 74, 98
LHC Large Hadron Collider 30, 94
LHS left-hand side 17, 81
LO lowest order 31, 50, 95
LQU local quantum uncertainty 38, 42, 48–50, 52, 95, 97
LSZ Lehmann-Symanzik-Zimmermann 23, 62

NDA naive dimensional analysis 29, 31, 40
NLO next-to-lowest order 95
NP new physics 4, 5, 22, 23, 25, 29, 30, 41, 42, 48–51, 53, 74, 93, 94, 97, 98
NWA narrow-width approximation 23, 24, 94

ODE ordinary differential equations 8

PDF parton distribution function 36, 50

QCD quantum chromodynamics 19, 53, 57, 60
QED quantum electrodynamics 15

QFT quantum field theory 4, 15, 16, 18–20, 23–25, 77–79, 87, 88, 90, 91, 93–95

QM quantum mechanics 3–5, 7, 14, 15, 17–20, 24, 25, 78, 79, 82

RHS right-hand side 15, 17, 24, 81, 85, 88, 89, 91

SM Standard Model 19, 20, 22, 24, 29–32, 34, 39, 41–44, 47–50, 57–61, 63, 64, 68, 70, 71, 73, 74, 93, 94, 96–98

SMEFT Standard Model EFT 22, 23, 29, 31, 32, 39, 40, 42, 47, 48, 50, 52, 93, 95, 97, 99

UV ultraviolet 21, 22, 25, 42, 59, 88

vev vacuum expectation value 22, 41

WKB Wentzel-Kramers-Brillouin 8, 10, 16, 18, 78–84, 90, 91, 94

Bibliography

[1] P. Lo Chiatto, *Interference Resurrection of the τ Dipole through Quantum Tomography*, 2408.04553.

[2] P. Lo Chiatto and F. Yu, *Consistent Electroweak Phenomenology of a Nearly Degenerate Z' Boson*, 2405.03396.

[3] P. Lo Chiatto, S. Schenk and F. Yu, *Quantum Imprint of the Anharmonic Oscillator*, 2308.01244.

[4] A. Lenard and F. J. Dyson, *Stability of Matter. II*, *Journal of Mathematical Physics* **9** (1968) 698.

[5] F. J. Dyson and A. Lenard, *Stability of Matter. I*, *Journal of Mathematical Physics* **8** (1967) 423.

[6] E. H. Lieb and W. E. Thirring, *Bound for the kinetic energy of fermions which proves the stability of matter*, *Phys. Rev. Lett.* **35** (1975) 687.

[7] J. S. Bell, *On the Einstein-Podolsky-Rosen paradox*, *Physics Physique Fizika* **1** (1964) 195.

[8] J. F. Clauser, M. A. Horne, A. Shimony and R. A. Holt, *Proposed experiment to test local hidden-variable theories*, *Phys. Rev. Lett.* **23** (1969) 880.

[9] S. J. Freedman and J. F. Clauser, *Experimental test of local hidden-variable theories*, *Phys. Rev. Lett.* **28** (1972) 938.

[10] M. C. Gutzwiller, *Chaos in classical and quantum mechanics*. Springer, New York, 1990.

[11] M. Berry, *Asymptotics, singularities and the reduction of theories*, in *Logic, Methodology and Philosophy of Science IX*, D. Prawitz, B. Skyrms and D. Westerståhl, eds., vol. 134 of *Studies in Logic and the Foundations of Mathematics*, pp. 597–607, Elsevier, (1995), DOI.

[12] S. Pascazio, *All you ever wanted to know about the quantum Zeno effect in 70 minutes*, *Open Systems & Information Dynamics* **21** (2014) 1440007 [1311.6645].

[13] I. I. Rabi, *Space Quantization in a Gyrating Magnetic Field*, *Phys. Rev.* **51** (1937) 652.

[14] L. S. Schulman, *Continuous and pulsed observations in the quantum zeno effect*, *Phys. Rev. A* **57** (1998) 1509.

[15] A. Bokulich and P. Bokulich, *Bohr's Correspondence Principle*, in *The Stanford Encyclopedia of Philosophy*, E. N. Zalta, ed., Metaphysics Research Lab, Stanford University, (2020).

[16] P. A. M. Dirac, *The fundamental equations of quantum mechanics*, *Proc. Roy. Soc. Lond. A* **109** (1925) 642.

[17] P. Ehrenfest, *Bemerkung über die angenäherte Gültigkeit der klassischen Mechanik innerhalb der Quantenmechanik*, *Z. Phys.* **45** (1927) 455.
[18] G. Wentzel, *Eine Verallgemeinerung der Quantenbedingungen für die Zwecke der Wellenmechanik*, *Z. Phys.* **38** (1926) 518.
[19] H. A. Kramers, *Wellenmechanik und halbzahlige Quantisierung*, *Z. Phys.* **39** (1926) 828.
[20] L. Brillouin, *La mécanique ondulatoire de Schrödinger; une méthode générale de resolution par approximations successives*, *Compt. Rend. Hebd. Seances Acad. Sci.* **183** (1926) 24.
[21] J. P. Boyd, *Asymptotic, Superasymptotic and Hyperasymptotic Series*, *Acta Applicandae Mathematicae* **56** (1999) 1.
[22] A. Zettl, *Sturm-Liouville theory*, vol. 121 of *Mathematical Surveys and Monographs*. American Mathematical Society, Providence, RI, 2005.
[23] V. A. Rubakov, *Classical theory of gauge fields*. Princeton University Press, Princeton, New Jersey, 5, 2002.
[24] T. Holstein, *Mobilities of positive ions in their parent gases*, *The Journal of Physical Chemistry* **56** (1952) 832 [https://doi.org/10.1021/j150499a004].
[25] C. Herring, *Critique of the heitler-london method of calculating spin couplings at large distances*, *Rev. Mod. Phys.* **34** (1962) 631.
[26] B. M. Smirnov and M. I. Chibisov, *Electron Exchange and Changes in the Hyperfine State of Colliding Alkaline Metal Atoms*, *Soviet Journal of Experimental and Theoretical Physics* **21** (1965) 624.
[27] A. Cherman and M. Unsal, *Real-Time Feynman Path Integral Realization of Instantons*, 1408.0012.
[28] A. Andreassen, D. Farhi, W. Frost and M. D. Schwartz, *Direct Approach to Quantum Tunneling*, *Phys. Rev. Lett.* **117** (2016) 231601 [1602.01102].
[29] W.-Y. Ai, B. Garbrecht and C. Tamarit, *Functional methods for false vacuum decay in real time*, *JHEP* **12** (2019) 095 [1905.04236].
[30] T. Steingasser and D. I. Kaiser, *Quantum tunneling from excited states: Recovering imaginary-time instantons from a real-time analysis*, 2402.00099.
[31] D. Sauzin, *Introduction to 1-summability and resurgence*, 1405.0356.
[32] J. Ecalle, *Les fonctions resurgentes, Vol. 1: Algebres de fonctions resurgentes*. Publications Mathematiques d'Orsay, 1981.
[33] J. Ecalle, *Les fonctions resurgentes, Vol. 2: Les fonctions resurgentes appliquees a l'iteration*. Publications Mathematiques d'Orsay, 1981.
[34] J. Ecalle, *Les fonctions resurgentes, Vol. 3: L'equation du pont et la classification analytique des objets locaux*. Publications Mathematiques d'Orsay, 1985.
[35] P. Flajolet and R. Sedgewick, *Analytic Combinatorics*. Cambridge University Press, 2009.
[36] F. J. Dyson, *Divergence of perturbation theory in quantum electrodynamics*, *Phys. Rev.* **85** (1952) 631.
[37] C. Bachas, *On the breakdown of perturbation theory*, *Theor. Math. Phys.* **95** (1993) 491 [hep-th/9212033].
[38] M. B. Voloshin, *Multiparticle amplitudes at zero energy and momentum in scalar theory*, *Nucl. Phys. B* **383** (1992) 233.
[39] E. N. Argyres, R. H. P. Kleiss and C. G. Papadopoulos, *Amplitude estimates for multi - Higgs production at high-energies*, *Nucl. Phys. B* **391** (1993) 42.
[40] J. Jaeckel and S. Schenk, *Exploring High Multiplicity Amplitudes in Quantum Mechanics*, *Phys. Rev. D* **98** (2018) 096007 [1806.01857].

[41] G. 't Hooft, *A Planar Diagram Theory for Strong Interactions*, *Nucl. Phys. B* **72** (1974) 461.
[42] A. J. Leggett, *Macroscopic Quantum Systems and the Quantum Theory of Measurement*, *Progress of Theoretical Physics Supplement* **69** (1980) 80.
[43] P. Debye, *Zur Theorie der spezifischen Wärmen*, *Annalen Phys.* **344** (1912) 789.
[44] S. Balibar, *The discovery of superfluidity*, *Journal of Low Temperature Physics* **146** (2007) 441.
[45] H. K. Onnes, *Further Experiments with Liquid Helium. D. On the Change of the Electrical Resistance of Pure Metals at very low Temperatures, etc. V. The Disappearance of the resistance of mercury*, pp. 264–266.
Springer Netherlands, Dordrecht, 1991.
10.1007/978-94-009-2079-8-16.
[46] J. Bardeen, L. N. Cooper and J. R. Schrieffer, *Theory of superconductivity*, *Phys. Rev.* **108** (1957) 1175.
[47] Y. Aharonov and D. Bohm, *Significance of electromagnetic potentials in the quantum theory*, *Phys. Rev.* **115** (1959) 485.
[48] L. Fonda, G. C. Ghirardi and A. Rimini, *Decay Theory of Unstable Quantum Systems*, *Rept. Prog. Phys.* **41** (1978) 587.
[49] A. S. Blum, *The state is not abolished, it withers away: How quantum field theory became a theory of scattering*, *Stud. Hist. Phil. Sci. B* **60** (2017) 46 [2011.05908].
[50] C. G. Callan, Jr., R. F. Dashen and D. J. Gross, *The Structure of the Gauge Theory Vacuum*, *Phys. Lett. B* **63** (1976) 334.
[51] R. Jackiw and C. Rebbi, *Vacuum Periodicity in a Yang-Mills Quantum Theory*, *Phys. Rev. Lett.* **37** (1976) 172.
[52] S. R. Coleman, *The Fate of the False Vacuum. 1. Semiclassical Theory*, *Phys. Rev. D* **15** (1977) 2929.
[53] C. G. Callan, Jr. and S. R. Coleman, *The Fate of the False Vacuum. 2. First Quantum Corrections*, *Phys. Rev. D* **16** (1977) 1762.
[54] A. H. Guth and S. H. H. Tye, *Phase Transitions and Magnetic Monopole Production in the Very Early Universe*, *Phys. Rev. Lett.* **44** (1980) 631.
[55] B. W. Lee, C. Quigg and H. B. Thacker, *Weak Interactions at Very High-Energies: The Role of the Higgs Boson Mass*, *Phys. Rev. D* **16** (1977) 1519.
[56] P. W. Higgs, *Broken Symmetries and the Masses of Gauge Bosons*, *Phys. Rev. Lett.* **13** (1964) 508.
[57] G. S. Guralnik, C. R. Hagen and T. W. B. Kibble, *Global Conservation Laws and Massless Particles*, *Phys. Rev. Lett.* **13** (1964) 585.
[58] M. Lindner, *Implications of Triviality for the Standard Model*, *Z. Phys. C* **31** (1986) 295.
[59] J. Baez, *How many fundamental constants are there?*, 2011.
[60] D. Baumann, *Cosmology*. Cambridge University Press, 7, 2022, 10.1017/9781108937092.
[61] A. Crivellin and B. Mellado, *Anomalies in particle physics and their implications for physics beyond the standard model*, *Nature Rev. Phys.* **6** (2024) 294 [2309.03870].
[62] A. V. Manohar, *Introduction to effective field theories*, *arXiv preprint arXiv: 1804.05863* (2018) .
[63] K. G. Wilson, *Renormalization group and critical phenomena. 1. Renormalization group and the Kadanoff scaling picture*, *Phys. Rev. B* **4** (1971) 3174.

[64] C. W. Bauer, S. Fleming and M. E. Luke, *Summing Sudakov logarithms in $B \to X_s\gamma$in effective field theory.*, *Phys. Rev. D* **63** (2000) 014006 [hep-ph/0005275].

[65] C. W. Bauer, S. Fleming, D. Pirjol and I. W. Stewart, *An Effective field theory for collinear and soft gluons: Heavy to light decays*, *Phys. Rev. D* **63** (2001) 114020 [hep-ph/0011336].

[66] C. W. Bauer, D. Pirjol and I. W. Stewart, *Soft collinear factorization in effective field theory*, *Phys. Rev. D* **65** (2002) 054022 [hep-ph/0109045].

[67] E. Fermi, *Tentativo di una teoria dell'emissione dei raggi beta*, *Ric. Sci.* **4** (1933) 491.

[68] M. Neubert, *Heavy quark symmetry*, *Phys. Rept.* **245** (1994) 259 [hep-ph/9306320].

[69] T. Appelquist and J. Carazzone, *Infrared Singularities and Massive Fields*, *Phys. Rev. D* **11** (1975) 2856.

[70] J. C. Criado and M. Pérez-Victoria, *Field redefinitions in effective theories at higher orders*, *JHEP* **03** (2019) 038 [1811.09413].

[71] R. Alonso, E. E. Jenkins and A. V. Manohar, *A Geometric Formulation of Higgs Effective Field Theory: Measuring the Curvature of Scalar Field Space*, *Phys. Lett. B* **754** (2016) 335 [1511.00724].

[72] R. Alonso, E. E. Jenkins and A. V. Manohar, *Geometry of the Scalar Sector*, *JHEP* **08** (2016) 101 [1605.03602].

[73] R. Gómez-Ambrosio, F. J. Llanes-Estrada, A. Salas-Bernárdez and J. J. Sanz-Cillero, *SMEFT is falsifiable through multi-Higgs measurements (even in the absence of new light particles)*, *Commun. Theor. Phys.* **75** (2023) 095202 [2207.09848].

[74] L. Graf, B. Henning, X. Lu, T. Melia and H. Murayama, *2, 12, 117, 1959, 45171, 1170086, . . . : a hilbert series for the qcd chiral lagrangian*, *JHEP* **01** (2021) 142 [2009.01239].

[75] B. Grzadkowski, M. Iskrzynski, M. Misiak and J. Rosiek, *Dimension-Six Terms in the Standard Model Lagrangian*, *JHEP* **10** (2010) 085 [1008.4884].

[76] H. Lehmann, K. Symanzik and W. Zimmermann, *On the formulation of quantized field theories*, *Nuovo Cim.* **1** (1955) 205.

[77] M. J. G. Veltman, *Unitarity and causality in a renormalizable field theory with unstable particles*, *Physica* **29** (1963) 186.

[78] D. A. Dicus, E. Sudarshan and X. Tata, *Factorization theorem for decaying spinning particles*, *Physics Letters B* **154** (1985) 79.

[79] A. Denner and S. Dittmaier, *Electroweak Radiative Corrections for Collider Physics*, *Phys. Rept.* **864** (2020) 1 [1912.06823].

[80] D. Berdine, N. Kauer and D. Rainwater, *Breakdown of the Narrow Width Approximation for New Physics*, *Phys. Rev. Lett.* **99** (2007) 111601 [hep-ph/0703058].

[81] C. F. Uhlemann and N. Kauer, *Narrow-width approximation accuracy*, *Nucl. Phys. B* **814** (2009) 195 [0807.4112].

[82] E. Fuchs, *Interference effects in new physics processes at the LHC*, Ph.D. thesis, U. Hamburg, Dept. Phys., Hamburg, 2015. 10.3204/DESY-THESIS-2015-037.

[83] J. S. Bell and R. Jackiw, *A PCAC puzzle: $\pi^0 \to \gamma\gamma$ in the σ model*, *Nuovo Cim. A* **60** (1969) 47.

[84] S. L. Adler, *Axial-vector vertex in spinor electrodynamics*, *Phys. Rev.* **177** (1969)

2426.
[85] G. 't Hooft, *Symmetry breaking through bell-jackiw anomalies*, *Phys. Rev. Lett.* **37** (1976) 8.
[86] N. S. Manton, *Topology in the Weinberg-Salam Theory*, *Phys. Rev. D* **28** (1983) 2019.
[87] C. H. Taubes, *The Existence of a Nonminimal Solution to the SU(2) Yang-Mills Higgs Equations on R**3*, *Commun. Math. Phys.* **86** (1982) 257.
[88] F. R. Klinkhamer and N. S. Manton, *A Saddle Point Solution in the Weinberg-Salam Theory*, *Phys. Rev. D* **30** (1984) 2212.
[89] A. Ringwald, *High-Energy Breakdown of Perturbation Theory in the Electroweak Instanton Sector*, *Nucl. Phys. B* **330** (1990) 1.
[90] O. Espinosa, *High-Energy Behavior of Baryon and Lepton Number Violating Scattering Amplitudes and Breakdown of Unitarity in the Standard Model*, *Nucl. Phys. B* **343** (1990) 310.
[91] L. McLerran, A. Vainshtein and M. Voloshin, *Electroweak interactions become strong at energy above $\sim$ 10 tev*, *Phys. Rev. D* **42** (1990) 171.
[92] J. M. Cornwall, *On the High-energy Behavior of Weakly Coupled Gauge Theories*, *Phys. Lett. B* **243** (1990) 271.
[93] S. H. H. Tye and S. S. C. Wong, *Bloch Wave Function for the Periodic Sphaleron Potential and Unsuppressed Baryon and Lepton Number Violating Processes*, *Phys. Rev. D* **92** (2015) 045005 [1505.03690].
[94] S. H. H. Tye and S. S. C. Wong, *Baryon Number Violating Scatterings in Laboratories*, *Phys. Rev. D* **96** (2017) 093004 [1710.07223].
[95] Y.-C. Qiu and S. H. H. Tye, *Role of Bloch Waves in baryon-number violating processes*, *Phys. Rev. D* **100** (2019) 033006 [1812.07181].
[96] C. Bachas and T. Tomaras, *Band Structure in Yang-Mills Theories*, *JHEP* **05** (2016) 143 [1603.08749].
[97] V. A. Kuzmin, V. A. Rubakov and M. E. Shaposhnikov, *On the Anomalous Electroweak Baryon Number Nonconservation in the Early Universe*, *Phys. Lett. B* **155** (1985) 36.
[98] A. D. Sakharov, *Violation of CP Invariance, C asymmetry, and baryon asymmetry of the universe*, *Pisma Zh. Eksp. Teor. Fiz.* **5** (1967) 32.
[99] H. Goldberg, *Breakdown of perturbation theory at tree level in theories with scalars*, *Phys. Lett. B* **246** (1990) 445.
[100] L. S. Brown, *Summing tree graphs at threshold*, *Phys. Rev. D* **46** (1992) R4125 [hep-ph/9209203].
[101] M. B. Voloshin, *Summing one loop graphs at multiparticle threshold*, *Phys. Rev. D* **47** (1993) R357 [hep-ph/9209240].
[102] B. H. Smith, *Summing one loop graphs in a theory with broken symmetry*, *Phys. Rev. D* **47** (1993) 3518 [hep-ph/9209287].
[103] A. S. Gorsky and M. B. Voloshin, *Nonperturbative production of multiboson states and quantum bubbles*, *Phys. Rev. D* **48** (1993) 3843 [hep-ph/9305219].
[104] E. N. Argyres, R. H. P. Kleiss and C. G. Papadopoulos, *Multiscalar amplitudes to all orders in perturbation theory*, *Phys. Lett. B* **308** (1993) 292 [hep-ph/9303321].
[105] M. V. Libanov, V. A. Rubakov, D. T. Son and S. V. Troitsky, *Exponentiation of multiparticle amplitudes in scalar theories*, *Phys. Rev. D* **50** (1994) 7553 [hep-ph/9407381].
[106] D. T. Son, *Semiclassical approach for multiparticle production in scalar theories*,

Nucl. Phys. B **477** (1996) 378 [hep-ph/9505338].

[107] V. V. Khoze, *Multiparticle Higgs and Vector Boson Amplitudes at Threshold*, *JHEP* **07** (2014) 008 [1404.4876].

[108] V. V. Khoze, *Multiparticle production in the large λn limit: realising Higgsplosion in a scalar QFT*, *JHEP* **06** (2017) 148 [1705.04365].

[109] G. Badel, G. Cuomo, A. Monin and R. Rattazzi, *The Epsilon Expansion Meets Semiclassics*, *JHEP* **11** (2019) 110 [1909.01269].

[110] G. Dvali and C. Gomez, *Black Hole's Quantum N-Portrait*, *Fortsch. Phys.* **61** (2013) 742 [1112.3359].

[111] G. Dvali and L. Eisemann, *Perturbative understanding of nonperturbative processes and quantumization versus classicalization*, *Phys. Rev. D* **106** (2022) 125019 [2211.02618].

[112] G. Dvali, G. F. Giudice, C. Gomez and A. Kehagias, *UV-Completion by Classicalization*, *JHEP* **08** (2011) 108 [1010.1415].

[113] W. Buchmuller and D. Wyler, *Effective Lagrangian Analysis of New Interactions and Flavor Conservation*, *Nucl. Phys. B* **268** (1986) 621.

[114] I. Brivio and M. Trott, *The Standard Model as an Effective Field Theory*, *Phys. Rept.* **793** (2019) 1 [1706.08945].

[115] A. Falkowski, M. Gonzalez-Alonso, A. Greljo, D. Marzocca and M. Son, *Anomalous Triple Gauge Couplings in the Effective Field Theory Approach at the LHC*, *JHEP* **02** (2017) 115 [1609.06312].

[116] D. Liu, A. Pomarol, R. Rattazzi and F. Riva, *Patterns of Strong Coupling for LHC Searches*, *JHEP* **11** (2016) 141 [1603.03064].

[117] A. Azatov, R. Contino, C. S. Machado and F. Riva, *Helicity selection rules and noninterference for BSM amplitudes*, *Phys. Rev. D* **95** (2017) 065014 [1607.05236].

[118] A. Helset and M. Trott, *On interference and non-interference in the SMEFT*, *JHEP* **04** (2018) 038 [1711.07954].

[119] A. Azatov, D. Barducci and E. Venturini, *Precision diboson measurements at hadron colliders*, *JHEP* **04** (2019) 075 [1901.04821].

[120] H. El Faham, G. Pelliccioli and E. Vryonidou, *Triple-gauge couplings in LHC diboson production: a SMEFT view from every angle*, 2405.19083.

[121] L. J. Dixon and Y. Shadmi, *Testing gluon selfinteractions in three jet events at hadron colliders*, *Nucl. Phys. B* **423** (1994) 3 [hep-ph/9312363].

[122] Y. Afik and J. R. M. n. de Nova, *Entanglement and quantum tomography with top quarks at the LHC*, *Eur. Phys. J. Plus* **136** (2021) 907 [2003.02280].

[123] ATLAS collaboration, *Observation of quantum entanglement in top-quark pairs using the ATLAS detector*, 2311.07288.

[124] A. J. Barr, M. Fabbrichesi, R. Floreanini, E. Gabrielli and L. Marzola, *Quantum entanglement and Bell inequality violation at colliders*, 2402.07972.

[125] S. A. Abel, M. Dittmar and H. K. Dreiner, *Testing locality at colliders via Bell's inequality?*, *Phys. Lett. B* **280** (1992) 304.

[126] S. Li, W. Shen and J. M. Yang, *Can Bell inequalities be tested via scattering cross-section at colliders ?*, 2401.01162.

[127] F. Maltoni, C. Severi, S. Tentori and E. Vryonidou, *Quantum detection of new physics in top-quark pair production at the LHC*, *JHEP* **03** (2024) 099 [2401.08751].

[128] E. H. Simmons, *Dimension-six Gluon Operators as Probes of New Physics*, *Phys. Lett. B* **226** (1989) 132.

[129] E. H. Simmons, *Higher dimension gluon operators and hadronic scattering*, *Phys. Lett. B* **246** (1990) 471.
[130] A. Azatov, J. Elias-Miro, Y. Reyimuaji and E. Venturini, *Novel measurements of anomalous triple gauge couplings for the LHC*, *JHEP* **10** (2017) 027 [1707.08060].
[131] R. Aoude and W. Shepherd, *Jet Substructure Measurements of Interference in Non-Interfering SMEFT Effects*, *JHEP* **08** (2019) 009 [1902.11262].
[132] G. Panico, F. Riva and A. Wulzer, *Diboson interference resurrection*, *Phys. Lett. B* **776** (2018) 473 [1708.07823].
[133] G. M. D'Ariano, M. G. A. Paris and M. F. Sacchi, *Quantum Tomography*, quant-ph/0302028.
[134] Y. Afik and J. R. M. n. de Nova, *Quantum information with top quarks in QCD*, *Quantum* **6** (2022) 820 [2203.05582].
[135] U. Fano, *Pairs of two-level systems*, *Rev. Mod. Phys.* **55** (1983) 855.
[136] PDF4LHC Working Group collaboration, *The PDF4LHC21 combination of global PDF fits for the LHC Run III*, *J. Phys. G* **49** (2022) 080501 [2203.05506].
[137] D. Clark, E. Godat and F. Olness, *Maneparse: a mathematica reader for parton distribution functions*, *Computer Physics Communications* (2016) .
[138] E. Schrödinger, *Discussion of probability relations between separated systems*, *Mathematical Proceedings of the Cambridge Philosophical Society* **31** (1935) 555–563.
[139] R. Horodecki, P. Horodecki, M. Horodecki and K. Horodecki, *Quantum entanglement*, *Reviews of Modern Physics* **81** (2009) 865.
[140] W. K. Wootters, *Entanglement of formation of an arbitrary state of two qubits*, *Physical Review Letters* **80** (1998) 2245.
[141] R. Horodecki, P. Horodecki and M. Horodecki, *Violating bell inequality by mixed spin-12 states: necessary and sufficient condition*, *Physics Letters A* **200** (1995) 340.
[142] N. Gisin, *Bell's inequality holds for all non-product states*, *Physics Letters A* **154** (1991) 201.
[143] W. Bernreuther, D. Heisler and Z.-G. Si, *A set of top quark spin correlation and polarization observables for the LHC: Standard Model predictions and new physics contributions*, *JHEP* **12** (2015) 026 [1508.05271].
[144] A. Peres, *Separability criterion for density matrices*, *Phys. Rev. Lett.* **77** (1996) 1413 [quant-ph/9604005].
[145] C. H. Bennett, D. P. DiVincenzo, C. A. Fuchs, T. Mor, E. Rains, P. W. Shor et al., *Quantum nonlocality without entanglement*, *Phys. Rev. A* **59** (1999) 1070 [quant-ph/9804053].
[146] A. Bera, T. Das, D. Sadhukhan, S. S. Roy, A. S. De and U. Sen, *Quantum discord and its allies: a review*, *arXiv preprint arXiv: 1703.10542* (2017) .
[147] Y. Afik and J. R. M. n. de Nova, *Quantum Discord and Steering in Top Quarks at the LHC*, *Phys. Rev. Lett.* **130** (2023) 221801 [2209.03969].
[148] D. Girolami, T. Tufarelli and G. Adesso, *Characterizing Nonclassical Correlations via Local Quantum Uncertainty*, *Phys. Rev. Lett.* **110** (2013) 240402 [1212.2214].
[149] M. Baumgart and B. Tweedie, *A New Twist on Top Quark Spin Correlations*, *JHEP* **03** (2013) 117 [1212.4888].
[150] M. M. Altakach, P. Lamba, F. Maltoni, K. Mawatari and K. Sakurai, *Quantum*

information and CP measurement in $H \to \tau^+\tau^-$ at future lepton colliders, 2211.10513.

[151] K. Ehatäht, M. Fabbrichesi, L. Marzola and C. Veelken, *Probing entanglement and testing Bell inequality violation with e+e-→τ+τ- at Belle II*, *Phys. Rev. D* **109** (2024) 032005 [2311.17555].

[152] K. Cheng, T. Han and M. Low, *Optimizing fictitious states for Bell inequality violation in bipartite qubit systems with applications to the tt^- system*, *Phys. Rev. D* **109** (2024) 116005 [2311.09166].

[153] D. Jeans, *Tau lepton reconstruction at collider experiments using impact parameters*, *Nucl. Instrum. Meth. A* **810** (2016) 51 [1507.01700].

[154] R. Aoude, E. Madge, F. Maltoni and L. Mantani, *Probing new physics through entanglement in diboson production*, *JHEP* **12** (2023) 017 [2307.09675].

[155] U. Haisch, L. Schnell and J. Weiss, *LHC tau-pair production constraints on a_τ and d_τ*, 2307.14133.

[156] S. Eidelman and M. Passera, *Theory of the tau lepton anomalous magnetic moment*, 0701260.

[157] F. Feruglio, P. Paradisi and O. Sumensari, *Implications of scalar and tensor explanations of $R_{D^{(*)}}$*, *JHEP* **11** (2018) 191 [1806.10155].

[158] I. Doršner, S. Fajfer, A. Greljo, J. F. Kamenik and N. Košnik, *Physics of leptoquarks in precision experiments and at particle colliders*, *Phys. Rept.* **641** (2016) 1 [1603.04993].

[159] K.-m. Cheung, *Muon anomalous magnetic moment and leptoquark solutions*, *Phys. Rev. D* **64** (2001) 033001 [hep-ph/0102238].

[160] I. Doršner, S. Fajfer and O. Sumensari, *Muon $g-2$ and scalar leptoquark mixing*, *JHEP* **06** (2020) 089 [1910.03877].

[161] A. Crivellin and M. Hoferichter, *Consequences of chirally enhanced explanations of $(g-2)_\mu$ for $h \to \mu\mu$ and $Z \to \mu\mu$*, *JHEP* **07** (2021) 135 [2104.03202].

[162] T. Aoyama et al., *The anomalous magnetic moment of the muon in the Standard Model*, *Phys. Rept.* **887** (2020) 1 [2006.04822].

[163] Muon g-2 collaboration, *Measurement of the Positive Muon Anomalous Magnetic Moment to 0.46 ppm*, *Phys. Rev. Lett.* **126** (2021) 141801 [2104.03281].

[164] A. S. Fomin, A. Y. Korchin, A. Stocchi, S. Barsuk and P. Robbe, *Feasibility of τ -lepton electromagnetic dipole moments measurement using bent crystal at the LHC*, *JHEP* **03** (2019) 156 [1810.06699].

[165] J. Fu, M. A. Giorgi, L. Henry, D. Marangotto, F. M. Vidal, A. Merli et al., *Novel Method for the Direct Measurement of the τ Lepton Dipole Moments*, *Phys. Rev. Lett.* **123** (2019) 011801 [1901.04003].

[166] J. Bernabeu, G. A. Gonzalez-Sprinberg, M. Tung and J. Vidal, *The Tau weak magnetic dipole moment*, *Nucl. Phys. B* **436** (1995) 474 [hep-ph/9411289].

[167] J. Bernabeu, G. A. Gonzalez-Sprinberg, J. Papavassiliou and J. Vidal, *Tau anomalous magnetic moment form-factor at super B/flavor factories*, *Nucl. Phys. B* **790** (2008) 160 [0707.2496].

[168] J. Bernabeu, G. A. Gonzalez-Sprinberg and J. Vidal, *Tau spin correlations and the anomalous magnetic moment*, *JHEP* **01** (2009) 062 [0807.2366].

[169] S. Eidelman, D. Epifanov, M. Fael, L. Mercolli and M. Passera, *τ dipole moments via radiative leptonic τ decays*, *JHEP* **03** (2016) 140 [1601.07987].

[170] A. Rajaraman, J. N. Howard, R. Riley and T. M. P. Tait, *The τ Magnetic Dipole Moment at Future Lepton Colliders*, *LHEP* **2** (2019) 5 [1810.09570].

[171] Belle collaboration, *An improved search for the electric dipole moment of the τ*

lepton, *JHEP* **04** (2022) 110 [2108.11543].

[172] G. A. Gonzalez-Sprinberg, A. Santamaria and J. Vidal, *Model independent bounds on the tau lepton electromagnetic and weak magnetic moments*, *Nucl. Phys. B* **582** (2000) 3 [hep-ph/0002203].

[173] DELPHI collaboration, *Study of tau-pair production in photon-photon collisions at LEP and limits on the anomalous electromagnetic moments of the tau lepton*, *Eur. Phys. J. C* **35** (2004) 159 [hep-ex/0406010].

[174] I. Galon, A. Rajaraman and T. M. P. Tait, *$H \to \tau^+\tau^-\gamma$ as a probe of the τ magnetic dipole moment*, *JHEP* **12** (2016) 111 [1610.01601].

[175] ATLAS collaboration, *Observation of the $\gamma\gamma \to \tau\tau$ Process in Pb+Pb Collisions and Constraints on the τ-Lepton Anomalous Magnetic Moment with the ATLAS Detector*, *Phys. Rev. Lett.* **131** (2023) 151802 [2204.13478].

[176] CMS collaboration, *Observation of τ lepton pair production in ultraperipheral lead-lead collisions at $\sqrt{s_{\mathrm{NN}}} = 5.02$ TeV*, *Phys. Rev. Lett.* **131** (2023) 151803 [2206.05192].

[177] M. Verducci, N. Vignaroli, C. Roda and V. Cavasinni, *A study of the measurement of the τ lepton anomalous magnetic moment in high energy lead-lead collisions at LHC*, 2307.15160.

[178] M. L. Laursen, M. A. Samuel and A. Sen, *Radiation Zeros and a Test for the g Value of the τ Lepton*, *Phys. Rev. D* **29** (1984) 2652.

[179] I. Rodriguez and O. A. Sampayo, *Tau anomalous couplings and radiation zeros in the e+ e- —> tau anti-tau gamma process*, hep-ph/0312316.

[180] M. Fael, L. Mercolli and M. Passera, *Towards a determination of the tau lepton dipole moments*, *Nucl. Phys. B Proc. Suppl.* **253-255** (2014) 103 [1301.5302].

[181] J. Aebischer, W. Dekens, E. E. Jenkins, A. V. Manohar, D. Sengupta and P. Stoffer, *Effective field theory interpretation of lepton magnetic and electric dipole moments*, *JHEP* **07** (2021) 107 [2102.08954].

[182] T. Hahn and M. Perez-Victoria, *Automatized one loop calculations in four-dimensions and D-dimensions*, *Comput. Phys. Commun.* **118** (1999) 153 [hep-ph/9807565].

[183] T. Hahn, *Generating Feynman diagrams and amplitudes with FeynArts 3*, *Comput. Phys. Commun.* **140** (2001) 418 [hep-ph/0012260].

[184] S. Banerjee, A. Y. Korchin and Z. Was, *Spin correlations in τ-lepton pair production due to anomalous magnetic and electric dipole moments*, *Phys. Rev. D* **106** (2022) 113010 [2209.06047].

[185] F. Maltoni, C. Severi, S. Tentori and E. Vryonidou, *Quantum tops at circular lepton colliders*, 2404.08049.

[186] M. Fabbrichesi and L. Marzola, *Quantum tomography with τ leptons at the FCC-ee*, 2405.09201.

[187] A. Elagin, P. Murat, A. Pranko and A. Safonov, *A New Mass Reconstruction Technique for Resonances Decaying to di-tau*, *Nucl. Instrum. Meth. A* **654** (2011) 481 [1012.4686].

[188] CMS collaboration, *Measurement of the tau lepton polarization in Z boson decays*, .

[189] L. Bianchini, B. Calpas, J. Conway, A. Fowlie, L. Marzola, C. Veelken et al., *Reconstruction of the Higgs mass in events with Higgs bosons decaying into a pair of τ leptons using matrix element techniques*, *Nucl. Instrum. Meth. A* **862** (2017) 54 [1603.05910].

[190] P. Bärtschi, C. Galloni, C. Lange and B. Kilminster, *Reconstruction of τ lepton pair invariant mass using an artificial neural network*, *Nucl. Instrum. Meth. A*

929 (2019) 29 [1904.04924].

[191] N. Tamir, I. Bessudo, B. Chen, H. Raiko and L. Barak, *Neural networks for boosted di-τ identification*, *JINST* **19** (2024) P07004 [2312.08276].

[192] L. Tani, N.-N. Seeba, H. Vanaveski, J. Pata and T. Lange, *A unified machine learning approach for reconstructing hadronically decaying tau leptons*, 2407.06788.

[193] A. Y. Korchin, E. Richter-Was, Y. Volkotrub and Z. Was, *τ-lepton pair spin in proton-proton LHC collisions for anomalous dipole moments*, 2407.17282.

[194] C. G. Timpson, *Perspective chapter: Why do we care about violating bell inequalities?*, in *Quantum Entanglement in High Energy Physics*, O. K. Baker, ed., (Rijeka), IntechOpen, (2023), DOI.

[195] M. Carena, A. Daleo, B. A. Dobrescu and T. M. P. Tait, *Z' gauge bosons at the Tevatron*, *Phys. Rev. D* **70** (2004) 093009 [hep-ph/0408098].

[196] P. Batra, B. A. Dobrescu and D. Spivak, *Anomaly-free sets of fermions*, *J. Math. Phys.* **47** (2006) 082301 [hep-ph/0510181].

[197] P. Langacker, *The Physics of Heavy Z' Gauge Bosons*, *Rev. Mod. Phys.* **81** (2009) 1199 [0801.1345].

[198] A. Hook, E. Izaguirre and J. G. Wacker, *Model Independent Bounds on Kinetic Mixing*, *Adv. High Energy Phys.* **2011** (2011) 859762 [1006.0973].

[199] P. Fileviez Perez and M. B. Wise, *Breaking Local Baryon and Lepton Number at the TeV Scale*, *JHEP* **08** (2011) 068 [1106.0343].

[200] B. A. Dobrescu and F. Yu, *Coupling-Mass Mapping of Dijet Peak Searches*, *Phys. Rev. D* **88** (2013) 035021 [1306.2629].

[201] B. A. Dobrescu and C. Frugiuele, *Hidden GeV-scale interactions of quarks*, *Phys. Rev. Lett.* **113** (2014) 061801 [1404.3947].

[202] D. B. Costa, B. A. Dobrescu and P. J. Fox, *General Solution to the U(1) Anomaly Equations*, *Phys. Rev. Lett.* **123** (2019) 151601 [1905.13729].

[203] S. Heeba and F. Kahlhoefer, *Probing the freeze-in mechanism in dark matter models with U(1)' gauge extensions*, *Phys. Rev. D* **101** (2020) 035043 [1908.09834].

[204] L. Michaels and F. Yu, *Probing new $U(1)$ gauge symmetries via exotic $Z \to Z'\gamma$ decays*, *JHEP* **03** (2021) 120 [2010.00021].

[205] M. Bauer, P. Foldenauer and M. Mosny, *Flavor structure of anomaly-free hidden photon models*, *Phys. Rev. D* **103** (2021) 075024 [2011.12973].

[206] LHC New Physics Working Group collaboration, *Simplified Models for LHC New Physics Searches*, *J. Phys. G* **39** (2012) 105005 [1105.2838].

[207] X.-P. Liu, Jia Wang and F. Yu, *A Tale of Two Portals: Testing Light, Hidden New Physics at Future e^+e^- Colliders*, *JHEP* **06** (2017) 077 [1704.00730].

[208] J. A. Dror, R. Lasenby and M. Pospelov, *Dark forces coupled to nonconserved currents*, *Phys. Rev. D* **96** (2017) 075036 [1707.01503].

[209] A. Albert et al., *Recommendations of the LHC Dark Matter Working Group: Comparing LHC searches for dark matter mediators in visible and invisible decay channels and calculations of the thermal relic density*, *Phys. Dark Univ.* **26** (2019) 100377 [1703.05703].

[210] A. Ismail, A. Katz and D. Racco, *On dark matter interactions with the Standard Model through an anomalous Z'*, *JHEP* **10** (2017) 165 [1707.00709].

[211] A. Ismail and A. Katz, *Anomalous Z' and diboson resonances at the LHC*, *JHEP* **04** (2018) 122 [1712.01840].

[212] J. A. Dror, R. Lasenby and M. Pospelov, *Light vectors coupled to bosonic currents*,

Phys. Rev. D **99** (2019) 055016 [1811.00595].
[213] P. Foldenauer, *Light dark matter in a gauged $U(1)_{L_\mu - L_\tau}$ model*, *Phys. Rev. D* **99** (2019) 035007 [1808.03647].
[214] H.-C. Cheng, X.-H. Jiang, L. Li and E. Salvioni, *Dark showers from Z-dark Z' mixing*, *JHEP* **04** (2024) 081 [2401.08785].
[215] X. Chu, T. Hambye and M. H. G. Tytgat, *The Four Basic Ways of Creating Dark Matter Through a Portal*, *JCAP* **05** (2012) 034 [1112.0493].
[216] R. Essig et al., *Working Group Report: New Light Weakly Coupled Particles*, in *Snowmass 2013: Snowmass on the Mississippi*, 10, 2013, 1311.0029.
[217] P. Ilten, Y. Soreq, M. Williams and W. Xue, *Serendipity in dark photon searches*, *JHEP* **06** (2018) 004 [1801.04847].
[218] M. Bauer, P. Foldenauer and J. Jaeckel, *Hunting All the Hidden Photons*, *JHEP* **07** (2018) 094 [1803.05466].
[219] M. Fabbrichesi, E. Gabrielli and G. Lanfranchi, *The Dark Photon*, 2005.01515.
[220] C. Antel et al., *Feebly-interacting particles: FIPs 2022 Workshop Report*, *Eur. Phys. J. C* **83** (2023) 1122 [2305.01715].
[221] F. Jegerlehner, *Renormalizing the standard model*, *Conf. Proc. C* **900603** (1990) 476.
[222] ALEPH, DELPHI, L3, OPAL, SLD, LEP Electroweak Working Group, SLD Electroweak Group, SLD Heavy Flavour Group collaboration, *Precision electroweak measurements on the Z resonance*, *Phys. Rept.* **427** (2006) 257 [hep-ex/0509008].
[223] B. Holdom, *Two U(1)'s and Epsilon Charge Shifts*, *Phys. Lett. B* **166** (1986) 196.
[224] Particle Data Group collaboration, *Review of Particle Physics*, *PTEP* **2022** (2022) 083C01.
[225] G. Breit and E. Wigner, *Capture of Slow Neutrons*, *Phys. Rev.* **49** (1936) 519.
[226] FCC collaboration, *FCC-ee: The Lepton Collider: Future Circular Collider Conceptual Design Report Volume 2*, *Eur. Phys. J. ST* **228** (2019) 261.
[227] CEPC Study Group collaboration, *CEPC Conceptual Design Report: Volume 2 - Physics & Detector*, 1811.10545.
[228] M. Frank, T. Hahn, S. Heinemeyer, W. Hollik, H. Rzehak and G. Weiglein, *The Higgs Boson Masses and Mixings of the Complex MSSM in the Feynman-Diagrammatic Approach*, *JHEP* **02** (2007) 047 [hep-ph/0611326].
[229] E. Fuchs and G. Weiglein, *Breit-Wigner approximation for propagators of mixed unstable states*, *JHEP* **09** (2017) 079 [1610.06193].
[230] J. Racker, *CP violation in mixing and oscillations in a toy model for leptogenesis with quasi-degenerate neutrinos*, *JHEP* **04** (2021) 290 [2012.05354].
[231] J. Racker, *CP violation in mixing and oscillations for leptogenesis. Part II. The highly degenerate case*, *JHEP* **11** (2021) 027 [2109.00040].
[232] M. Beuthe, *Oscillations of neutrinos and mesons in quantum field theory*, *Phys. Rept.* **375** (2003) 105 [hep-ph/0109119].
[233] A. Pilaftsis, *Resonant CP violation induced by particle mixing in transition amplitudes*, *Nucl. Phys. B* **504** (1997) 61 [hep-ph/9702393].
[234] G. Cacciapaglia, A. Deandrea and S. De Curtis, *Nearby resonances beyond the Breit-Wigner approximation*, *Phys. Lett. B* **682** (2009) 43 [0906.3417].
[235] J. de Blas, J. M. Lizana and M. Perez-Victoria, *Combining searches of Z' and W' bosons*, *JHEP* **01** (2013) 166 [1211.2229].
[236] B. A. Dobrescu and F. Yu, *Dijet and electroweak limits on a Z' boson coupled to quarks*, *Phys. Rev. D* **109** (2024) 035004 [2112.05392].

[237] G. D. Kribs, G. Lee and A. Martin, *Effective field theory of Stückelberg vector bosons*, *Phys. Rev. D* **106** (2022) 055020 [2204.01755].
[238] K. S. Babu, C. F. Kolda and J. March-Russell, *Implications of generalized Z-Z′ mixing*, *Phys. Rev. D* **57** (1998) 6788 [hep-ph/9710441].
[239] D. Curtin, R. Essig, S. Gori and J. Shelton, *Illuminating dark photons with high-energy colliders*, *JHEP* **02** (2015) 157 [1412.0018].
[240] A. Greljo, P. Stangl, A. E. Thomsen and J. Zupan, *On $(g-2)_\mu$ from gauged $u(1)_X$*, *JHEP* **07** (2022) 098 [2203.13731].
[241] K. Harigaya, E. Petrosky and A. Pierce, *Precision Electroweak Tensions and a Dark Photon*, 2307.13045.
[242] D. Qiu and Y.-L. Tang, *Electroweak Precision Measurements of a Nearly-Degenerate Z′-Z System*, 2309.16794.
[243] N. M. Coyle and C. E. M. Wagner, *Resolving the muon $g-2$ tension through Z′-induced modifications to σ_{had}*, *JHEP* **12** (2023) 071 [2305.02354].
[244] B. Misra and E. C. G. Sudarshan, *The Zeno's Paradox in Quantum Theory*, *J. Math. Phys.* **18** (1977) 756.
[245] T. G. Rizzo, *Z′ phenomenology and the LHC*, in *Theoretical Advanced Study Institute in Elementary Particle Physics: Exploring New Frontiers Using Colliders and Neutrinos*, pp. 537–575, 10, 2006, hep-ph/0610104.
[246] C. T. Hill and E. H. Simmons, *Strong Dynamics and Electroweak Symmetry Breaking*, *Phys. Rept.* **381** (2003) 235 [hep-ph/0203079].
[247] A. Leike, *The Phenomenology of extra neutral gauge bosons*, *Phys. Rept.* **317** (1999) 143 [hep-ph/9805494].
[248] A. Pais, *Remark on baryon conservation*, *Phys. Rev. D* **8** (1973) 1844.
[249] Y. Tosa, R. E. Marshak and S. Okubo, *Baryon and Lepton Numbers as Broken Local Symmetries*, *Phys. Rev. D* **27** (1983) 444.
[250] C. D. Carone and H. Murayama, *Possible light U(1) gauge boson coupled to baryon number*, *Phys. Rev. Lett.* **74** (1995) 3122 [hep-ph/9411256].
[251] M. A. Melvin, *Elementary particles and symmetry principles*, *Rev. Mod. Phys.* **32** (1960) 477.
[252] T. Gherghetta, J. Kersten, K. Olive and M. Pospelov, *Evaluating the price of tiny kinetic mixing*, *Phys. Rev. D* **100** (2019) 095001 [1909.00696].
[253] J. L. Feng, H. Tu and H.-B. Yu, *Thermal Relics in Hidden Sectors*, *JCAP* **10** (2008) 043 [0808.2318].
[254] L. Ackerman, M. R. Buckley, S. M. Carroll and M. Kamionkowski, *Dark Matter and Dark Radiation*, *Phys. Rev. D* **79** (2009) 023519 [0810.5126].
[255] J. L. Feng, M. Kaplinghat, H. Tu and H.-B. Yu, *Hidden Charged Dark Matter*, *JCAP* **07** (2009) 004 [0905.3039].
[256] M. Bohm, H. Spiesberger and W. Hollik, *On the One Loop Renormalization of the Electroweak Standard Model and Its Application to Leptonic Processes*, *Fortsch. Phys.* **34** (1986) 687.
[257] M. E. Peskin and T. Takeuchi, *A New constraint on a strongly interacting Higgs sector*, *Phys. Rev. Lett.* **65** (1990) 964.
[258] M. E. Peskin and T. Takeuchi, *Estimation of oblique electroweak corrections*, *Phys. Rev. D* **46** (1992) 381.
[259] J. H. Christenson, J. W. Cronin, V. L. Fitch and R. Turlay, *Evidence for the 2π Decay of the K_2^0 Meson*, *Phys. Rev. Lett.* **13** (1964) 138.
[260] R. G. Stuart, *General renormalization of the gauge invariant perturbation expansion near the Z0 resonance*, *Phys. Lett. B* **272** (1991) 353.

[261] A. Sirlin, *Observations concerning mass renormalization in the electroweak theory*, *Phys. Lett. B* **267** (1991) 240.
[262] A. Sirlin, *Theoretical considerations concerning the Z0 mass*, *Phys. Rev. Lett.* **67** (1991) 2127.
[263] M. Nowakowski and A. Pilaftsis, *On gauge invariance of Breit-Wigner propagators*, *Z. Phys. C* **60** (1993) 121 [hep-ph/9305321].
[264] A. Denner and J.-N. Lang, *The Complex-Mass Scheme and Unitarity in perturbative Quantum Field Theory*, *Eur. Phys. J. C* **75** (2015) 377 [1406.6280].
[265] H. Feshbach, *Unified theory of nuclear reactions*, *Annals Phys.* **5** (1958) 357.
[266] D. Espriu, J. Manzano and P. Talavera, *Flavor mixing, gauge invariance and wave function renormalization*, *Phys. Rev. D* **66** (2002) 076002 [hep-ph/0204085].
[267] A. Lewandowski, *LSZ-reduction, resonances and non-diagonal propagators: fermions and scalars*, *Nucl. Phys. B* **937** (2018) 394 [1710.07165].
[268] A. Lewandowski, *LSZ-reduction, resonances and non-diagonal propagators: Gauge fields*, *Nucl. Phys. B* **935** (2018) 40 [1803.11434].
[269] K. Sakurai and W. Yin, *Suppression of Higgs mixing by "quantum Zeno effect"*, *Eur. Phys. J. C* **83** (2023) 498 [2204.01739].
[270] CDF collaboration, *High-precision measurement of the W boson mass with the CDF II detector*, *Science* **376** (2022) 170.
[271] M. Martinez, R. Miquel, G. Rolandi and R. Tenchini, *Precision tests of the electroweak interaction at the Z pole*, *Rev. Mod. Phys.* **71** (1999) 575.
[272] S. Cassel, D. M. Ghilencea and G. G. Ross, *Electroweak and Dark Matter Constraints on a Z-prime in Models with a Hidden Valley*, *Nucl. Phys. B* **827** (2010) 256 [0903.1118].
[273] D. Boyanovsky and J. Chen, *Kinetic mixing between a Higgs boson and a nearly degenerate dark scalar: Oscillations and displaced vertices*, *Phys. Rev. D* **96** (2017) 096007 [1708.05328].
[274] A. Kamada, T. Kuwahara, S. Matsumoto, Y. Watanabe and Y. Watanabe, *Mediator decay through mixing with degenerate spectrum*, 2404.06793.
[275] R. Feynman, R. Leighton and M. Sands, *The Feynman Lectures on Physics, Vol. 3: Quantum Mechanics*. California Institute of Technology, 1964.
[276] T. Aoyama, T. Kinoshita and M. Nio, *Theory of the Anomalous Magnetic Moment of the Electron*, *Atoms* **7** (2019) 28.
[277] R. Boughezal et al., *Theory Techniques for Precision Physics – Snowmass 2021 TF06 Topical Group Report*, 2209.10639.
[278] F. Maltoni et al., *TF07 Snowmass Report: Theory of Collider Phenomena*, 2210.02591.
[279] C. A. Hurst, *The Enumeration of Graphs in the Feynman-Dyson Technique*, *Proc. Roy. Soc. Lond. A* **214** (1952) 44.
[280] C. M. Bender and T. T. Wu, *Statistical Analysis of Feynman Diagrams*, *Phys. Rev. Lett.* **37** (1976) 117.
[281] C. M. Bender and S. A. Orszag, *Advanced mathematical methods for scientists and engineers I: Asymptotic methods and perturbation theory*. Springer, 1999.
[282] M. Mariño, *Lectures on non-perturbative effects in large N gauge theories, matrix models and strings*, *Fortsch. Phys.* **62** (2014) 455 [1206.6272].
[283] D. Dorigoni, *An Introduction to Resurgence, Trans-Series and Alien Calculus*, *Annals Phys.* **409** (2019) 167914 [1411.3585].
[284] M. Mariño, *Advanced Topics in Quantum Mechanics*. Cambridge University Press,

12, 2021, 10.1017/9781108863384.

[285] E. Brezin, G. Parisi and J. Zinn-Justin, *Perturbation Theory at Large Orders for Potential with Degenerate Minima*, *Phys. Rev. D* **16** (1977) 408.

[286] E. B. Bogomolny and V. A. Fateev, *Large Orders Calculations in the Gauge Theories*, *Phys. Lett. B* **71** (1977) 93.

[287] E. B. Bogomolny, *Calculation of Instanton - Anti-Instanton Contributions in Quantum Mechanics*, *Phys. Lett. B* **91** (1980) 431.

[288] M. Stone and J. Reeve, *Late Terms in the Asymptotic Expansion for the Energy Levels of a Periodic Potential*, *Phys. Rev. D* **18** (1978) 4746.

[289] P. Achuthan, H. J. W. Muller-Kirsten and A. Wiedemann, *Perturbation Theory and Boundary Conditions: Analogous Treatments of Anharmonic Oscillators and Double Wells and Similarly Related Potentials and the Calculation of Exponentially Small Contributions to Eigenvalues*, *Fortsch. Phys.* **38** (1990) 78.

[290] J. Q. Liang and H. J. W. Muller-Kirsten, *Quantum tunneling for the sine-Gordon potential: Energy band structure and Bogomolny-Fateev relation*, *Phys. Rev. D* **51** (1995) 718.

[291] J. Zinn-Justin, *Multi - Instanton Contributions in Quantum Mechanics*, *Nucl. Phys. B* **192** (1981) 125.

[292] J. Zinn-Justin, *Multi - Instanton Contributions in Quantum Mechanics. 2.*, *Nucl. Phys. B* **218** (1983) 333.

[293] J. Zinn-Justin, *Instantons in Quantum Mechanics: Numerical Evidence for a Conjecture*, *J. Math. Phys.* **25** (1984) 549.

[294] I. I. Balitsky and A. V. Yung, *Instanton Molecular Vacuum in $N = 1$ Supersymmetric Quantum Mechanics*, *Nucl. Phys. B* **274** (1986) 475.

[295] I. I. Balitsky and A. V. Yung, *Collective - Coordinate Method for Quasizero Modes*, *Phys. Lett. B* **168** (1986) 113.

[296] H. Aoyama, H. Kikuchi, I. Okouchi, M. Sato and S. Wada, *Valley views: Instantons, large order behaviors, and supersymmetry*, *Nucl. Phys. B* **553** (1999) 644 [hep-th/9808034].

[297] H. Aoyama, H. Kikuchi, I. Okouchi, M. Sato and S. Wada, *Valleys in quantum mechanics*, *Phys. Lett. B* **424** (1998) 93 [quant-ph/9710064].

[298] J. Zinn-Justin and U. D. Jentschura, *Multi-instantons and exact results I: Conjectures, WKB expansions, and instanton interactions*, *Annals Phys.* **313** (2004) 197 [quant-ph/0501136].

[299] J. Zinn-Justin and U. D. Jentschura, *Multi-instantons and exact results II: Specific cases, higher-order effects, and numerical calculations*, *Annals Phys.* **313** (2004) 269 [quant-ph/0501137].

[300] U. D. Jentschura and J. Zinn-Justin, *Instantons in quantum mechanics and resurgent expansions*, *Phys. Lett. B* **596** (2004) 138 [hep-ph/0405279].

[301] M. Marino, R. Schiappa and M. Weiss, *Nonperturbative Effects and the Large-Order Behavior of Matrix Models and Topological Strings*, *Commun. Num. Theor. Phys.* **2** (2008) 349 [0711.1954].

[302] M. Marino, *Nonperturbative effects and nonperturbative definitions in matrix models and topological strings*, *JHEP* **12** (2008) 114 [0805.3033].

[303] M. Unsal, *Theta dependence, sign problems and topological interference*, *Phys. Rev. D* **86** (2012) 105012 [1201.6426].

[304] I. Aniceto and R. Schiappa, *Nonperturbative Ambiguities and the Reality of Resurgent Transseries*, *Commun. Math. Phys.* **335** (2015) 183 [1308.1115].

[305] G. V. Dunne and M. Unsal, *Uniform WKB, Multi-instantons, and Resurgent*

Trans-Series, *Phys. Rev. D* **89** (2014) 105009 [1401.5202].

[306] E. M. Malatesta, G. Parisi and T. Rizzo, *Two-loop corrections to large order behavior of φ^4 theory*, *Nuclear Physics B* **922** (2017) 293 [1704.04458].

[307] C. M. Bender and T. T. Wu, *Anharmonic oscillator*, *Phys. Rev.* **184** (1969) 1231.

[308] C. M. Bender and T. T. Wu, *Anharmonic oscillator. 2: A Study of perturbation theory in large order*, *Phys. Rev. D* **7** (1973) 1620.

[309] J. J. Loeffel, A. Martin, B. Simon and A. S. Wightman, *Pade approximants and the anharmonic oscillator*, *Phys. Lett. B* **30** (1969) 656.

[310] T. Sulejmanpasic and M. Ünsal, *Aspects of perturbation theory in quantum mechanics: The BenderWu Mathematica ® package*, *Comput. Phys. Commun.* **228** (2018) 273 [1608.08256].

[311] M. Serone, G. Spada and G. Villadoro, *The Power of Perturbation Theory*, *JHEP* **05** (2017) 056 [1702.04148].

[312] L. T. Giorgini, U. D. Jentschura, E. M. Malatesta, G. Parisi, T. Rizzo and J. Zinn-Justin, *Two-Loop Corrections to the Large-Order Behavior of Correlation Functions in the One-Dimensional N-Vector Model*, *Phys. Rev. D* **101** (2020) 125001 [2005.01485].

[313] L. T. Giorgini, U. D. Jentschura, E. M. Malatesta, G. Parisi, T. Rizzo and J. Zinn-Justin, *Correlation functions of the anharmonic oscillator: Numerical verification of two-loop corrections to the large-order behavior*, *Phys. Rev. D* **105** (2022) 105012 [2111.12765].

[314] C. Bachas, *A Proof of exponential suppression of high-energy transitions in the anharmonic oscillator*, *Nucl. Phys. B* **377** (1992) 622.

[315] J. M. Cornwall and G. Tiktopoulos, *Functional Schrodinger equation approach to high-energy multiparticle scattering*, *Phys. Lett. B* **282** (1992) 195.

[316] J. M. Cornwall and G. Tiktopoulos, *The Functional Schrodinger equation approach to high-energy multileg amplitudes*, *Phys. Rev. D* **47** (1993) 1629.

[317] J. M. Cornwall and G. Tiktopoulos, *Semiclassical matrix elements for the quartic oscillator*, *Annals Phys.* **228** (1993) 365.

[318] S. Y. Khlebnikov, *Semiclassical transition probabilities for interacting oscillators*, *Nucl. Phys. B* **436** (1995) 428 [hep-ph/9401318].

[319] J. Jaeckel and S. Schenk, *Exploring high multiplicity amplitudes: The quantum mechanics analogue of the spontaneously broken case*, *Phys. Rev. D* **99** (2019) 056010 [1811.12116].

[320] A. Voros, *Exact anharmonic quantization condition (in one dimension)*, *Institute for Mathematics and Its Applications* **95** (1997) 189.

[321] R. Balian and C. Bloch, *Solution of the Schrodinger Equation in Terms of Classical Paths*, *Annals Phys.* **85** (1974) 514.

[322] J. L. Dunham, *The Wentzel-Brillouin-Kramers Method of Solving the Wave Equation*, *Physical Review* **41** (1932) 713.

[323] S. Codesido and M. Marino, *Holomorphic Anomaly and Quantum Mechanics*, *J. Phys. A* **51** (2018) 055402 [1612.07687].

[324] A. Voros, *The return of the quartic oscillator. The complex WKB method*, *Annales de l'I.H.P. Physique théorique* **39** (1983) 211.

[325] N. Fröman and P. O. Fröman, *JWKB approximation*. North-Holland Publishing Company Amsterdam, 1965.

[326] R. Balian, G. Parisi and A. Voros, *Discrepancies from asymptotic series and their relation to complex classical trajactories*, *Phys. Rev. Lett.* **41** (1978) 1141.

[327] A. Voros, *Spectre de l'équation de schrödinger et méthode bkw*, *Publications*

Mathématiques d'Orsay **81** (1981) 1.

[328] H. J. Silverstone, *JWKB connection-formula problem revisited via Borel summation*, *Phys. Rev. Lett.* **55** (1985) 2523.

[329] F. Fischbach, A. Klemm and C. Nega, *WKB Method and Quantum Periods beyond Genus One*, *J. Phys. A* **52** (2019) 075402 [1803.11222].

[330] G. Basar, G. V. Dunne and M. Unsal, *Quantum Geometry of Resurgent Perturbative/Nonperturbative Relations*, *JHEP* **05** (2017) 087 [1701.06572].

[331] M. Kreshchuk and T. Gulden, *The Picard–Fuchs equation in classical and quantum physics: application to higher-order WKB method*, *J. Phys. A* **52** (2019) 155301 [1803.07566].

[332] I. S. Gradshteyn and I. M. Ryzhik, *Table of Integrals, Series, and Products*. Academic Press, 2007.

[333] G. V. Dunne and M. Unsal, *Resurgence and Trans-series in Quantum Field Theory: The CP(N-1) Model*, *JHEP* **11** (2012) 170 [1210.2423].

[334] G. V. Dunne and M. Ünsal, *Continuity and Resurgence: towards a continuum definition of the $\mathbb{CP}$(N-1) model*, *Phys. Rev. D* **87** (2013) 025015 [1210.3646].

[335] B. Simon and A. Dicke, *Coupling constant analyticity for the anharmonic oscillator*, *Annals Phys.* **58** (1970) 76.

[336] S. Y. Khlebnikov, *Semiclassical approach to multiparticle production*, *Phys. Lett. B* **282** (1992) 459.

[337] M. V. Libanov, D. T. Son and S. V. Troitsky, *Exponentiation of multiparticle amplitudes in scalar theories. 2. Universality of the exponent*, *Phys. Rev. D* **52** (1995) 3679 [hep-ph/9503412].

[338] F. L. Bezrukov, M. V. Libanov, D. T. Son and S. V. Troitsky, *Singular classical solutions and tree multiparticle cross-sections in scalar theories*, in *10th International Workshop on High-energy Physics and Quantum Field Theory (NPI MSU 95)*, pp. 228–238, 9, 1995, hep-ph/9512342.

[339] S. Schenk, *The breakdown of resummed perturbation theory at high energies*, *JHEP* **03** (2022) 100 [2109.00549].

[340] V. V. Khoze and S. Schenk, *Multiparticle amplitudes in a scalar EFT*, *JHEP* **05** (2022) 134 [2203.03654].

[341] V. V. Khoze and J. Reiness, *Review of the semiclassical formalism for multiparticle production at high energies*, *Phys. Rept.* **822** (2019) 1 [1810.01722].

[342] S. L. Adler, *Axial vector vertex in spinor electrodynamics*, *Phys. Rev.* **177** (1969) 2426.

[343] G. 't Hooft, *Computation of the Quantum Effects Due to a Four-Dimensional Pseudoparticle*, *Phys. Rev. D* **14** (1976) 3432.

[344] R. W. Batterman, *The Devil in the Details: Asymptotic Reasoning in Explanation, Reduction, and Emergence*. New York: Oxford University Press, 2002.

[345] S. Graffi, V. Grecchi and B. Simon, *Borel summability: Application to the anharmonic oscillator*, *Phys. Lett. B* **32** (1970) 631.

[346] J. P. Eckmann, J. Magnen and R. Sénéor, *Decay properties and borel summability for the Schwinger functions inP(Φ)2 theories*, *Communications in Mathematical Physics* **39** (1974) 251.

[347] J. Magnen and R. Seneor, *Phase Space Cell Expansion and Borel Summability for the Euclidean phi**4 in Three-Dimensions Theory*, *Commun. Math. Phys.* **56** (1977) 237.

[348] A. Grassi, M. Marino and S. Zakany, *Resumming the string perturbation series*, *JHEP* **05** (2015) 038 [1405.4214].

[349] M. C. Gonzalez-Garcia and M. Maltoni, *Phenomenology with Massive Neutrinos*, *Phys. Rept.* **460** (2008) 1 [0704.1800].
[350] K. Lande, E. T. Booth, J. Impeduglia, L. M. Lederman and W. Chinowsky, *Observation of long-lived neutral v particles*, *Phys. Rev.* **103** (1956) 1901.
[351] V. L. Fitch, P. A. Piroue and R. B. Perkins, *Mass Difference of Neutral K Mesons*, *Nuovo Cim.* **22** (1961) 1160.
[352] R. H. Good, R. P. Matsen, F. Muller, O. Piccioni, W. M. Powell, H. S. White et al., *Regeneration of Neutral K Mesons and Their Mass Difference*, *Phys. Rev.* **124** (1961) 1223.
[353] ARGUS collaboration, *Observation of B0 - anti-B0 Mixing*, *Phys. Lett. B* **192** (1987) 245.
[354] Q. Liu, I. Low and T. Mehen, *Minimal entanglement and emergent symmetries in low-energy QCD*, *Phys. Rev. C* **107** (2023) 025204 [2210.12085].
[355] Belle collaboration, *Observation of Bell inequality violation in B mesons*, *J. Mod. Opt.* **51** (2004) 991 [quant-ph/0310192].
[356] F. Benatti and R. Floreanini, *Bell's locality and ε'/ε*, *Phys. Rev. D* **57** (1998) R1332.
[357] M. Fabbrichesi, R. Floreanini, E. Gabrielli and L. Marzola, *Bell inequality is violated in $B^0 \to j/\psi K^*(892)^0$ decays*, *Phys. Rev. D* **109** (2024) L031104.
[358] CMS collaboration, *Probing entanglement in top quark production with the CMS detector*, .
[359] C. Abel et al., *Measurement of the Permanent Electric Dipole Moment of the Neutron*, *Phys. Rev. Lett.* **124** (2020) 081803 [2001.11966].
[360] W.-Y. Ai, J. S. Cruz, B. Garbrecht and C. Tamarit, *Consequences of the order of the limit of infinite spacetime volume and the sum over topological sectors for CP violation in the strong interactions*, *Phys. Lett. B* **822** (2021) 136616 [2001.07152].
[361] E. Witten, *Cosmic separation of phases*, *Phys. Rev. D* **30** (1984) 272.
[362] M. Kamionkowski, A. Kosowsky and M. S. Turner, *Gravitational radiation from first-order phase transitions*, *Phys. Rev. D* **49** (1994) 2837.
[363] P. Athron, C. Balázs, A. Fowlie, L. Morris and L. Wu, *Cosmological phase transitions: From perturbative particle physics to gravitational waves*, *Prog. Part. Nucl. Phys.* **135** (2024) 104094 [2305.02357].
[364] E. Madge, E. Morgante, C. Puchades-Ibáñez, N. Ramberg, W. Ratzinger, S. Schenk et al., *Primordial gravitational waves in the nano-Hertz regime and PTA data — towards solving the GW inverse problem*, *JHEP* **10** (2023) 171 [2306.14856].
[365] M. Beneke, A. P. Chapovsky, A. Signer and G. Zanderighi, *Effective theory approach to unstable particle production*, *Phys. Rev. Lett.* **93** (2004) 011602 [hep-ph/0312331].
[366] M. Beneke, A. P. Chapovsky, A. Signer and G. Zanderighi, *Effective theory calculation of resonant high-energy scattering*, *Nucl. Phys. B* **686** (2004) 205 [hep-ph/0401002].
[367] S. Cao and D. Boyanovsky, *Effective field theory of particle mixing*, *Phys. Rev. D* **109** (2024) 036038 [2310.17070].
[368] G. Sigl and G. Raffelt, *General kinetic description of relativistic mixed neutrinos*, *Nucl. Phys. B* **406** (1993) 423.
[369] A. Pilaftsis and T. E. J. Underwood, *Resonant leptogenesis*, *Nucl. Phys. B* **692** (2004) 303 [hep-ph/0309342].
[370] A. Cervera-Lierta, J. I. Latorre, J. Rojo and L. Rottoli, *Maximal Entanglement in*

High Energy Physics, *SciPost Phys.* **3** (2017) 036 [1703.02989].

[371] S. R. Beane, D. B. Kaplan, N. Klco and M. J. Savage, *Entanglement Suppression and Emergent Symmetries of Strong Interactions*, *Phys. Rev. Lett.* **122** (2019) 102001 [1812.03138].

[372] I. Low and T. Mehen, *Symmetry from entanglement suppression*, *Phys. Rev. D* **104** (2021) 074014 [2104.10835].

[373] M. Carena, I. Low, C. E. M. Wagner and M.-L. Xiao, *Entanglement suppression, enhanced symmetry, and a standard-model-like Higgs boson*, *Phys. Rev. D* **109** (2024) L051901 [2307.08112].

[374] K. Kowalska and E. M. Sessolo, *Entanglement in flavored scalar scattering*, *JHEP* **07** (2024) 156 [2404.13743].

[375] S. Chang and G. Jacobo, *Consequences of Minimal Entanglement in Bosonic Field Theories*, 2409.13030.

[376] M. Duch, A. Strumia and A. Titov, *New physics in spin entanglement*, 2403.14757.

[377] B. A. Dobrescu and I. Mocioiu, *Spin-dependent macroscopic forces from new particle exchange*, *JHEP* **11** (2006) 005 [hep-ph/0605342].

[378] B. S. Cirelson, *QUANTUM GENERALIZATIONS OF BELL'S INEQUALITY*, *Lett. Math. Phys.* **4** (1980) 93.

[379] S. Popescu and D. Rohrlich, *Quantum nonlocality as an axiom*, *Found. Phys.* **24** (1994) 379.

[380] M. Eckstein and P. Horodecki, *Probing the limits of quantum theory with quantum information at subnuclear scales*, *Proc. Roy. Soc. Lond. A* **478** (2022) 20210806 [2103.12000].

[381] J. M. Cornwall, D. N. Levin and G. Tiktopoulos, *Uniqueness of spontaneously broken gauge theories*, *Phys. Rev. Lett.* **30** (1973) 1268.

[382] J. M. Cornwall, D. N. Levin and G. Tiktopoulos, *Derivation of Gauge Invariance from High-Energy Unitarity Bounds on the s Matrix*, *Phys. Rev. D* **10** (1974) 1145.

[383] C. E. Vayonakis, *Born Helicity Amplitudes and Cross-Sections in Nonabelian Gauge Theories*, *Lett. Nuovo Cim.* **17** (1976) 383.

[384] N. Dondi, I. Kalogerakis, D. Orlando and S. Reffert, *Resurgence of the large-charge expansion*, *JHEP* **05** (2021) 035 [2102.12488].

Prisco Lo Chiatto

Johannes Gutenberg Universität Mainz plochiat@uni-mainz.de

Updated as of 18/03/25

Education

November 2021 - October 2024	PhD in Theoretical High Energy Physics at **Johannes Gutenberg Universität Mainz** • **MPA** Fellowship • Thesis Title: Quantum Effects in the Search for New Physics
Oct 2020 - July 2021	ERASMUS+ student at **Heidelberg University**
Oct 2019 - Oct 2021	Master degree in Theoretical and computational Physics **Università degli Studi di Modena e Reggio Emilia** Thesis title: Theoretical Analysis and Sensitivity Study for the NA62 Experiment of the Decay of the K Meson into two Pions and a Pseudoscalar Particle Final Grade: 110/110 *cum laude*
Sep 2016 - Jul 2019	Undergraduate degree in Physics **Università degli Studi di Modena e Reggio Emilia**

Seminars and Presentations

24th May 2024	Seminar at **Universidad de Granada** (Granada, Spain)
18th Apr 2024	Seminar at **Max Planck Institut für Physik** (Munich, Germany)
1st Feb 2024	Seminar at **IPPP Durham** (Durham, UK)
14th Dec 2023	Seminar at **Ruprecht Karl Universität Heidelberg** (Heidelberg, Germany)
15 May 2023	Invited online talk at the journal club of the Particle Physics and Cosmology group of **Universidade Federal de Minas Gerais** (Belo Horizonte, Brasil)
12 May 2023	HEPCOS seminar at **SUNY Buffalo** (Buffalo, NY, USA)
09 May 2023	Talk at **Phenomenology 2023 Symposium** (Pittsburgh, PA, USA)
03 Jun 2021	Online presentation to Rare Decays working group of **NA62**
22 Apr 2021	Online presentation to Rare Decays working group of **NA62**
3 Sep 2020	Online presentation to Rare Decays working group of **NA62**
Oct 2020	Online presentations to RICH working group of **NA62**

Publications

NA62 Collaboration *Recent results from the NA62 experiment at CERN* PoS QNP2024 (2025), 222
NA62 Collaboration *Search for hadronic decays of feebly-interacting particles at NA62* Eur.Phys.J.C 85 (2025) 5, 571
NA62 Collaboration *Search for Physics beyond the Standard Model at NA62* PoS ICHEP2024 (2025), 445
NA62 Collaboration *Observation of the $K^+ \to \pi^+ \nu\bar{\nu}$ decay and measurement of its branching ratio* JHEP 02 (2025), 191, JHEP 02 (2025), 191
NA62 Collaboration *First detection of a tagged neutrino in the NA62 experiment* Phys.Lett.B 863 (2025), 139345
NA62 Collaboration *Search for K+ decays into the +e+e e+e final state* Phys.Lett.B 859 (2024) 139122
P. Lo Chiatto *Interference Resurrection of the τ Dipole through Quantum Tomography* arXiv:2408.04553
P. Lo Chiatto, F. Yu *Consistent Electroweak Phenomenology of a Nearly Degenerate Z' Boson* Phys.Rev.D 111 (2025) 3, 035001 **P. Lo Chiatto**, S. Schenk, F. Yu *Quantum Imprint of the Anharmonic Oscillator* arXiv:2308.01244
P. Lo Chiatto, A. Bizzeti, and F. Bucci *First Estimate of the Sensitivity for the Decay $K^+ \to \pi^+ \pi^0 a$* NA62-22-01 (NA62 Internal Note)

NA62 Collaboration *Search for K+ decays into the +e+e e+e final state* Phys. Lett. B 846 (2023)
NA62 Collaboration *A Study of the $K^+ \to \pi e^+ \nu\gamma$ decay* JHEP 09 (2023) 040
NA62 Collaboration *Improved calorimetric particle identification in NA62 using machine learning techniques* arXiv:2304.10580
NA62 Collaboration *Search for dark photon decays to $\mu^+\mu^-$ at NA62* JHEP 09 (2023) 035
NA62 Collaboration *High level perfomance of the NA62 RICH detector* Nucl.Instrum.Meth.A 1045 (2023) 167583
NA62 Collaboration *New measurement of radiative decays at the NA62 Experiment at CERN: $K_{e3\gamma}$* PoS DISCRETE 2020-2021 (2022) 055
NA62 Collaboration *Search for K^+ decays to a lepton and invisible particles* PoS DISCRETE 2020-2021 (2022) 056
NA62 Collaboration *Searches for lepton flavour/number violation in K^+ and π^0 decays at the NA62 experiment* PoS NuFact 2021 (2022) 130
NA62 Collaboration *Search for K^+ decays to a lepton and invisible particles* PoS NuFact2021 (2022) 157
NA62 Collaboration *Measurement of the very rare $K^+ \to \pi^+ \nu\bar{\nu}$ decay at the NA62 experiment at CERN* PoS NuFact 2021 (2022) 176
NA62 Collaboration *Search for heavy neutral lepton production at the NA62 experiment* PoS EPS-HEP2021 (2022) 686
NA62 Collaboration *Search for lepton number and flavour violation in K^+ and π^0 decays* PoS DISCRETE 2020-2021 (2022) 686
NA62 Collaboration *New measurement of the radiative decay $Ke3\gamma$ at the NA62 experiment at CERN* PoS PANIC 2021 (2022) 427
NA62 Collaboration *Preliminary results of the $K^+ \to \pi^0 e^+ \nu\gamma$ decay study at the NA62 experiment* PoS EPS-HEP 2021 (2022) 553
NA62 Collaboration *NA62 results on Dark Sector searchs* Frascati Phys.Ser. 74 (2022) 269-284